# Ethyl octyl ether synthesis

## from 1-octanol and ethanol or diethyl carbonate on acidic ion-exchange resins

Jordi Guilera Sala

Universitat de Barcelona

# Ethyl octyl ether synthesis

## from 1-octanol and ethanol or diethyl carbonate on acidic ion-exchange resins

**Jordi Guilera Sala**

under the supervision of:

**Dra. Eliana Ramírez Rangel**

**Prof. Dr. Javier Tejero Salvador**

# Ethyl octyl ether synthesis from 1-octanol and ethanol or diethyl carbonate on acidic ion-exchange resins

Doctoral thesis to obtain the degree of doctor in

## Engineering and Advanced Technologies

presented by:

**Jordi Guilera Sala**

performed in the “Applied Kinetics and Catalysis” research group,

Chemical Engineering Department,

University of Barcelona

approved by:

**Dra. Eliana Ramírez Rangel**

University of Barcelona

**Prof. Dr. Javier Tejero Salvador**

University of Barcelona

Barcelona, June 2013

# List of publications

**Authors:** J. Guilera, R. Bringué, E. Ramírez, M. Iborra, J. Tejero
**Title:** Synthesis of ethyl octyl ether from diethyl carbonate and 1-octanol over solid catalysts. A screening study
**Journal:** Applied Catalysis A-General
**Volume:** 413-414 **Pages:** 21-29 **Year:** 2012

**Authors:** J. Guilera, R. Bringué, E. Ramírez, M. Iborra and J. Tejero
**Title:** Comparison between ethanol and diethyl carbonate as ethylating agents for ethyl octyl ether synthesis over acidic ion-exchange resins
**Journal:** Industrial & Engineering Chemistry Research
**Volume:** 51 **Pages:** 16525-16530 **Year:** 2012

**Authors:** C. Casas, J. Guilera, E. Ramírez, R. Bringué, M. Iborra and J. Tejero
**Title:** Reliability of the synthesis of $C_{10}$–$C_{16}$ linear ethers from 1-alkanols over acidic ion-exchange resins
**Journal:** Biomass Conversion and Biorefinery
**Volume:** 3 **Pages:** 27-37 **Year:** 2013

# Works in progress

**Authors:** J. Guilera, E. Ramírez, M. Iborra, J. Tejero, F. Cunill
**Title:** Synthesis of ethyl octyl ether by reaction between 1-octanol and ethanol over Amberlyst 70
**Journal:** Green Syntheses
**Publication status:** Accepted

**Authors:** J. Guilera, E. Ramírez, C. Fité, M. Iborra, J. Tejero
**Title:** Thermal stability and water effect on ion-exchange resins in ethyl octyl ether production at high temperature
**Journal:** Applied Catalysis A-General
**Publication status:** Revise and resubmit

**Authors:** J. Guilera, E. Ramírez, M. Iborra, J. Tejero, F. Cunill
**Title:** Experimental study of chemical equilibria of the liquid-phase alcohol dehydration to 1-ethoxy-octane and to ethoxyethane
**Journal:** Journal of Chemical & Engineering Data
**Publication status:** Revise and resubmit

**Authors:** J. Guilera, L. Hankova, K. Jerabek, E. Ramírez, J. Tejero
**Title:** Influence of the functionalization degree of acidic ion-exchange resins on ethyl octyl ether formation
**Journal:** Catalysis Today
**Publication status:** Under revision

**Authors:** J. Guilera, R. Bringué, E. Ramírez, J. Tejero, F. Cunill
**Title:** Kinetics of ethyl octyl ether formation from ethanol and 1-octanol dehydration catalyzed by Amberlyst 70
**Journal:** Chemical Engineering Journal
**Publication status:** Under revision

# Conference contributions

**Authors:** J. Guilera, C. Casas, E. Ramírez, R. Bringué, M. Iborra
**Title:** Synthesis of ethyl octyl ether from diethyl carbonate and 1-octanol over solid catalysts
**Kind of participation:** Poster
**Conference:** Ubiochem I (Utilisation of biomass for fuels and chemicals)
**Place of celebration:** Cordoba (SPAIN) **Year:** 2010 (May)

**Authors:** J. Guilera, E. Ramírez, R. Bringué, M. Iborra and J. Tejero
**Title:** Comparison between ethanol and diethyl carbonate as ethylating agents for ethyl octyl ether production over high swollen acid resins
**Kind of participation:** Poster
**Conference:** X EUROPACAT (European Congress on Catalysis)
**Place of celebration:** Glasgow (SCOTLAND) **Year:** 2011 (August)

**Authors:** C. Casas, J. Guilera, E. Ramírez, R. Bringué, M. Iborra and J. Tejero
**Title:** Reliability of the synthesis of $C_{10}$-$C_{16}$ linear ethers from 1-alkanols over acidic ion exchange resins
**Kind of participation:** Poster
**Conference:** XIX ISAF (International Symposium on Alcohol Fuels)
**Place of celebration:** Verona (ITALY) **Year:** 2011 (October)

**Authors:** J. Guilera, E. Ramírez, C. Fité, M. Iborra, J. Tejero
**Title:** Water effects on the activity of ion-exchange resins as catalysts of the reaction between ethanol and 1-octanol at high temperature
**Kind of participation:** Poster
**Conference:** 15$^{th}$ ICC (International Congress on Catalysis)
**Place of celebration:** Munich (GERMANY) **Year:** 2012 (July)

**Authors:** J. Guilera, L. Hankova, K. Jerabek, E. Ramírez, J. Tejero
**Title:** Influence of the sulfonation degree of acidic ion-exchange resins on ethyl octyl ether formation
**Kind of participation:** Oral communication
**Conference:** CAFC10 (Congress on Catalysis Applied to Fine Chemicals)
**Place of celebration:** Turku (FINLAND) **Year:** 2013 (June)

**Authors:** J. Guilera, R. Bringué, E. Ramírez, J. Tejero, F. Cunill
**Title:** Kinetics of 1-octanol and ethanol dehydration to ethyl octyl ether over Amberlyst 70
**Kind of participation:** Poster
**Conference:** XI EUROPACAT (European Congress on Catalysis)
**Place of celebration:** Lyon (FRANCE) **Year:** 2013 (September)

# Contents

Chapter 1

# General introduction

## 1.1 Oil influence in our society

Population and income growth are the two most powerful driving forces behind the demand for energy. Since 1900 world population has more than quadrupled, real income has grown by a factor of 25, and primary energy consumption by a factor of 23. Over the last 20 years world population has increased by 1.6 thousand million people, and it is foreseen to rise by 1.4 thousand million over the next 20 years. The world's real income has risen by 87% over the past 20 years and it is likely to rise by 100% over the next 20 years. At the global level, the most fundamental relationship in energy economics remains robust: more people with more income means that the production and consumption of energy will rise (see Fig. 1.1) [1].

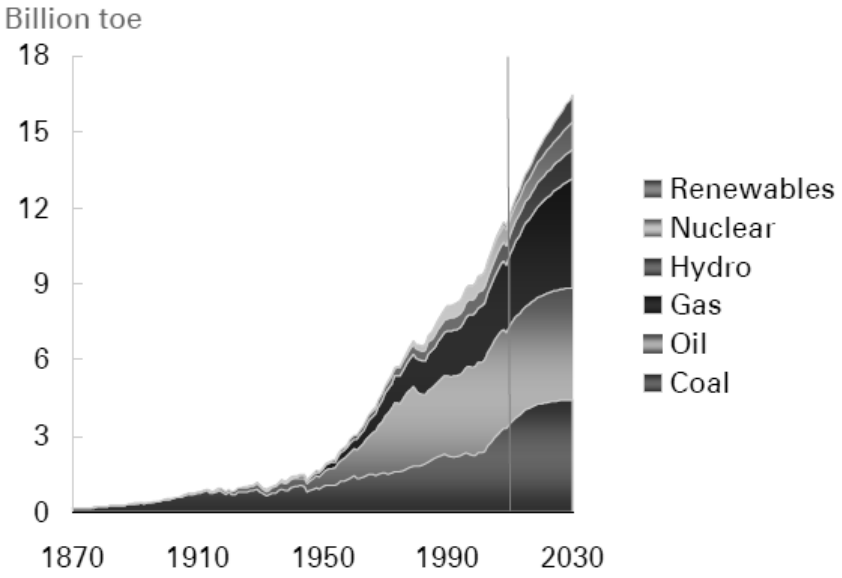


Fig. 1.1: World commercial energy consumption [1].

As globalization proceeds, the next 20 years are likely to see rapid growth of low and medium income economies. In 2011, all of the net energy consumption growth (+2.5%) took place in emerging economies, with China alone accounting for 71% of the global growth. In contrast, consumption in high-income economies fell 0.8%, the third decline in the past four years [2].

Oil remains the world's leading fuel. However, oil continues to suffer a long run decline in market share, while gas steadily gains. The diversification of the fuel mix is being driven by the power sector, where non-fossil fuels, lead by renewables, account for more than half of the growth. In transport, diversification is driven by policy and enabled by technology, with biofuels accounting for nearly a third of energy demand growth. The rate at which renewables are introduced the global energy, 18% of the growth in energy to 2030, is similar to the emergence of nuclear power in the 1970s and 1980s. Continued policy support, high oil prices and technological innovations all contribute to the rapid expansion of biofuels [1], [3], [4].

The United States and Brazil will continue to dominate biofuel production, together they would account for 68% of total output in 2030 (see Fig.1.2). Smaller scale production started more recently in Europe from France, Germany and Spain. The exponential growth of biofuels production is largely due to bioethanol. Thus, bioethanol has become the most promising biofuel and is considered as the only feasible short to medium alternative to fossil transport fuel. Besides, the potential of bioethanol to create jobs is immense in farming, biorefineries, the chemical industry, the fuel supply sector and fuel-flexible vehicle engineering [1], [5].

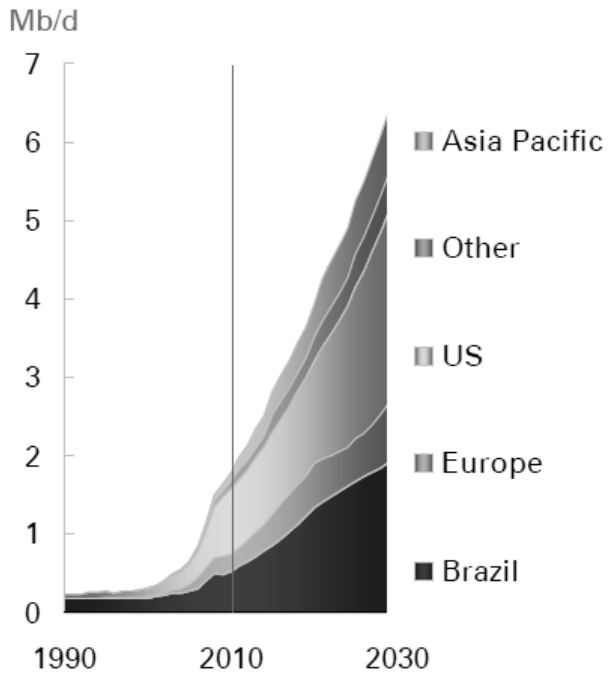


Fig. 1.2: Biofuel worldwide supply [1].

## 1.2 Bioethanol

Ethanol produced from renewable sources is called bioethanol. Ethanol has good properties in spark ignition internal combustion engines. Thus, the most straightforward way to use bioethanol is to blend it with gasoline. Bioethanol fuel is currently used in internal combustion engines as 5-26% anhydrous bioethanol blends to gasoline (< 5% in Europe and India, 10% in US, 22-26% mandatory blends in Brazil) or as pure fuel of hydrated bioethanol (named as E100) [6].

Refiners blend bioethanol directly to gasoline; however, ethanol addition results in a significant increase in gasoline vapour pressure, which is an important constraint. An indirect way to introduce bioethanol to gasoline is by producing bioethers such as ethyl tert-butyl ether (ETBE). The introduction of bioethers in reformulated gasoline leads to a reduction in emissions of

exhaust pollutants such as volatile organic compounds and particles. Likewise, fuel asymmetric branched ethers have higher octane numbers, and in this way, allow refiners to substitute other less desirable components e.g. aromatics and olefins. Besides, blending bioethers into gasoline is more energy efficient than that of bioethanol, with an additional saving of 24 kg of $CO_2$-equivalent/GJ of bioethanol [7], [8].

Ethanol is unable to be directly used in diesel engines. Nonetheless, to blend bioethanol with conventional diesel has been evaluated since 1980s. Over the last years, this topic has been a subject of research due to diesel fuel is foreseen to grow much faster than gasoline over the next 20 years. In addition, interest in maximizing the production of diesel fuel is specially high in Europe. European refineries do not produce enough diesel fuel, and consequently, European countries are importing diesel and exporting gasoline to the United States [9], [10]. However, the use of ethanol-diesel blends has some limitations. With respect to conventional diesel, ethanol-diesel blend has lower viscosity and lubricity, reduced ignitability and cetane number, higher volatility and lower miscibility. In order to overcome these difficulties, the use of cetane enhancers and solvent additives are needed to recover the potential of these blends [9], [11].

Analogously as gasoline, a more attractive way to introduce bioethanol to the diesel pool is by producing suitable compounds, namely bioethanol-derived components. Quoted alternative diesel compositions can contain $C_4$-$C_{10}$ oligomers of dehydrated ethanol and ethyl glycerol ethers [12]–[14]. Nevertheless, oligomers do not have the combustion advantages of oxygenated compounds and ethyl glycerol ethers have been proven to be disadvantageous with regard to the undesired particle emissions [15]. With the aim of avoiding the above disadvantages, Eberhard recently patented the use of diesel fuel based on ethanol (60-90% v/v) that contains linear dialkyl ethers (up to 20% v/v) [15]. The interest in using linear dialkyl ethers in diesel fuel is caused by their high cetane number and other desirable fuel properties, such as lower pour and cloud point [16], [17]. Additionally, the use of an alcohol from a renewable origin to form such ethers is an opportunity to increase the biofuel percentage in the diesel pool.

## 1.3 Ethyl octyl ether

A bioethanol-derived component that has excellent properties as diesel fuel is ethyl octyl ether (EOE), IUPAC name: 1-ethoxy-octane. EOE is an asymmetrical ether of 10 carbon atoms, $C_{10}H_{22}O$ (see Fig. 1.3). EOE has 10 w/w % oxygen content, 187ºC boiling, $d_4^{20}$ of 0.771, cetane number of 97 and satisfactory lubricity [18]. In addition of the good properties as diesel component, EOE as an alkyl ether also has a wide variety of potential industrial uses such as component of dyes, paints, rubbers, resins and lubricants [19]–[21].

Fig. 1.3: EOE structure.

Linear ethers can be formed by the bimolecular dehydration of primary linear alcohols over acid catalysts. Alcohol dehydration reaction is highly useful for obtaining symmetrical ethers from primary alcohols such as dimethyl ether, di-n-butyl ether, di-n-pentyl ether, di-n-hexyl ether or di-n-octyl ether. In the case of using secondary alcohols, the obtained selectivities to ethers are lower, as a result of the olefinic by-product obtained by monomolecular dehydration [22]–[25].

So far, the dehydration of alcohols has been industrially catalyzed by sulfuric acid [15]. However, it is widely known that solid catalysts have the advantage of easier separation and they yield a reaction product free of blacken compounds. Accordingly, it is desirable to obtain solid acid catalysts that exhibit activities and selectivities at least comparable to their homogeneous counterparts in order to obtain an economic and environmental viable process. Besides, by using a solid catalyst it is possible to carry out the ether production on a fixed, fluidized or mobile bed process. Over the last years, it has found that acidic ion-exchange resins are able to catalyze the dehydration of primary alcohols to linear symmetrical ethers with high selectivity (97-99%) [22], [25]–[27].

## 1.4 Acidic ion-exchange resins as catalysts

Ion-exchange consists of the interchange of ions between two phases. In particular, ion-exchange resins are useful because of the insolubility of the resin phase. After contact with the ion-containing solution, the resin can be separated by filtration. They are also adaptable to continuous processes involving columns. Their insolubility renders them environmentally compatible since the cycle of loading/regeneration/reloading allows them to be used for many years. Ion-exchange resins have been used since 1940's in water softening, removal of toxic metals from water in the environment, wastewater treatment, hydrometallurgy, sensors, chromatography, and biomolecular separations [28]. In Fig. 1.4 it is shown an illustrative example of the beads of an ion-exchange resin.

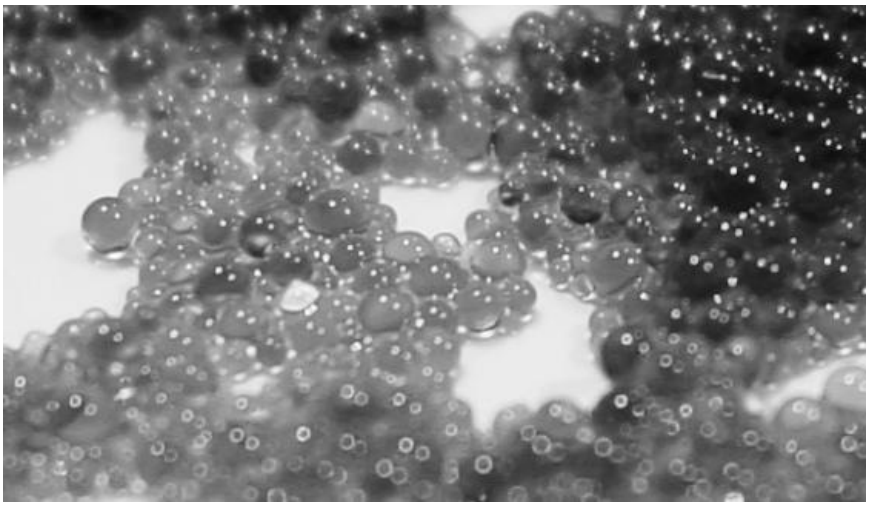

Fig. 1.4: Ion-exchange resin beads.

Ion-exchange resins are also used as catalysts, both in place of homogeneous catalysts such as sulfuric acid and to immobilize metallic catalysts [29]. As concerns to acid catalysts, most commercial acidic ion-exchange resins are based on a polystyrene-divinylbenzene (PS-DVB) copolymer. The continuous operation of cation-exchange resins through numerous load/regeneration cycles depends on their physical stability, i.e., the ability of the beads to resist fracture and disintegration into smaller irregular particles. Fig. 1.5 shows an illustrative example of breaking of polymer matrix when heated. It was found that the manner in which they are prepared from unfunctionalized PS-DVB beads is critical to their stability. The reaction with concentrated sulfuric acid must be done on beads that are fully swollen in an inert solvent; dichloroethane, methylene chloride and trichloroethylene give good results since they are excellent swelling solvents. After sulfonation, the concentrated sulfuric acid in contact with the beads must not be diluted too rapidly with water because the swelling forces created by hydration of the sulfonic acid ligands will cause the beads to shatter; washing with sulfuric acid solutions of progressively lower acidity allows hydration to occur slowly. The resins must then be packed in a manner that maintains their complete hydration or they must be slowly hydrated prior to use [28].

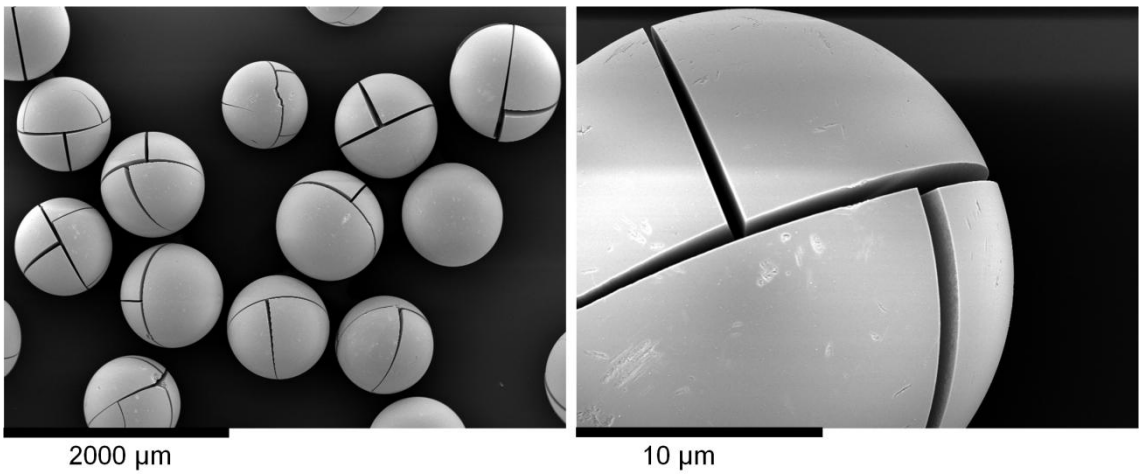


Fig. 1.5: Scanning electron micrograph of broken polymer matrix of a resin.

Acidic PS-DVB ion-exchange resins are attractive catalysts because, compared to most other solid acids, they exhibit higher concentrations of acid sites (~5 meq $H^+$/g) and the strength of the acid sites tends to be highly uniform. On the contrary, the strength of the acid groups are lower than those found on zeolitic and similar solid acids [24], [26], [30], [31]. The exchange capacity of acidic resins are chiefly conditionated by their molecular accessibility, namely, by their ability to be crossed by reactants and products moving to and from the active sites. On these grounds, it appears quite obvious that any application of acidic ion-exchange resins ought to be preceded by a careful examination of the resin morphology [32].

PS-DVB copolymer carriers are divided into two groups. Historically, the first type of PS-DVB resins was the gel-type ones. Gel-type resins are copolymerized without porogen; hence, their porosity only appears in a swollen state. In the 1960s a second type of resins was developed, the macroreticular ones [28]. Addition of a solvent to the mixture of monomers during the polymerization induces creation of permanent pores, stable even in absence of swelling. Thanks to it, the resulting polymers contain pores at least partially stable even in absence of swelling (a schematic diagram of a macroreticular resin is displayed in Fig. 1.6). These so-called macroreticular resins have permanent macropores which can be detected in dry state. Nevertheless, even in the macroreticular resins new pores appear by the swelling of the polymer in suitable solvent [32].

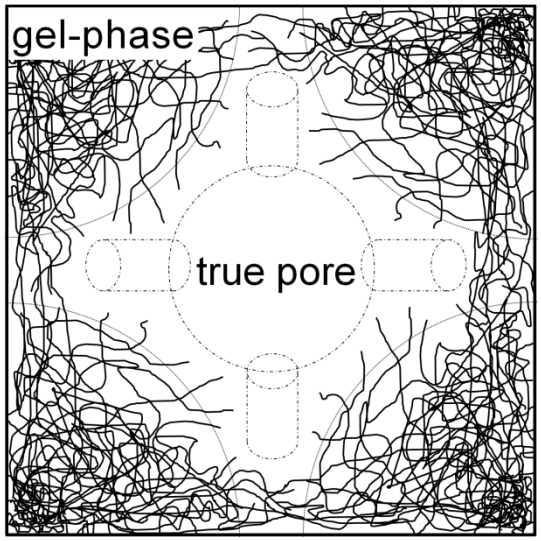


Fig. 1.6: Morphology of a macroreticular resin [33].

Complete porosity of polymeric supports cannot be characterized by conventional porosimetric methods as mercury intrusion or nitrogen adsorption since they require completely dry samples. Using such data to interpret resin effects observed e.g. in reactions carried out in solvents does require the assumption that the morphology is not changed significantly when the resin is wetted with solvent. This assumption is clearly not valid using hydrophilic polymeric catalysts in a polar reaction environment. Therefore, in order to study the morphology of gel-type and macroreticular catalysts, other characterization techniques are needed. To date, the only procedure employed to assess the morphology of ion-exchange resins in a swollen state has been the Inverse Steric Exclusion Chromatography (ISEC) technique. This method is based on measurements of elution volumes of standard solutes with known molecular sizes, by using chromatographic column filled with the investigated swollen polymer [33]–[37].

Attempts to obtain porosimetric data from ISEC technique have been reported in the open literature since 1975. Ten years later, Jerabek proposed an approach based on modelling of the porous structure as a set of discrete fractions, each composed of pores having simple geometry and uniform sizes. From that point of view, gel-phase porosity is described as zones of different chain density. According to this model, the pore size of the gel-phase is represented as total rod length per unit of volume ($nm^{-2}$) [34], [35].

The morphological information given by ISEC technique has been used in successful correlation on catalytic activity of ion-exchangers. In polar reaction systems the catalyst swelling is comparable to that of water, hence, it is expected that the internal catalyst morphology to be also similar. Recently, several studies on alcohol dehydration to ethers had make use of ISEC description to correlate ion-exchange morphology with catalytic results [22], [26], [38]. In these works, it is observed that the accessibility of the reactants to acid centres is the key factor to describe the catalytic results. Consequently, the ISEC technique is attracting increased interest from resin designers and exploiters [39].

Besides acidity and morphological properties, on the selection of a suitable acidic resin for a given reaction it is important that the catalyst retains its activity and selectivity for some time. With respect to acid resins, a great disadvantage of its industrial use is their low thermal stability. In general, thermal deactivation by sulfonic groups leaching hinders their application at high temperature. Most PS-DVB resins are stable up to 150ºC, but the maximum operating temperature of some highly used resins is even lower [40], [41]. Thermal resistance to desulphonation of PS-DVB resins can be enhanced by adding electron withdrawing groups to the sulfonated phenyl ring, such as chlorine atoms. Therefore, in some reactions that are catalyzed by acidic ion-exchange resins, the operating temperature can be increased to obtain higher reaction rates and, therefore, to have a more economically feasible reaction unit [30].

## 1.5 Reaction kinetic modelling

The modelling of a reaction process is necessary for further reactor design purposes. When an acidic ion-exchange resin is used as catalyst, analogously as other solid catalysts, it is compulsory that at least one reactant in the fluid phase interact with the solid surface, and get fixed on it. Therefore, chemical reaction takes part in a complex process, where different elemental catalytic steps are involved. The reaction process consists of the following seven stages (see Fig. 1.7):

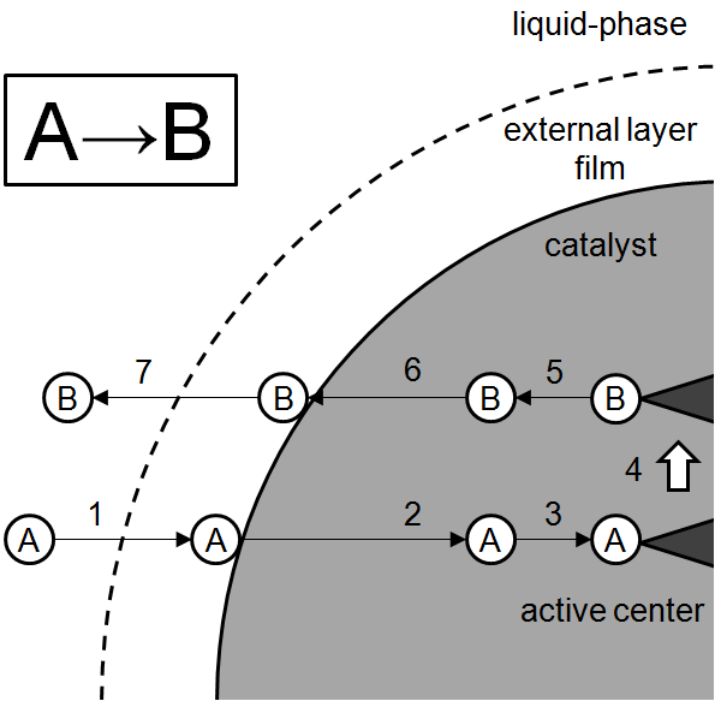


Fig. 1.7: Steps of the catalytic process in a reaction A → B.

1. Diffusion of reactants from bulk liquid-phase to the external resin surface (external mass transfer).
2. Diffusion of reactants through the catalyst (internal mass transfer).
3. Adsorption of reactants on resin active sites.
4. Chemical reaction between adsorbed species or between adsorbed species with fluid phase ones.
5. Desorption of reaction products.
6. Diffusion of products through the catalyst (internal mass transfer).
7. Diffusion of products from external resin surface to bulk liquid phase (external mass transfer).

Steps 1, 2, 6 and 7, concerning to mass transfers, are of physical nature, while steps 3, 4 and 5 are of chemical nature. Mass transfer resistances strongly depend on the flow conditions in the reactor and the particle size of the catalyst. Varying these parameters it is possible to check the physical transfer limitations of the reaction. If physical steps are very fast, there is no resistance to the mass transfer from the bulk liquid to the resin surface and from the resin surface to the active sites. Thus, the concentration around the catalyst sites is supposed to be the same as that of the liquid bulk phase. Under these conditions, the mass transfer steps do not affect the reaction rate of the catalytic reaction. Therefore, the reaction rate is the intrinsic one and can be computed from the reaction mechanism assuming that the concentration at the catalyst site is the same as that of the liquid surrounding catalyst sites.

A plausible intrinsic reaction mechanism of acidic resins catalytic reactions is that the reactants chemisorb on the surface and react while in the adsorbed state. The process of adsorption A on a sulfonic group σ is represented by (single site adsorption)

$$A + \sigma \leftrightarrow A\sigma$$

and the reaction between adsorbed molecules, for instance, by

$$A\sigma + B\sigma \leftrightarrow C\sigma + D\sigma$$

The developed kinetic expressions for explaining this process are based on 3 assumptions: a) the solid surface contains a fixed number of active sites b) all the active sites are identical c) the active sites reactivity does not depend on quantity and nature of the rest of compounds present on the solid surface during the reaction, it only depends on temperature. However, it is worth mentioning that assumptions (b) and (c) are inaccurate using ion-exchangers as catalyst [37], [39], [42].

Classical kinetic models catalyzed by solids comes from Langmuir isotherm development using species concentration near from active sites instead of occupied sites fraction (Langmuir and Hinshelwood) or surface molar concentrations (Hougen and Watson), which are difficult to determine experimentally. In Langmuir-Hinshelwood-Hougen-Watson (LHHW) formalism, the reaction is between adsorbed molecules, while in Eley-Rideal (ER) formalisms, it is considered that some reactants are not adsorbed so that reaction occurs directly between an adsorbed reactant with reactants present in the liquid-phase. In both cases, in the absence of external and internal mass resistances, general procedure consists of proposing a rate-limiting step (reactants adsorption, products desorption or surface reaction), and then to develop equations depending on possible different active sites involved in the catalytic process. Usually, many different possible kinetic models can be proposed to explain reaction data, but all of them possess the same general structure (eq. 1.1), so it is compulsory to check all of them to reach those fit better the experimental reaction rate data and provide values of thermodynamically parameters [43], [44].

$$\text{reaction rate} = \frac{[\text{kinetic term}][\text{driving force}]}{[\text{adsorption term}]} \qquad \text{eq. 1.1}$$

## 1.6 Scope of the thesis

Ethyl octyl ether has excellent properties as a diesel compound and it can be an industrial option to introduce bioethanol indirectly to the diesel pool. The aim of this thesis is to study the catalytic reaction process for obtaining such product. This involves the selection of a suitable reaction pathway and catalysts, as well as, thermochemical and kinetic evaluation of the process, which are necessary for a reactor design purposes.

In **Chapter 2**, materials, catalysts and experimental apparatus used in this work are described. In **Chapter 3**, the production of ethyl octyl ether from ethanol and 1-octanol dehydration is evaluated. In this study, several acidic ion-exchange resins are compared to establish a relation between morphological parameters and catalytic activity to the desired product. In **Chapter 4**, the synthesis of ethyl octyl ether from a mixture of diethyl carbonate over several solid catalysts is studied. Again, the influence of the morphological parameters of the catalysts is related to the activity. In **Chapter 5**, both ethanol and diethyl carbonate, are compared as ethylating agents of 1-octanol to give ethyl octyl ether over some of the best catalysts found. In **Chapter 6**, the evolution of catalytic activity to form ethyl octyl ether from ethanol and 1-octanol along time is evaluated. Temperature and water effects are highlighted. In **Chapter 7**, the thermochemical data of the ethyl octyl ether formation from ethanol and 1-octanol is obtained. Besides, a kinetic model able to predict the reaction rates on the best catalyst found, Amberlyst 70, is proposed. In **Chapter 8**, the possibility of increasing the selectivity to ethyl octyl ether on acidic resins by using partially sulfonated resins is explored. **Chapter 9** summarizes the results obtained in the scope of this work and it gives recommendations for future research.

Chapter 2

# Experimental

## 2.1 Chemicals

1-octanol (OcOH) (≥ 99%, Acros), ethanol (EtOH) (≥ 99.8%, Panreac), diethyl carbonate (DEC) (≥98%, Fluka), diethyl ether (DEE) (≥99%, Panreac), di-n-octyl ether (DNOE) (≥ 97%, Fluka), 1-octene (≥ 97%, Fluka), 1,4-dioxane (≥ 99.8, Sigma), 1-pentanol (≥99%, Sigma), sulphuric acid (>95%, Lac-ner) and 1,2-dichloroethane (DCE) (99.8%, Acros) were used without further purification. EOE was synthesized and purified in our lab by rectification to 99%. Bidistilled water was also used.

## 2.2 Catalysts

A great part of experiments shown in this work was performed by using commercial acidic PS-DVB resins (described in section 2.2.1). Besides, in chapter 4, it was used other types of commercial solid catalysts such as basic resins, acidic nafion, a zeolite and two aluminas (described in section 2.2.2). Eventually, in chapter 8, a series of PS-DVB resins were prepared by sulfonation of a polymer carrier, and subsequently, tested (described in section 8.3).

### 2.2.1 Acidic PS-DVB resins

17 acidic PS-DVB resins were used as catalysts, supplied by Purolite (CT 124, 224 and 482), Aldrich (Dowex 50Wx8, 50Wx4 and 50Wx2) and Rohm and Haas France (Amberlyst 15, 16, 31, 35, 36, 39, 46, 48, 70, 121 and XE804). The main properties of tested ion-exchange resins are presented in Table 2.1.

Table 2.1: Characteristics of used ion-exchange resins.

| catalyst | structure | acid capacity (meq $H^+$/g) | sulfonation type[a] | DVB (%)[b] | porous information in dry state[c] | | |
|---|---|---|---|---|---|---|---|
| | | | | | $d_{pore}$ (nm) | $\Sigma V_{pore}$ ($cm^3$/g) | $S_{BET}$ ($m^2$/g) |
| Amberlyst 15 | macroreticular | 4.81 | CS | 20 | 31.8 | 0.33 | 42 |
| Amberlyst 35 | macroreticular | 5.32 | OS | 20 | 23.6 | 0.21 | 29 |
| Amberlyst 48 | macroreticular | 5.62 | OS | high | 31.0 | 0.25 | 34 |
| Amberlyst 46 | macroreticular | 0.87 | SS | high | 19.2 | 0.26 | 57 |
| Amberlyst 16 | macroreticular | 4.80 | CS | 12 [45] | 29.7 | 0.01 | 2 |
| Amberlyst 36 | macroreticular | 5.40 | OS | 12 [46] | 27.0 | 0.14 | 21 |
| Amberlyst 39 | macroreticular | 5.06 | CS | 8 [47] | 17.6 | <0.01 | <1 |
| Purolite CT482[d] | macroreticular | 4.25 | CS | n. a. | 26.8 | 0.06 | 9 |
| Amberlyst XE804[d] | macroreticular | 3.17 | CS | n. a. | 20.7 | 0.02 | 4 |
| Amberlyst 70[d] | macroreticular | 2.65 | CS | 8 | - | - | <1 |
| Dowex 50Wx8 | gel-type | 4.83 | CS | 8 | - | - | <1 |
| Purolite CT 124 | gel-type | 5.00 | CS | 4 | - | - | <1 |
| Purolite CT 224 | gel-type | 5.34 | OS | 4 | - | - | 1 |
| Dowex 50Wx4 | gel-type | 4.95 | CS | 4 | - | - | <1 |
| Amberlyst 31 | gel-type | 4.80 | CS | 4 [46] | - | - | <1 |
| Dowex 50Wx2 | gel-type | 4.83 | CS | 2 | - | - | 1 |
| Amberlyst 121 | gel-type | 4.80 | CS | 2 [48] | - | - | <1 |

[a] CS=conventionally sulfonated; OS=oversulfonated; SS=surface sulfonated or low sulfonated [b] information not warranted for the authors [c] obtained from gas adsorption-desorption (described in section 2.3.3) [d] chlorinated resin.

Macroreticular resins include polymers of high crosslinking degree (Amberlyst 15, 35, 46 and 48), medium (Amberlyst 16 and 36) and low (Amberlyst 39 and 70); gel-type ones include resins containing 8% DVB (Dowex 50Wx8), 4% (Purolite CT 124 and 224; Dowex50Wx4 and Amberlyst 31) and 2% (Dowex 50Wx2 and Amberlyst 121). As for sulfonation degree, selected resins include conventionally sulfonated, oversulfonated and low sulfonated. Amberlyst 35 is an oversulfonated versions of Amberlyst 15; Amberlyst 36 an oversulfonated version of Amberlyst 16; and CT 224 an oversulfonated version of CT 124. Amberlyst 46 has its sulfonic groups located only on the surface of the gel-phase microspheres and it can be considered a surface sulfonated version of Amberlyst 15. Special properties of the chlorinated resins (Amberlyst 70 and XE804; and Purolite CT482) have to be emphasized. They have chlorine atoms in its structure to improve their thermal stability.

In the dry state, macroreticular resins with high crosslinking degree have permanent porosity, whereas low-crosslinked resins show low surface areas and pore volumes. As for gel-type resins, they do not present permanent porosity so that they are collapsed in dry state. However, gas adsorption-desorption data are not useful to describe the morphology in swollen state neither that of macroreticular resins nor that of gel-type ones.

Accordingly, morphological properties of acidic PS-DVB resins discussed in this work are obtained from ISEC technique, using water as the mobile phase due to the hydrophilic character of the catalytic tests, described in section 1.4.

**True pores**

Macroreticular resins are synthesized in the presence of a solvent, miscible with the monomers but the formed polymer is insoluble in it. Thanks to it, the resulting polymers contain pores at least partially stable even in absence of swelling (a schematic diagram of a macroreticular resin is displayed in Fig. 1.6). This family of pores is usually called macropores and they are permanent pores. Unambiguously, as "true" pores can be evaluated pores having diameter greater than 8 nm [38]. To characterize these pores it is possible to use the cylindrical model [33]. Table 2.2 summarizes the true pores information of the tested catalysts. Macroreticular catalysts show pore diameter between 9 and 19 nm, a total pore volume between 0.16 and 1.05 $cm^3/g$ and a total surface between 46 and 214 $m^2/g$. Obviously, gel-type resins did not showed any true pores so they are not described.

Table 2.2: Properties of resin true pores morphology using ISEC technique.

| catalyst | $d_{pore}$ (nm) | $\Sigma V_{pore}$ ($cm^3/g$) | $\Sigma S$ ($m^2/g$) |
|---|---|---|---|
| Amberlyst 15 | 12.4 ± 1.3 | 0.616 ± 0.004 | 192 ± 30 |
| Amberlyst 35 | 12.6 ± 0.3 | 0.720 ± 0.089 | 199 ± 5 |
| Amberlyst 48 | 12.3 ± 0.7 | 0.568 ± 0.007 | 186 ± 14 |
| Amberlyst 46 | 10.3 ± 4.7 | 0.470 ± 0.110 | 186 ± 31 |
| Amberlyst 16 | 15.5 ± 0.2 | 0.188 ± 0.002 | 46 ± 3 |
| Amberlyst 36 | 14.8 ± 4.6 | 0.259 ± 0.109 | 68 ± 8 |
| Amberlyst 39 | 15.0 ± 4.2 | 0.155 ± 0.002 | 56 ± 3 |
| Purolite CT482 | 18.5 ± 0.2 | 1.051 ± 0.259 | 214 ± 27 |
| Amberlyst XE804 | 8.5 ± 0.4 | 0.518 ± 0.037 | 243 ± 5 |
| Amberlyst 70 | 13.5 ± 0.4 | 0.220 ± 0.049 | 66 ± 13 |

By comparing ISEC true pore description (Table 2.2) and the information of nitrogen adsorption (Table 2.1), it is clear that the morphology of the resins changes drastically swollen in water. In the dry state, surface areas were much lower ($0<S_{dry}<60$ $m^2/g$) than those measured in swollen state ($46<S_{swollen}<214$ $m^2/g$). This fact can be observed as well for pore volumes. Accordingly, mean pore diameter values were larger in dry state ($17<d_{pore}<32$ nm) than in swollen state ($9<d_{pore}<19$ nm). This is because in the swollen state it appears new pores in the mesopore range not detected in dry state (diameter 8-20 nm).

In general, the high-crosslinked resins showed, both swollen in water and in dry state, higher pore volumes and higher surface areas than those of the low-crosslinked ones. As for low-crosslinked macroreticular resins (Amberlyst 39 and 70), their morphology was almost collapsed in dry state, whereas they present a much more expanded structure in swollen state

($56<S_{swollen}<66$ $m^2/g$). Besides, the only pores detected in dry state for Amberlyst 39 and 70 were the large ones ($18<d_{pore}<27$ nm).

**Gel-phase**

A great advantage of ISEC technique is that it provides a description of a set of discrete gel-phase fractions, each with its own characteristic value of the polymer chain density. As a result that acid centres are located in the gel-phase and reactants and products must diffuse through it, the morphological information of the gel-phase of acidic PS-DVB resins is highly valuable in interpreting their catalytic behaviour. Gel-phase fractions are currently normalized as 0.1, 0.2, 0.4, 0.8 and 1.5 $nm^{-2}$ [36]. The sum of computed cumulative volumes of the swollen gel fraction used is the specific volume of the swollen phase parameter ($V_{sp}$) (Table 2.3).

Table 2.3: $V_{sp}$ of resin gel-phase using ISEC technique.

| catalyst | $V_{sp}$ ($cm^3/g$) |
|---|---|
| Amberlyst 15 | 0.622 ± 0.006 |
| Amberlyst 35 | 0.504 ± 0.003 |
| Amberlyst 48 | 0.514 ± 0.003 |
| Amberlyst 46 | 0.190 ± 0.030 |
| Amberlyst 16 | 1.136 ± 0.065 |
| Amberlyst 36 | 1.261 ± 0.065 |
| Amberlyst 39 | 1.643 ± 0.048 |
| Purolite CT482 | 1.081 ± 0.072 |
| Amberlyst XE804 | 0.834 ± 0.101 |
| Amberlyst 70 | 1.149 ± 0.021 |
| Dowex 50Wx8 | 1.404 ± 0.067 |
| Purolite CT 124 | 2.006 ± 0.077 |
| Purolite CT 224 | 1.859 ± 0.152 |
| Dowex 50Wx4 | 1.900 ± 0.043 |
| Amberlyst 31 | 2.096 ± 0.092 |
| Dowex 50Wx2 | 2.677 ± 0.022 |
| Amberlyst 121 | 3.154 ± 0.031 |

The pattern of volume distribution among the five discrete fractions of macroreticular resins, gel-type ones and chlorinated macroreticular ones is displayed in Fig. 2.1, 2.2 and 2.3, respectively. Concerning standard macroreticular resins (see Fig. 2.1); the main volume fraction is in the densest zone, 1.5 $nm^{-2}$ zone, poorly accessible. As an exemption, Amberlyst 39 presents its main volume fraction in the 0.8 $nm^{-2}$ zone. This behaviour is explained by the lower DVB content (8%) than those of common macroreticular resins (12-20%). In addition, it is clearly observed a trend between $V_{sp}$ and DVB content: as higher is the DVB content in the polymer structure, lower the ability to swell is. Accordingly, $V_{sp}$ values follows this trend: high-crosslinked (Amberlyst 15, 35 and 48) < medium-crosslinked (Amberlyst 16 and 36) < low-crosslinked (Amberlyst 39).

The difference among resins with the same crosslinking degree is the sulfonation degree, Amberlyst 15, 16 and 39 are conventionally sulfonated resins, whereas Amberlyst 35, 36 and 48 are oversulfonated ones (see Table 1). It is expected that oversulfonated resins have a stiffer structure. This fact is observed for the $V_{sp}$ values of Amberlyst 35 and 48, lower than that of their homologue Amberlyst 15, as well as for the gel-type resins Purolite CT 124 (conventionally sulfonated) and Purolite CT 224 (oversulfonated). Nevertheless, this trend is not observed between the medium-crosslinked macroreticular resins (Amberlyst 16 and 36) and they show comparable $V_{sp}$ values.

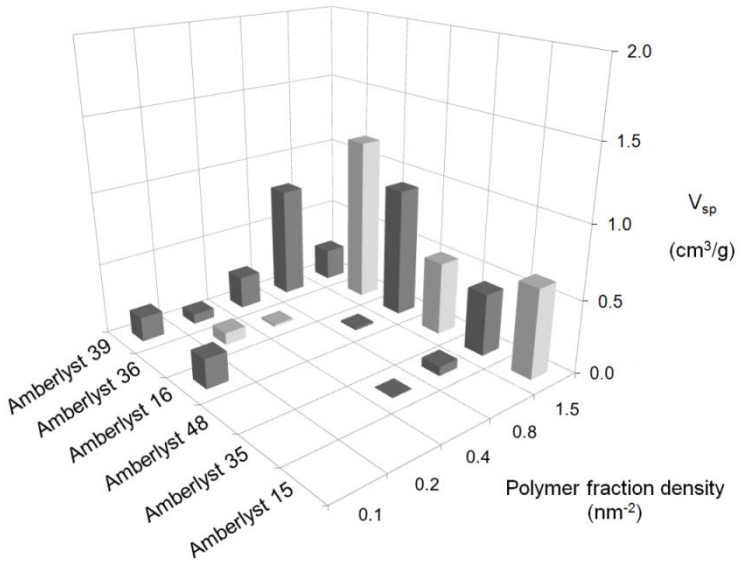


Fig. 2.1: ISEC gel-phase pattern of conventional macroreticular resins.

As for gel-type resins, $V_{sp}$ values are clearly higher than those of macroreticular catalysts (see Fig. 2.2). By comparing the $V_{sp}$ values of the gel-type resins, it is observed the same trend than in macroreticular ones: as lower is the DVB content higher the $V_{sp}$ value is. Thus, $V_{sp}$ values follows this trend: 8% DVB (Dowex 50Wx8) < 4% DVB (Purolite CT 124 and 224; Dowex 50Wx4 and Amberlyst 31) < 2 % DVB (Dowex 50Wx2 and Amberlyst 121). With regard to the distribution of the fraction density zones, Amberlyst 121 shows the least dense structure and it presents its main volume fraction density between 0.2-0.4 $nm^{-2}$. On the other extreme, Dowex 50Wx8 shows a high dense resin with a poor accessible gel-phase.

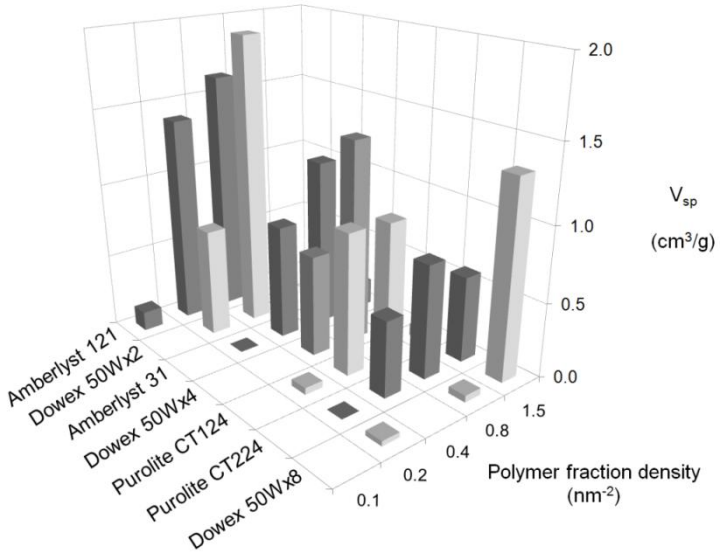


Fig. 2.2: ISEC gel-phase pattern of gel-type resins.

On the other hand, some macroreticular resins have chlorine atoms in its structure to improve their thermal stability [26], [30]. Amberlyst 70 presents a low dense gel-phase zone in the 0.4 $nm^{-2}$ zone (see Fig. 2.3). This high space between polymer chains is only comparable to gel-type catalyst as Dowex 50Wx2 and none of conventional macroreticular resin exhibits similar characteristics. Consequently, Amberlyst 70 is a highly suitable catalyst for polar environments. However in dry state its structure is almost completely collapsed. On the other hand, Purolite CT482 and Amberlyst XE804 show a more rigid gel-phase, and hence, their dry state structures are not collapsed. Thus, Purolite CT482 and Amberlyst XE804 are apparently more suitable thermal stable resins than Amberlyst 70 in lipophilic reaction mixtures.

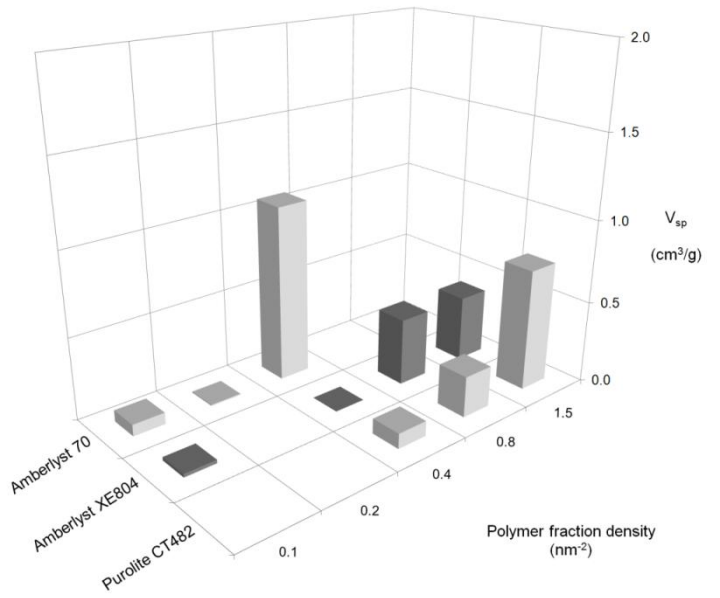


Fig. 2.3: ISEC gel-phase pattern of chlorinated macroreticular resins.

### 2.2.2 Others

Other catalysts tested include basic ion-exchange resins, acidic nafion, the zeolite H-BEA-25 and aluminas. They were supplied by Rohm and Haas (Amberlyst 26 OH, Amberlyst 21), Sigma (Nafion® NR 50, acid γ-Al2O3, basic γ-Al2O3) and Sudchemie (H-BEA-25). The main properties of tested basic resins are shown in Table 2.4. Both basic resins have macroreticular structure. Amberlyst 21 is a weak anion-exchange resin with high basic capacity, whereas Amberlyst 26 is a strong one with low basic capacity. Nafion® NR50 is a gel-type copolymer of Teflon® and perfluoro-alkanesulfonic monomers. Fluorine atoms of polymer chains upgrade thermal stability of NR50 and give a higher acid strength than PS-DVB resins but lower acid capacity (0.89 meq $H^+$/g).

Table 2.4: Properties of tested basic resins.

| catalyst | basic strength | type | basic capacity (meq $OH^-$/g) | $S_{BET}$ ($m^2$/g) |
|---|---|---|---|---|
| Amberlyst 21 | weak | macroreticular | 4.6 [41] | 35 [41] |
| Amberlyst 26 OH | strong | macroreticular | 2-2.6 [49], [50] | 30 [41] |

Properties of the zeolite (H-BEA-25) and two aluminas (γ-Al2O3) are presented in Table 2.5. Both aluminas were supplied as activated form. Tested inorganic catalysts presents relevantly lower acid or basic capacity than the polymeric ones. In contrast, the surface areas in dry state are higher, with H-BEA-25 leading.

Table 2.5: Properties of tested zeolite and aluminas.

| | H-BEA-25 | acid γ-$Al_2O_3$ | basic γ-$Al_2O_3$ |
|---|---|---|---|
| $SiO_2/Al_2O_3$ | 25 | | |
| Brönsted acid sites (meq $H^+$/g) | 1.2 | 0.46 | |
| Brönsted basic sites (meq $OH^-$/g) | | | 0.57 |
| $S_{BET}$ ($m^2$/g)[a] | 503 | 151 | 139 |
| $V_{pore}$ ($cm^3$/g)[a] | 0.663 | 0.255 | 0.265 |
| $d_{pore}$ (nm)[a] | 10.8 | 5.7 | 6.2 |
| $d_p$ (mm) | 0.008 | 0.105 | 0.105 |

[a] obtained from gas adsorption-desorption (described in section 2.3.3)

## 2.3 Apparatus and analysis

The experimental data on the synthesis of EOE were obtained from two different experimental devices, a batch and a fixed-bed reactor. Alternative devices used in this work are also presented.

### 2.3.1 Batch reactor

The first set-up consists in a 100-mL nominal stainless steel autoclave operated in batch mode. The temperature was controlled to within ± 0.1ºC by an electrical furnace. The pressure was set at 25 bar by means of $N_2$ to maintain the liquid-phase. A reactor outlet was connected directly to a sampling valve, which injected 0.2 µL of liquid into a GLC apparatus. Reaction was controlled by a computer with a designed LabView software program. A scheme of the experimental set-up is shown in Fig. 2.4.

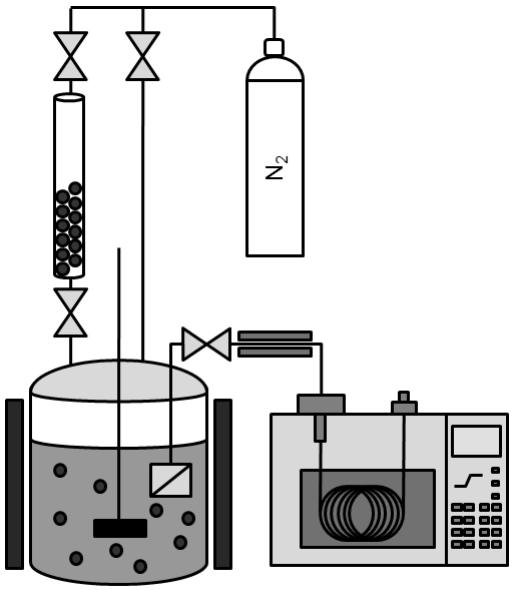


Fig. 2.4: Experimental set-up of the batch reactor.

Analyses were carried out by means of a HP-GLC apparatus equipped with a TCD. A 50m × 0.2mm × 0.5µm capillary column, methyl siloxane HP-Pona (Agilent), was used to separate and quantify the compounds present in the reaction mixture. The oven was temperature programmed to start at 50ºC with a 10ºC/min ramp up to 250ºC and held for 6 min. Helium (≥ 99.998%, Linde) was used as the carrier gas. All chemical species were identified by using a second GLC apparatus equipped with mass spectrometer GC/MS 5973 (Agilent) and chemical database software. In each set of experiments, standard samples of 5 mL have been prepared with different compounds proporcions and analyzed to correlate the chromatographic area with the weight percentage of the reaction medium.

### 2.3.2 Fixed-bed reactor

The second set-up consists in a 20-mL continuous fixed-bed reactor (PID Eng & Tech). The liquid mixture was pumped by a HPLC pump (Gilson 307). The pressure was set at 25 bar by means of a micrometric regulating valve to maintain the liquid-phase. The reactor bed consisted of resin homogeneously diluted with inert quartz (Chapter 6) or inert SiC particles (Chapter 7). The inert was used to keep the bed isothermal, and also to assure good contact between reactants and catalyst avoiding back-mixing and channelling. The temperature was controlled to within ± 1ºC by an electrical furnace. A scheme of the experimental set-up is shown in Fig. 2.5.

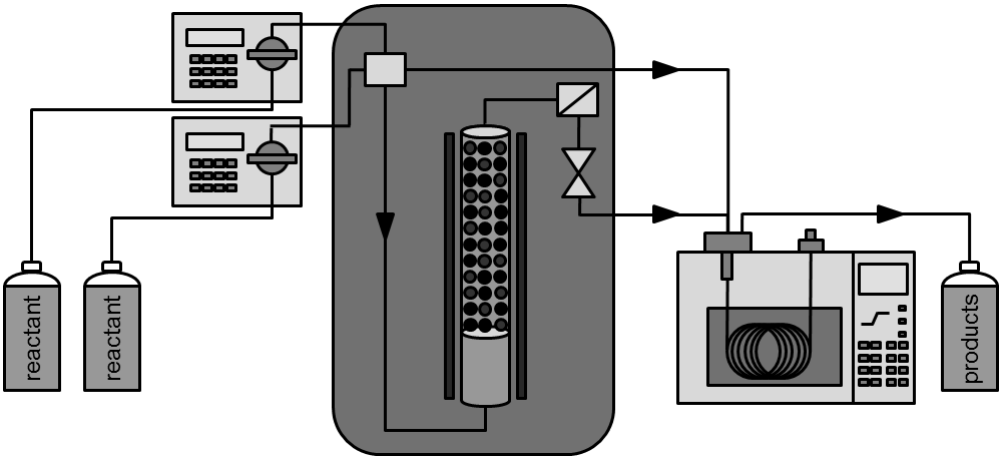


Fig. 2.5: Experimental set-up of the fixed-bed reactor.

Samples of liquid reaction medium were taken on-line from the reactor inlet and outlet. Their composition was determined in an HP6890A GLC (Hewlett Packard) equipped with TCD detector. A 50m × 0.2mm × 0.5µm capillary column HP-Pona (Agilent) was used to separate and quantify the compounds present in the reaction mixture. The oven was temperature programmed to start at 50ºC with a 25ºC/min ramp up to 250ºC and held for 6 min. Helium (≥ 99.998%, Linde) was used as the carrier gas. All chemical species were identified by a second GLC apparatus equipped with mass spectrometer GC/MS 5973 (Agilent) and chemical database software. In each set of experiments, standard samples of 5 mL have been prepared with different compounds proporcions and analyzed to correlate the chromatographic area with the weight percentage of the reaction medium.

### 2.3.3 Auxiliary devices

#### ISEC

The morphology of ion-exchange resins in a swollen state has been assessed by means of the ISEC technique. The ISEC apparatus consisted of HPLC pump (Waters 510), sampling valve, stainless steel column (4.27 $cm^3$) and a refractometric detector (Shodex RI-100). The detector signal was connected to a computer and the sampling data was synchronized with the mobile phase flow rate using a drop counter. Catalysts were crushed, sieved in swollen state ($0.250<d_p<0.125$ mm) and placed overnight in the mobile phase (0.2N $Na_2SO_4$). Then, the swollen catalyst was packed in the column by flowing the mobile phase during around 30 minutes (~5 mL/min). Later on, the filled column was placed in the apparatus. During the chromatographic measurements the standard solutes (deuterium oxide, sugars and dextranes) were injected independently (20 µL). Elution volumes were determined on the basis of the first statistical moments of the chromatographic peaks. And for each standard solutethe measurement was three times repeated for minimization and determination of the experimental error. At the end of the measurements, the catalyst was washed with distilled water, quantitatively extruded from the column dried overnight (T=110ºC), and finally weighted. Additionally, the swollen morphology of the starting polymer was also characterized by ISEC measurements using THF as the mobile phase and n-alkanes and polystyrenes as standard solutes.

For description of the true pores was used conventional model of cylindrical pores. Morphology of the swollen gel was described using the Ogston model defining pores as spaces between randomly oriented rigid rods representing the polymer chains. Instead pore diemeter, the pore size is then defined as polymer chain concentration in units of length per unit of volume. Model of the gel part of the polymer morphology was composed of five discrete fractions with the polymer chain density 0.1, 0.2, 0.4, 0.8 and 1.5 $nm^{-2}$. The ISEC data treatment was based on adjusting the volumes of the model fractions with the aim to minimize differences between experimental elution volumes of standard solutes and values computed on the base of the morphology model. A complete description of the procedure can be found elsewhere [33].

#### Distillation column

A 1 meter distillation column packed with Pall rings was used to purify ethyl octyl ether (Fisher Scientific). Pressure was set at 0.1 bar.

#### Karl-Fischer

A Karl Fischer automatic titrator (Orion AF8) was used to determine the water content of resins.

**Laser diffraction Size Analyzer**

Particle size of resins was measured in several media by means of a LS 13320 Laser Diffraction Particle Size Analyzer. Resins samples, previously dried at 110ºC at vacuum, were soaked for 2 days in the solvent to assure that resins were completely swollen by the solvent.

**Scanning Electron Microscopy**

The resin morphology and the homogeneity of the catalytic bed were examined by using Scanning Electron Microscopy (SEM) analysis (Hitachi H-2300). The samples were dried at 110ºC under vacuum overnight, and subsequently, sputtered with a thin gold layer before imaging.

**Gas adsorption-desorption**

Catalyst BET surface area ($S_{BET}$), pore volue ($V_{pore}$) and pore diameter ($d_{pore}$) in dry state was obtained by nitrogen adsorption-desorption at -196ºC (Accusorb ASAP 2020, Micrometrics). Kripton was used for surface areas < 1 $m^2/g$. $S_{BET}$ was obtained by BET method. $V_{pore}$ was obtained by the volume of gas adsorbed at relative pressure $(P/P_0)=0.99$. $d_{pore}$ was computed as $4V_{pore}/S$. The samples were previously dried at 110ºC under vacuum overnight.

Chapter 3

# Synthesis of ethyl octyl ether from ethanol and 1-octanol over acidic ion-exchange resins. A screening study

AN EXTENDED VERSION OF THIS CHAPTER HAS BEEN PUBLISHED IN:

C. Casas, J. Guilera, E. Ramírez, R. Bringué, M. Iborra and J. Tejero. Reliability of the synthesis of $C_{10}$–$C_{16}$ linear ethers from 1-alkanols over acidic ion-exchange resins. *Biomass Conversion and Biorefinery*. **2013**. 3 (1) 27-37.

## 3.1 Introduction

Linear symmetrical $C_{10}$-$C_{16}$ ethers can be synthesized by the bimolecular dehydration reaction of primary alcohols, such as 1-pentanol, 1-hexanol or OcOH over acid catalysts [22]. As these alcohols can be obtained from hydroformylation of linear olefins, this could be a way to upgrade $C_4$ to $C_7$ cuts from catalytic cracking. Moreover, some of these alcohols could be produced from renewable sources such as bioethanol or glucose. Corville et al. have reported EtOH dimerisation to butanol over MgO at 450ºC while Tsuchida et al. obtained butanol, hexanol and OcOH over nonstoichiometric hydroxypatite between 400-450ºC [51], [52]. Recently, promising works involving syntheses of such alcohols from biomass are being developed; Dekishima et al. engineered an Escherichia coli strain to obtain 1-hexanol from glucose, extending a previous work in which 1-butanol was efficiently synthesized from glucose in Escherichia coli [53].

Thus, glucose and bioethanol are potential raw materials to produce renewable additives for commercial gasoil. Co-etherification of alcohol with bioethanol is another way of introducing renewable materials into diesel. As an example, asymmetrical $C_{10}$ ethyl octyl ether (EOE) could be produced by reaction between EtOH and OcOH. Since the oil industry addresses efforts to introduce a given percentage of bioethanol to diesel market, EOE could be a way to incorporate bioethanol to diesel pool avoiding the problems of direct blending to diesel fuels. In this way, EOE and other ethers derived from EtOH can enhance the biofuel content in diesel blends without a reduction of the fuel quality.

Ion-exchange resins are efficient and selective in the dehydration of 1-pentanol to di-n-pentyl ether, 1-hexanol to di-n-hexyl ether and OcOH to DNOE. Thus, it seems likely that ion-exchange resins might be efficient catalysts in the co-dehydration between EtOH and OcOH. As a consequence, the aim of this chapter is to study the reaction in liquid-phase on a series of polymeric catalysts. The relationship between morphology and catalytic behaviour of tested resins is discussed.

## 3.2 Experimental procedure

Catalytic tests were performed in the batch reactor (described in section 2.3.1). Resins were previously dried at 110ºC for 3 h at atmospheric pressure and subsequently at 110 under vacuum overnight. Then, the reactor was loaded 1 g of commercial dried resin and 70 mL of alcohol mixture, OcOH and EtOH 1:1 molar ratio (57 g). The reaction mixture was pressurized to 25 bar by means of $N_2$ heated to 150ºC and stirred at 500 rpm. The time the mixture reached 150ºC was considered as zero time of the experiment. Heating time was about 20 min, and alcohol conversion at zero time was always less than 0.5 %. Liquid samples were taken out hourly and analyzed online to follow the reaction until the end of the experiment (6h). Working conditions were selected since, as quoted in literature, liquid phase reactions of dehydration of 1-pentanol and 1-hexanol to linear ethers take place at these conditions in the same set-up free

of external and internal mass transfer influences [26], [54]. In all the experiments, mass balance was accomplished within an accuracy of ± 5 %.

Alcohol conversion, selectivity to EOE, as well as molar and mass yield to EOE+DNOE relative to alcohol, was computed in each experiment by the following expressions,

$$X_{EtOH+OcOH} = \frac{\text{mole of alcohol reacted}}{\text{initial mole of alcohol}} \times 100 \quad [\%, \text{mol/mol}] \qquad \text{eq. 3.1}$$

$$S^{EOE}_{EtOH+OcOH} = \frac{\text{mole of alcohol reacted to form EOE}}{\text{mole of alcohol reacted}} \times 100 \quad [\%, \text{mol/mol}] \qquad \text{eq. 3.2}$$

$$Y^{EOE+DNOE}_{EtOH+OcOH} = \frac{\text{mole of alcohol reacted to form EOE and DNOE}}{\text{initial mole of alcohol}} \times 100 \quad [\%, \text{mol/mol}] \qquad \text{eq. 3.3}$$

$$Y'^{EOE+DNOE}_{EtOH+OcOH} = \frac{\text{mass of formed EOE and DNOE}}{\text{initial mass of alcohol}} \times 100 \quad [\%, \text{w/w}] \qquad \text{eq. 3.4}$$

Selectivity to the main side products DEE and DNOE were computed analogously as eq. 3.2. Definition of eqs. 3.1 and 3.2 are not the classical ones; however, they are used in order to quantify the combined amount of alcohol that reacts to produce EOE. Similarly, eq. 3.3 give the yield of long chain ethers (EOE + DNOE) obtained from the mixture of EtOH and OcOH. In addition, mass yield is defined in eq. 2.4 as the mass of long chain ether produced per mass of reactants loaded.

## 3.3 Results and discussion

### 3.3.1 Description of the reaction between OcOH and EtOH

Experiments showed that reaction between OcOH and EtOH yields EOE and water as products. In addition, DNOE and DEE were obtained as by-products from the intermolecular dehydration of two OcOH or two EtOH molecules, respectively (see Fig. 3.1). Intramolecular OcOH dehydration took place in very low extent since very small amounts (<0.05 % w/w) of $C_8$ alkenes (octenes) were detected, only in some experiments. However, intramolecular dehydration of EtOH did not take place since ethylene was not detected in any case.

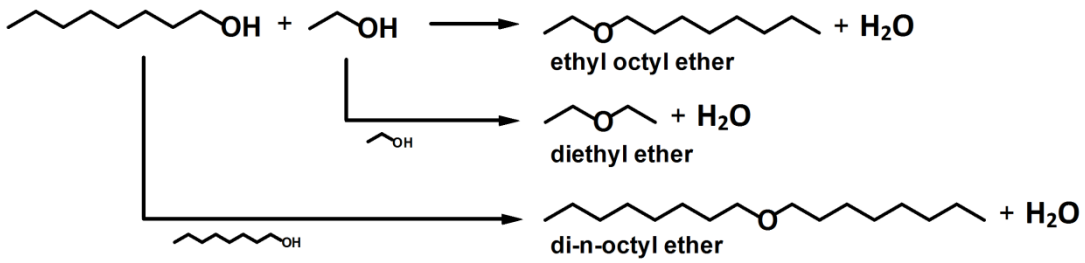


Fig. 3.1: Reaction scheme of EOE production from OcOH and EtOH.

Fig. 3.2 plots the composition distribution over Amberlyst 121, as an example. The etherification reactions proceeded smoothly from the beginning (DEE, EOE and DNOE); being EOE and DEE formed in similar amounts, and DNOE in lower amounts. Therefore, EtOH was much more reactive than OcOH. As observed, octenes were not detected over a gel-type resin such as Amberlyst 121. In fact, they were only detected over high-crosslinked macroreticular ones.

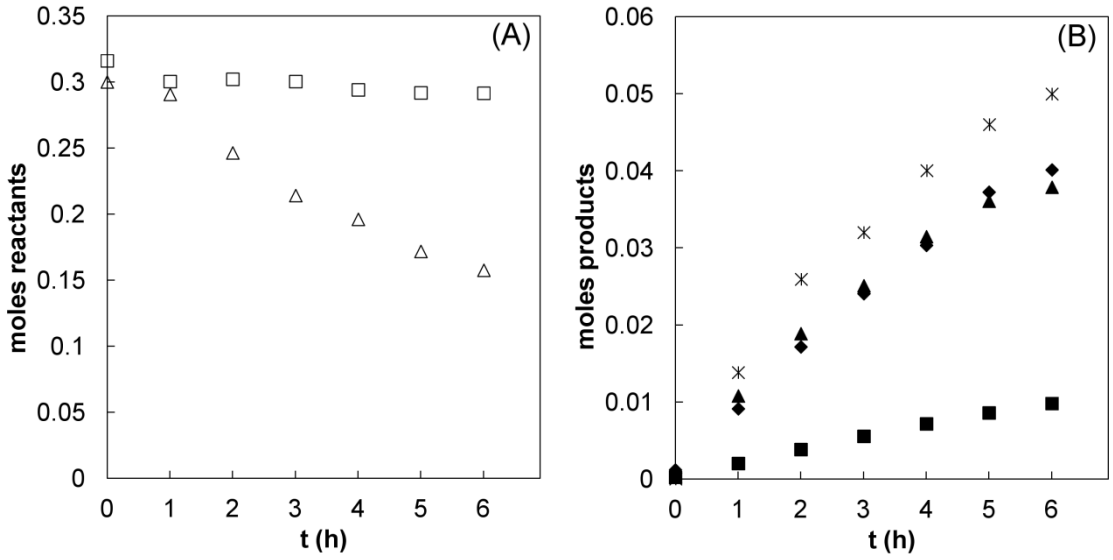


Fig. 3.2: Reactans (A) and products (B) profiles of OcOH and EtOH co-etherification over Amberlyst 121. T=150ºC, 500 rpm, W=1 g, $R_{OcOH/EtOH}$=1.
□ OcOH; ∆ EtOH; + water; ♦ EOE;▲ DEE; ■ DNOE.

The reaction was carried out over several acidic ion-exchange resins. As Fig. 3.3 shows, the favoured reaction was the formation of the ether with lower molecular weight, less bulky and hindered (moles DEE > moles EOE > moles DNOE). Unlike the reaction of dehydration of linear n-alkanols, the synthesis of EOE (15-46%) competes with the formation of DEE (43-83%) and DNOE (2-11%) as by-products, what explains the low selectivity to EOE compared to the quoted selectivity to symmetrical ethers from pure n-alkanols (57-99%) [22].

From an industrial standpoint, the differences between EOE, DNOE and DEE as possible candidates for diesel blends are relevant. DEE has a potential interest as a diesel compound because it is completely produced from (bio)ethanol. In addition, the cetane number of DEE is really high (~90) in comparison to that of EtOH (~8) or that of commercial diesel fuel (40–55) [55]. However, the high volatility of DEE is a serious drawback for its addition in large quantities to diesel blends. On the other hand, EOE and DNOE are linear long chain ethers with excellent properties as diesel components [16]. At present, production of EOE may be limited by the OcOH availability. In any case, the combined production of EOE and DNOE is useful for diesel blends.

### 3.3.2 Resin morphology influence on selectivity

Table 3.1 summarizes the results of the catalyst tests and Fig. 3.3 reveals that the ether distribution was highly related to the resin morphology. Long chain ethers (EOE and DNOE) were maximized using low-DVB content macroreticular resins and gel-type ones. On the contrary, the formation of DEE was highly favoured over medium and high-DVB content resins. Selectivity greatly depends on the morphology of ion-exchangers and the $V_{sp}$ was found to clearly influence the selectivity to long chain ethers. High and medium DVB% macroreticular resins have the lowest $V_{sp}$ values, in the range of 0.5-1.3 $cm^3/g$, whereas gel-type ones gather $V_{sp}$ values close to 2 $cm^3/g$ and even higher than 3 $cm^3/g$ in the case of Amberlyst 121. The higher combined selectivity to EOE and to DNOE were found on Amberlyst 70 (macroreticular, low DVB%), and gel-type resins Dowex 50Wx4 and Amberlyst 121 with selectivity values ranging from 41-46 % for EOE and 7-11 % for DNOE.

Table 3.1: Conversion of alcohol and selectivity to linear ethers.
T=150ºC, 500 rpm, $W_{cat}$=1 g, t=6h, $R_{OcOH/EtOH}$=1.

| catalyst | $X_{EtOH+OcOH}$ (%) | $S^{EOE}_{EtOH+OcOH}$ (%) | $S^{DEE}_{EtOH+OcOH}$ (%) | $S^{DNOE}_{EtOH+OcOH}$ (%) |
|---|---|---|---|---|
| Amberlyst 15 | 26.0 | 17.1 | 80.5 | 2.4 |
| Amberlyst 35 | 26.5 | 15.2 | 82.8 | 2.0 |
| Amberlyst 16 | 30.2 | 21.9 | 75.7 | 2.5 |
| Amberlyst 36 | 29.4 | 20.6 | 77.2 | 2.2 |
| Amberlyst 39 | 27.7 | 35.1 | 59.7 | 5.2 |
| Amberlyst 70 | 20.5 | 42.8 | 49.2 | 8.0 |
| CT 224 | 28.7 | 39.3 | 53.4 | 7.3 |
| Amberlyst 31 | 28.6 | 36.8 | 56.5 | 6.7 |
| Dowex 50Wx4 | 26.5 | 40.8 | 52.0 | 7.2 |
| Amberlyst 121 | 27.1 | 45.7 | 43.1 | 11.2 |

The behaviour of Amberlyst 70 should be highlighted as showed selectivity to EOE of 43%. Such selectivity value is comparable to gel-type PS-DVB resins, and quite higher than the other macroreticular resins. This fact can be explained because the distribution of gel-phase zones of different density of Amberlyst 70 is similar to that of gel-type resins, and spaces appeared in swollen state are wider than in macroreticular resins. It is clearly seen when it is compared to Amberlyst 39 morphology: despite having similar $V_{sp}$ values, gel-phase density of Amberlyst 70 is lower.

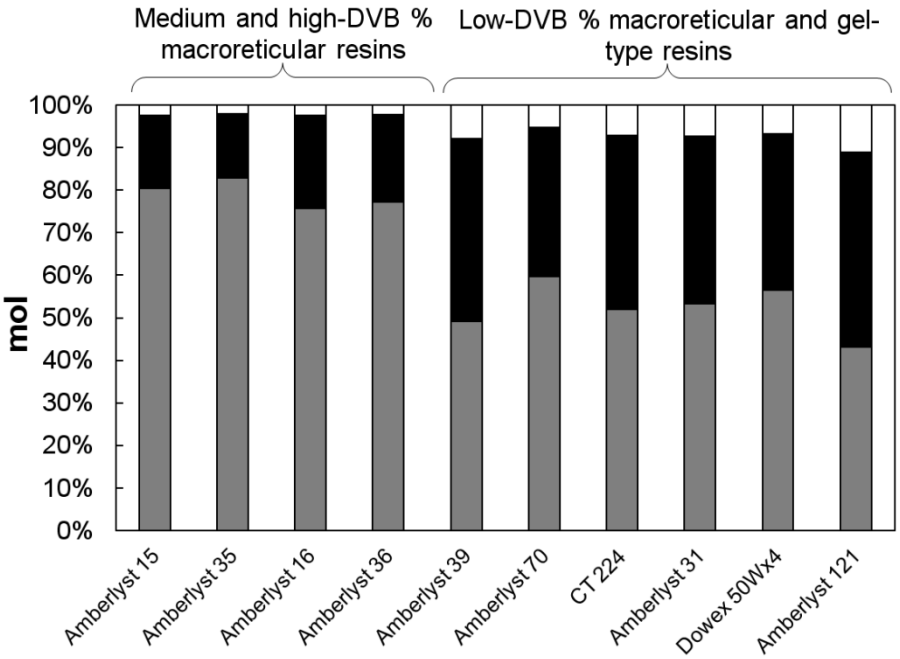


Fig. 3.3: Ether distribution of different ion-exchangers.
T=150ºC, 500 rpm, $W_{cat}$=1, t=6h, $R_{OcOH/EtOH}$=1. ■ DEE; ■ EOE; □ DNOE.

Selectivity values have been plotted in Fig. 3.4. Selectivity to long chain ethers (EOE and DNOE) is maximized by using resins with high $V_{sp}$ values. This behaviour can be explained by the fact that resins with low DVB% have a more flexible structure, and highly swell by the action of alcohols and the formed water according to their $V_{sp}$ values. The spaces between polymer chains of gel-type resins are wide enough to allow OcOH access more easily to acid centres compared to macroreticular resins, and in this way to compete efficiently with the EtOH for the acid sites. As Table 3.1 shows, Amberlyst 121 is the most selective to EOE, and in addition to DNOE, in such a way that combined selectivity to EOE and DNOE is higher than selectivity to DEE. On the contrary, the formation of the shortest ether, DEE, was clearly higher over high DVB% resins. In stiffer swollen resins such as Amberlyst 15 or 35 (macroreticular, high and medium DVB%), OcOH permeation is hindered whereas EtOH reach most of acid sites. As a result, DEE is preferably obtained in these macroreticular resins.

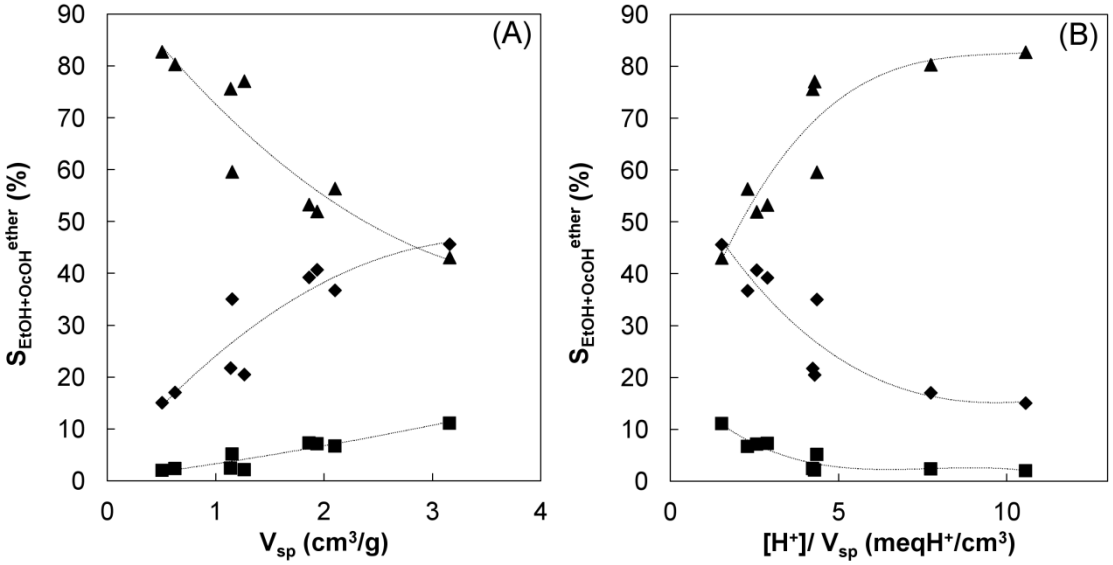


Fig. 3.4: Influence of $V_{sp}$ (A) and $[H^+]/V_{sp}$ on selectivity to linear ethers. T=150ºC, 500 rpm, $W_{cat}$=1 g, t=6h, $R_{OcOH/EtOH}$=1. ♦ $S_{EtOH+OcOH}^{EOE}$; ▲ $S_{EtOH+OcOH}^{DEE}$; ■ $S_{EtOH+OcOH}^{DNOE}$.

By comparing conventionally sulfonated and oversulfonated resins, it can be inferred from Table 3.1 that a higher acid capacity does not enhance the selectivity to long chain ether. In this way, from selectivities to EOE and DNOE of Amberlyst 15 and 35 or Amberlyst 16 and 36 it is observed that on Amberlyst 35 and Amberlyst 36 selectivity to long chain ethers was lower than on their conventionally sulfonated analogues. Moreover, since oversulfonated resins have higher acid strength than the other resins [30], it is drawn that dehydration to linear ether is favoured on the resins with less acid strength. Fig. 3.4B plot selectivity to linear ether against the parameter $[H^+]/V_{sp}$, sulphonic groups density per volume unit of swollen gel-phase. As seen, highly selective resins have low $[H^+]/V_{sp}$ values (Dowex 50Wx4; Amberlyst 31, 70 and 121), whereas the less selective Amberlyst 15 and 35 show high $[H^+]/V_{sp}$ values. As a result, DEE is formed over oversulfonated stiff resins in higher amounts than on their conventionally sulfonated analogues. Therefore, acid sites density per volume unit of swollen gel-phase would be an excellent guide to predict long chain ether formation.

### 3.3.3 Resin morphology influence on yield

Resin morphology has a decisive effect on the yield to EOE and DNOE. Amberlyst 121 gives the best results, followed by Amberlyst 31, CT 224 and Dowex 50Wx4. As a rule, lower yields were obtained over high and medium DVB% macroreticular resins (see Table 3.2). These resins maximized the production of DEE since their stiff structure is not able to accommodate longer molecules as easily as the more flexible structure of gel-type resins with 2-4 DVB% or the macroreticular ones with 8 DVB%. As a result, small ether molecules such as DEE are formed preferentially. By considering mass yields, more useful to evaluate immediately the industrial profit of the use of catalysts; for instance, working in batch-wise at 150ºC (500 rpm, catalyst loading 1.72%) on Amberlyst 121, it would be obtained 14.9 kg of a mixture of EOE and DNOE

at 6h per 100 kg of equimolar mixture of OcOH and EtOH. It is noted that EOE production from bioethanol has the drawback that a relevant quantity of EtOH is converted to DEE, which is much less attractive as a diesel component than EOE or DNOE.

Table 3.2: Conversion of alcohol and selectivity to linear ethers.
T=150ºC, 500 rpm, $W_{cat}$=1 g, t=6h, $R_{OcOH/EtOH}$=1.

| catalyst | $Y^{EOE+DNOE}_{EtOH+OcOH}$ (%, mol/mol) | $Y'^{EOE+DNOE}_{EtOH+OcOH}$ (%, w/w) |
|---|---|---|
| Amberlyst 15 | 5.1 | 4.9 |
| Amberlyst 35 | 4.6 | 4.4 |
| Amberlyst 16 | 7.3 | 6.9 |
| Amberlyst 36 | 6.7 | 6.3 |
| Amberlyst 39 | 11.1 | 10.7 |
| Amberlyst 70 | 10.4 | 10.2 |
| CT 224 | 13.4 | 13.0 |
| Amberlyst 31 | 12.5 | 11.9 |
| Dowex 50Wx4 | 12.7 | 12.3 |
| Amberlyst 121 | 15.4 | 14.9 |

It is expected than the gel-type resins not only give good ether yields at 150ºC but they were stable enough for industrial operation since they have been tested at a temperature very close to the maximum operating one [40], [41]. In reactions wherein water is released, hydrolysis of -$SO_3H$ groups by the action of water with liberation of $H_2SO_4$ and formation of sulphone bridges between chains is a reliable mechanism for ion-exchange deactivation [56]. However, kinetic runs performed on CT 224 heated at vacuum for more 80 h at 180ºC show an activity loss of only 2 % compared with fresh catalyst in the dehydration of 1-pentanol to di-n-pentyl ether [38]. So gel-type resins are quite attractive for industrial use: they offer good yields based on high selectivity in addition to reasonable thermal stability. It is to be noted that Amberlyst 70 has slightly low yields compared with Amberlyst 39. This fact is attributable to the low acid capacity (about 53 % of that of Amberlyst 39). However, Amberlyst 70 is highly selective and has high thermal stability. Based on selectivity and thermal stability it is clear that this resin is an attractive option for a future processes for obtaining $C_{10}$-$C_{16}$ linear ethers. As far as specific lifetime experiments and its possible regeneration among production cycles, stability studies on Amberlyst 70 can be found in the open literature for nonene oligomerization [57]. The activity of Amberlyst 70 was fully recovered after drying, indicating that loss of activity was caused exclusively by water inhibition and it was reversible. Thus, it is concluded that Amberlyst 70 would be an excellent catalyst for obtaining long linear ethers in industry. The possibility of working at temperatures as high as 190ºC at reliable reaction rates with good selectivity and reasonable thermal stability is significant.

## 3.4 Conclusions

EOE can be successfully formed from the reaction between OcOH and EtOH over acidic ion-exchange resins. However, selectivity to the asymmetrical EOE (15-46 %) is much lower than those of symmetrical ethers from pure alkanols (57-99 %). This is a result that EOE synthesis competes with the formation of DEE (43-83 %) and DNOE (2-11 %) as by-products.

The resin morphology is decisive to optimize the production to long chain ethers (EOE and DNOE). Selectivity to EOE is enhanced in gel-type and low-DVB% macroreticular resins since they have wide spaces in the swollen state, being Amberlyst 121 the most suitable in terms of yield maximization. Due to the high selectivity to ether and its high thermal stability, Amberlyst 70 is a very attractive catalyst for synthesize EOE.

Chapter 4

# Synthesis of ethyl octyl ether from diethyl carbonate and 1-octanol over solid catalysts

A REVISED VERSION OF THIS CHAPTER HAS BEEN PUBLISHED IN:

J. Guilera, R. Bringué, E. Ramírez, M. Iborra, J. Tejero. Synthesis of ethyl octyl ether from diethyl carbonate and 1-octanol over solid catalysts. A screening study. Applied Catalysis A: General. **2012**. 413-414 (31) 21-29.

## 4.1 Introduction

Chapter 3 proved that EOE can be successfully formed from the alcohol co-dehydration of OcOH and EtOH over acidic ion-exchange resins. Another promising green alkylation route to produce asymmetrical ethers is achieved with carbonates. Dimethyl carbonate has been proposed as methylating agent of several substances and reacts either as a methoxycarbonylating or as a methylating agent depending on the operation conditions [58]. In particular, the OcOH alkylation from dimethyl carbonate clearly showed to be more efficient than using directly methanol [59]. As dimethyl carbonate, DEC is generally accepted as an environmentally benign ethylating agent [60]–[64]. An advantage of using DEC with respect to dimethyl carbonate is that it can be obtained from EtOH (eq. 4.1). As a consequence, EOE would be a synthetic bio-fuel and could get the proper tax reduction, compensating partially their production costs higher than current commercial diesel.

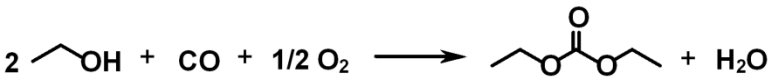


eq. 4.1

An industrial drawback to use alkyl carbonates is that their decomposition generates $CO_2$ as a by-product. However, the formation of carbonates from $CO_2$ is an interesting way for recycling it to fuels. Several advances in this direction have been reported and cyclic carbonate synthesis is already been industrialized [65]–[67]. Focused on linear carbonates, $CO_2$ reacts with alcohols in the presence of metal complexes (eq. 4.2). Due to the problems with the hydrolysis of the carbonate, 3 Á molecular sieves were used as drying agents to extract out the formed water. By using a dehydrative agent, an interesting dimethyl carbonate yield was achieved (55% based on methanol) and by-products were not significantly produced [68].

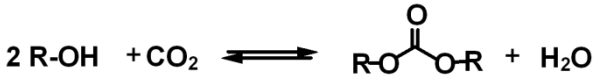


eq. 4.2

Chapter 3 revealed that EOE was synthesized successfully from EtOH and OcOH over acidic low-crosslinked resins at mild conditions (T=150ºC, P=25 bar). The present chapter is devoted to study the liquid-phase synthesis of EOE from DEC and OcOH over solid catalysts. A catalyst screening is carried out in order to select suitable catalysts for obtaining EOE.

## 4.2 Experimental procedure

Amberlyst 21 was previously converted to $OH^-$ form and both basic resins were first dried by methanol percolation [69], then in an oven at 80ºC for 3 h at atmospheric pressure and finally at 80ºC under vacuum overnight. Acidic resins were dried at 110ºC for 3 h at atmospheric pressure and subsequently at 110ºC under vacuum overnight. The residual water content of dried resins was determined by a Karl Fisher titrator (Orion AF8). Analytical volumetric titrations showed <3% (w/w) of residual water in the tested resins. Otherwise, H-BEA-25 was activated at 500ºC and both aluminas were treated at 300ºC in an atmospheric oven; subsequently dried at 110ºC under vacuum overnight.

Catalytic tests were performed in the batch reactor (described in section 2.3.1). The reactor was loaded with 70 mL of OcOH / DEC mixture, heated up to the desired temperature and stirred at 500 rpm. A molar ratio of $R_{OcOH/DEC}$ = 2 was used. Pressure was set at 25 bar with $N_2$ to maintain the liquid-phase. When the mixture reached the working temperature, 2 g of dried catalyst was injected into the reactor from an external cylinder by shifting with $N_2$. Catalyst injection was taken as zero time. Temperature was set at 100ºC for basic resins (because of their low thermal stability), 150ºC for all the other catalysts. Resins were used with the commercial distribution of particles sizes, and zeolite and aluminas as a powder. Working conditions were selected since, as quoted in literature, liquid-phase reactions of dehydration of 1-pentanol and 1-hexanol to linear ethers take place at these conditions in the same set-up free of external and internal mass transfer influences [26], [54]. It is to be noted that molecular size of such alcohols and ethers is similar to that of DEC and EOE, respectively.

In each experiment, DEC conversion ($X_{DEC}$), selectivity to EOE ($S_{DEC}^{EOE}$) and yield to EOE with respect to DEC ($Y_{DEC}^{EOE}$) were followed hourly by eqs. 4.3, 4.4 and 4.5, respectively.

$$X_{DEC} = \frac{\text{mole of DEC reacted}}{\text{mole of DEC initially}} \times 100 \quad [\%\,,\ \text{mol/mol}] \qquad \text{eq. 4.3}$$

$$S_{DEC}^{EOE} = \frac{\text{mole of DEC reacted to EOE}}{\text{mole of DEC reacted}} \times 100 \quad [\%\,,\ \text{mol/mol}] \qquad \text{eq. 4.4}$$

$$Y_{DEC}^{EOE} = \frac{\text{mole of DEC reacted to form EOE}}{\text{mole of DEC reacted initially}} \times 100 = X_{DEC} \cdot S_{DEC}^{EOE} \quad [\%\,,\ \text{mol/mol}] \qquad \text{eq. 4.5}$$

Experiments performed on Amberlyst 21, Amberlyst 26 OH, H-BEA-25, Amberlyst 15, Amberlyst 35, Amberlyst 48, Amberlyst 46, Amberlyst 70, CT 224 and Dowex 50Wx2 were replicated two times to assure the reproducibility of the results. Thus, data shown in this chapter has a relative experimental error lower than 1.2% for $X_{DEC}$, 2.0% for $S_{DEC}^{EOE}$ and 2.6% for $Y_{DEC}^{EOE}$ (95% confidence level) at 8h of reaction time.

## 4.3 Results and discussion

### 4.3.1 Preliminary experiments

Blank experiments without catalyst were performed at 150ºC. The non-catalyzed reaction allowed only the carboxyethylation of OcOH to ethyl octyl carbonate (EOC) but in small amounts ($X_{DEC}$ = 6% at 6h) and always $X_{DEC}$ < 1% at the initial time. In addition, it is seen that decomposition of carbonates (DEC and EOC) was not significant in the absence of catalyst. On the other hand, decomposition of DEC to DEE was checked over Amberlyst 121. Results state that the acidic resin decomposes significantly DEC to DEE ($X_{DEC}$ = 17% at 6h).

### 4.3.2 Catalyst screening

Table 4.1 summarizes the results of the catalyst screening runs. In general, the runs carried out over basic resins and both aluminas showed that DEC reactivity was low; therefore the EOE synthesis was not relevantly achieved. In the case of basic resins, the low conversions were probably due to the low working temperature. Unlike basic catalysts, DEC conversion is improved over acidic catalysts. Specifically, the two types of catalysts that showed a relevant activity were acidic resins and the zeolite, although at the working temperature the higher yields were achieved over acidic resins. Similarly, zeolites were found to be less active catalyst to produce di-n-pentyl ether than acidic ion-exchange resins [70]. Nevertheless, H-BEA-25 is less active but more selective to EOE than CT 224 and it is to be mentioned that zeolites have been reported as suitable catalyst to produce linear fuel at a higher temperature range of 250-350ºC [71].

Table 4.1: Conversion and yield over some acidic and basic catalysts at 6h.
$R_{OcOH/DEC}$ =2, $W_{cat}$=2 g, 500 rpm.

| type | | catalyst | $X_{DEC}$ (%) | $S_{DEC}^{EOE}$ (%) | $Y_{DEC}^{EOE}$ (%) | T (ºC) |
|---|---|---|---|---|---|---|
| basic | resin | Amberlyst 26 OH | 10 | - | - | 100 |
| | | Amberlyst 21 | 11 | - | - | 100 |
| | alumina | γ-$Al_2O_3$ | 7 | 3 | 0.2 | 150 |
| acidic | resin | CT 224 | 92 | 34 | 31 | 150 |
| | | Nafion 50 | 60 | 32 | 19 | 150 |
| | zeolite | H-BEA-25 | 17 | 65 | 11 | 150 |
| | alumina | γ-$Al_2O_3$ | 6 | 4 | 0.2 | 150 |

Fig. 4.1 shows the liquid product distribution along time over CT 224 (Fig. 4.1A) and H-BEA-25 (Fig. 4.1B). In addition to EOE, DNOE, DEE, EtOH and EOC, other by-products were detected in low amount (<3% molar): water, di-n-octyl carbonate (DOC), olefins and branched ethers, not shown for the sake of clarity. As seen, the product distribution profiles showed quite different trends along time. Over H-BEA-25, all products increased its molar percentage with time and EOC was low along the experiment. On the contrary, on CT 224 a maximum in the concentration profile for EtOH and EOC was observed. As these products were consumed, the moles of EOE were increased steadily. It seems that on CT 224 transesterification to EOC is faster than its decomposition to EOE. This trend is opposite to that observed on the zeolite where EOC is decomposed as it is formed. As expected selectivity to EOE rise steadily through the experiment.

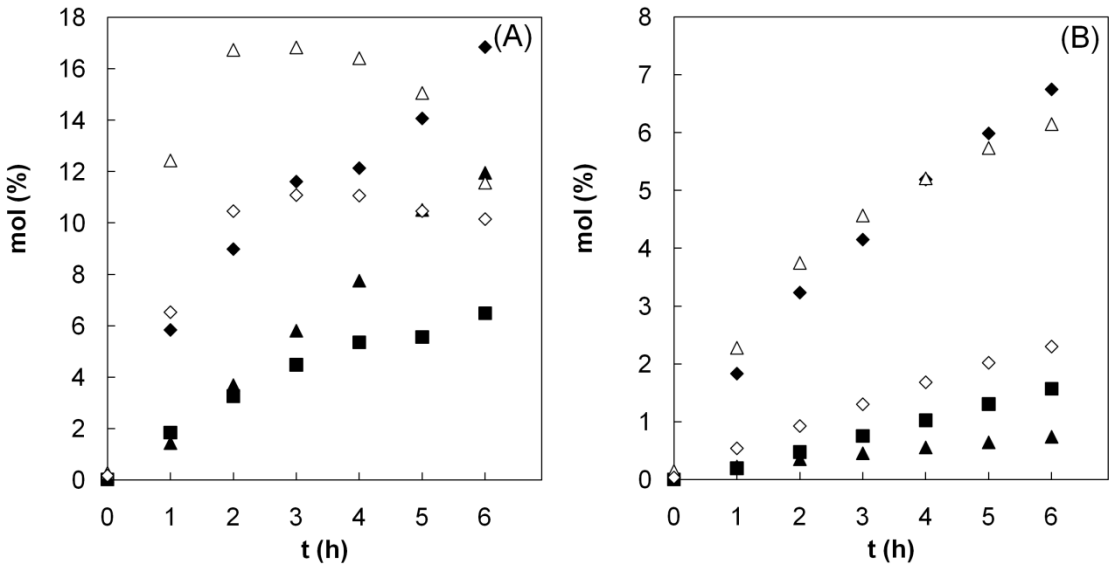


Fig. 4.1: Product distribution profile in liquid-phase along time over CT 224 (A) and H-BEA-25 (B). T=150ºC, $R_{OcOH/DEC}$ =2, $W_{cat}$=2 g, 500 rpm. Δ EtOH; ◊ EOC; ♦ EOE; ▲ DEE; ■ DNOE.

The EtOH and EOC profiles suggest the reaction scheme of Fig. 4.2, in agreement with those reported in open literature to synthesize ethers from dimethyl carbonate [59], [72]. EOE synthesis proceeds in two consecutive steps; the first (a) is the carboxylation of DEC to produce EOC and the second (b) the decomposition of EOC to EOE. The carboxylation step (a) would be kinetically favoured over acidic resins. However, reaction network is complex and the following side reactions take place in the reaction system:

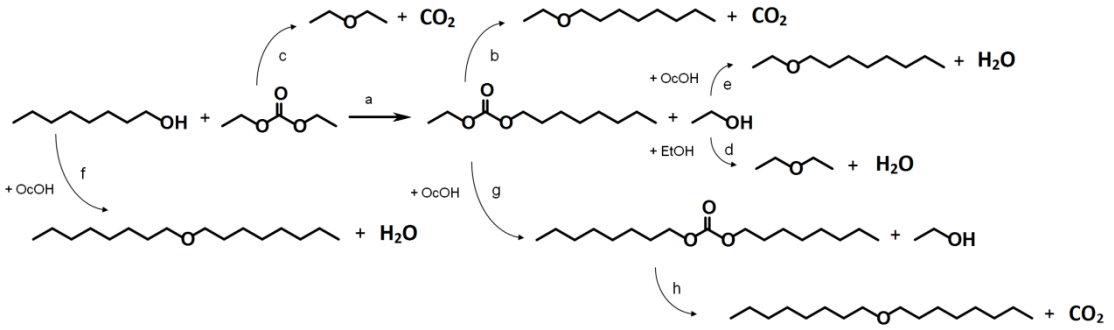


Fig. 4.2: Reaction scheme of EOE synthesis from DEC and OcOH.

(1) DEC decomposition to DEE (c), which is undesired because of the extra consumption of DEC. (2) Carboxyocthylation of EOC (g) and subsequent decomposition to DNOE (h) as revealed by the presence of DOC as by-product. (3) Additionally to carbonate decomposition routes, linear ethers can be also produced from alcohols dehydration (d, e, f), because water was detected in the mixture as by-product. Since the formed EtOH was partially dehydrated either with another EtOH (d) or with OcOH (e), it could be considered as an intermediate rather than a final product. As a result, the initial molar ratio (OcOH / DEC) would be an important factor to hinder the dehydration of EtOH to DEE and, as a consequence, to increase the selectivity to EOE [73].

As the preliminary catalyst screening revealed that the highest EOE yield was achieved over acidic PS-DVB resins on a catalyst weight basis, 13 resins of different morphology and acid capacity were tested for 8h. The product distribution trends for all acidic resin runs were similar to that shown in Fig. 4.1A and at 8h almost all DEC was converted to ethylated products. However, there was still a significant amount of the intermediate products (EOC and EtOH), which should be able to produce more EOE.

Table 4.2 shows DEC conversion, EOE selectivity and yield for tested acidic PS-DVB resins after 8h. As a general rule, gel-type resins show a better behaviour than macroreticular ones. It is also seen that in both gel-type and macroreticular resins EOE yield increases as the DVB% decreases, as a consequence of the higher DEC conversions and EOE selectivities observed. By comparing the macroreticular conventionally sulfonated resins Amberlyst 15, Amberlyst 16 and Amberlyst 39 resins with Amberlyst 46 it is seen that EOE yield on the last one is far smaller than on the other three resins, as expected because of the very low number of acid

sites of Amberlyst 46. The low EOE yield is mainly due to the very low DEC conversion since EOE selectivity of Amberlyst 46 is only a bit lesser. Amberlyst 15 has only about a 5% of $-SO_3H$ groups placed at the polymer surface (≈0.25 meq $H^+$/g) [74]. Since this quantity is a third of the acid capacity of Amberlyst 46 (sulfonated only at the polymer surface) it can be inferred that in macroreticular resins other than Amberlyst 46 the reaction takes place essentially in the gel-phase. Such gel-phase becomes active by the swelling of the polymer by permeation of alcohol and the retention of part of water released in the reaction.

Table 4.2: $X_{DEC}$ / $S_{DEC}^{EOE}$ / $Y_{DEC}^{EOE}$ (%) at 8h of acidic resins related to their structure type, DVB content and sulfonation degree. T=150ºC, $R_{OcOH/DEC}$=2, $W_{cat}$=2 g, 500 rpm.

| type | DVB (%) | conventional sulfonated | oversulfonated | surface sulfonated | chlorinated |
|---|---|---|---|---|---|
| macroreticular | High | 79.3 / 27.4 / 21.8[a] | 69.8 / 27.0 / 18.8[b] | 24.8 / 23.1 / 5.7[d] | |
| | | | 83.7 / 29.03/ 24.3[c] | | |
| | 12 | 85.4 / 32.5/ 27.8[e] | 91.7 / 29.6/ 26.9[f] | | |
| | 8 | 93.6 / 32.6 / 30.5[g] | | | 83.6 / 38.1/ 31.8[h] |
| gel-type | 8 | 90.9 / 33.2 / 30.2[i] | | | |
| | 4 | 91.7 / 32.1 / 29.5[j] | 95.0 / 34.9 / 33.1[k] | | |
| | 2 | 96.6 / 34.3 / 33.2[l] | | | |
| | | 95.8 / 34.6 / 33.2[m] | | | |

[a]Amberlyst 15, [b]Amberlyst 35, [c]Amberlyst 48, [d]Amberlyst 46, [e]Amberlyst 16, [f]Amberlyst 36, Amberlyst 39, [h]Amberlyst 70, [i]Dowex 50Wx8, [j]CT 124, [k]CT 224, [l]Dowex 50Wx2, [m]Amberlyst 121

Catalytic behaviour of Amberlyst 15, Amberlyst 16 and Amberlyst 39 can be explained looking at the structure of the swollen gel-phase. Gel-phase density of swollen resins decreases in the order Amberlyst 15 > Amberlyst 16 > Amberlyst 39. The number of accessible sites to the reaction in Amberlyst 39 is higher, and spaces between polymer chains allow OcOH and DEC to permeate and to accommodate better reaction intermediates. As a consequence, a higher DEC conversion and EOE selectivity is observed on Amberlyst 39. Similarly, Amberlyst 36 gives a better EOE yield than Amberlyst 35.

In the case of gel-type resins the higher EOE yield obtained on Amberlyst 121 and Dowex 50Wx2 are due to the fact that they show the higher $V_{sp}$ values. In this way they are more swollen in the reaction medium and, in addition, with a polymer density of 0.4 $nm^{-2}$ they give a better selectivity to EOE. Finally, by comparing data of Amberlyst 39 and Amberlyst 70, both resins conventionally sulfonated, it is seen that the latter shows a better EOE yield in spite of its acid capacity is about the half of that of Amberlyst 39. Although they have similar swollen gel-phase volume, Amberlyst 70 has lower polymer density of 0.4 $nm^{-2}$ than Amberlyst 39. Again, the wider spaces between polymer chains favoured the diffusion of OcOH and EOE as well as less steric restriction for the reaction intermediate.

However, the effect of the sulfonation degree is not clear because does not always upgrade the EOE yield (see Table 4.2). For instance, comparing among macroreticular resins with high percentage of DVB, whose amount of sulfonic groups decrease following Amberlyst 48 > Amberlyst 35 > Amberlyst 15, EOE yield did not reveal any direct effect of the sulfonation type. Likewise, the pairs Amberlyst 16 / Amberlyst 36 (macroreticular, 12 % DVB) and CT 124 / CT 224 (gel-type, 4% DVB) did not throw light on it. This behaviour could be explained by the fact that an extra sulfonation results in a higher number of acid centers but it also increases the stiffness of its structure. These two parameters have a contrary effect on the synthesis of EOE.

In order to state the influence of the resin structure on the catalytic behaviour, the effect of acid capacity and morphological parameters in swollen state on EOE yield was studied. Firstly, Fig. 4.3A plots the EOE yield versus the acid capacity. As shown, acid capacities of tested resins were similar (except for the particular resins Amberlyst 46 and Amberlyst 70) but they showed quite different activities in terms of EOE yield. It is also seen that gel-type resins gave higher yields than macroreticular ones at the same acid capacity, highlighting the significant role of the resin structure.

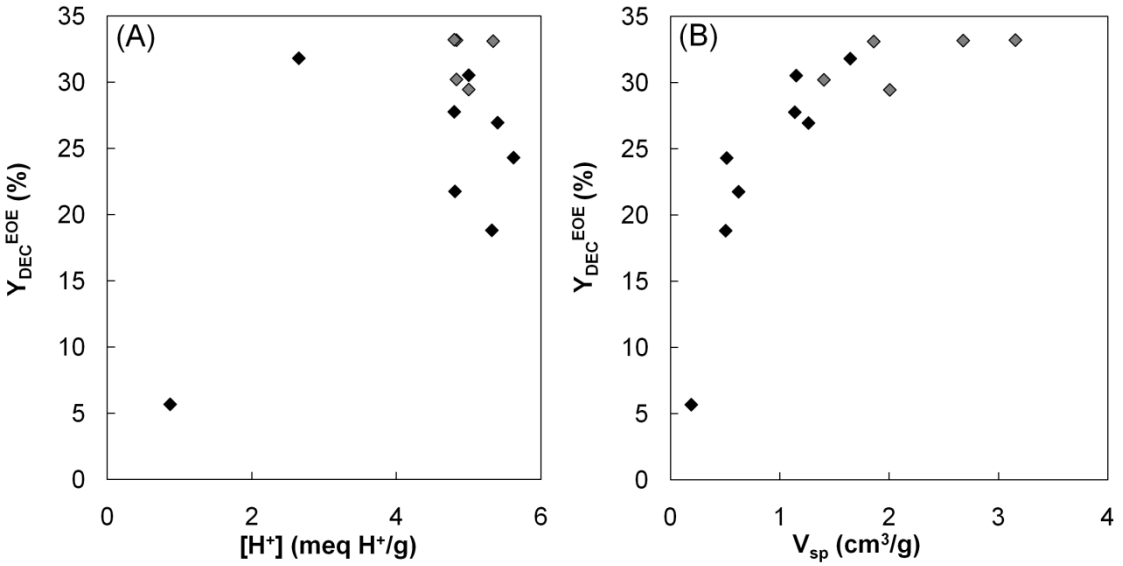


Fig. 4.3: Influence of resin acid capacity (A) and of $V_{sp}$ (B) on yield to EOE with respect to DEC at 8h. T=150ºC, $R_{OcOH/DEC}$=2, $W_{cat}$=2 g, 500 rpm. ♦Macroreticular; ♦Gel-type.

As mentioned above, $V_{sp}$ (specific volume of swollen polymer) is a parameter that allows knowing how much the resin swells in the reaction medium. Fig. 4.3B shows the positive effect of $V_{sp}$ on the yield to EOE. It is seen that measured EOE yield increases with $V_{sp}$ until a plateau is reached for $V_{sp}$ values of 2 $cm^3/g$. Both in macroreticular and in gel-type resins as $V_{sp}$ increases density of polymer gel-phase decreases. As a result, gel-phase is flexible enough and it could accommodate better the reaction intermediates, and the higher space between the polymer chains allows large molecules such as OcOH to access easier to a larger number of

acid centers. Resins with low DVB content have lower polymer fraction density in a polar medium and higher $V_{sp}$. Fig. 4.4A illustrates that the yield increased on decreasing the DVB resin content. Accordingly, in order to obtain efficiently large molecules such as EOE, ion-exchange resins with $V_{sp}$ of 2 $cm^3/g$ or higher which correspond to resins with less than 8% of DVB are the most suitable. Between tested resins gel-type Amberlyst 121, CT-224 and Dowex 50Wx2 fulfil such requirements.

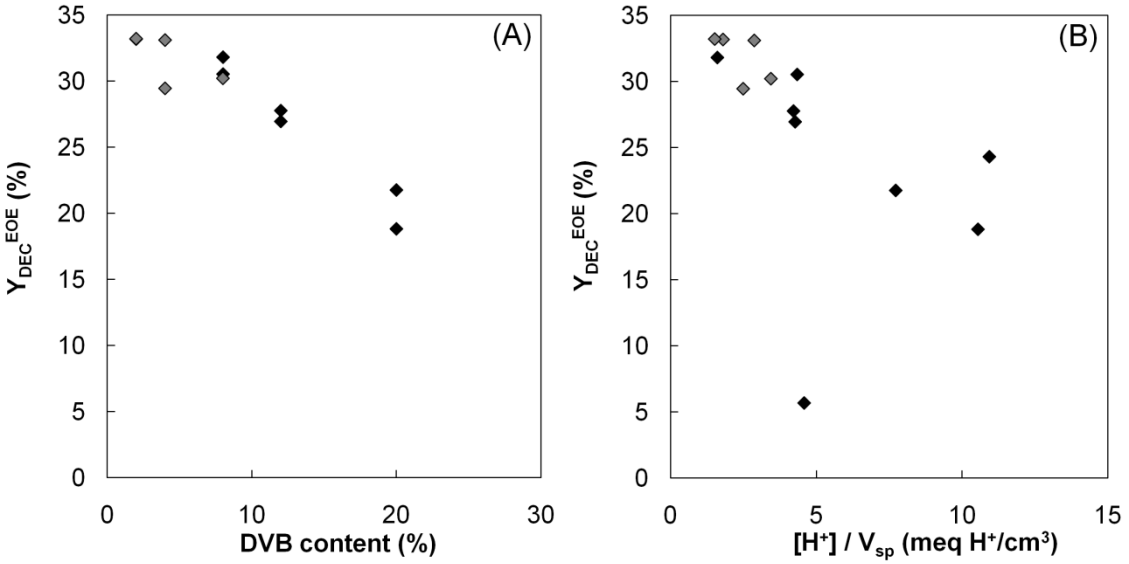


Fig. 4.4: Influence of resin DVB content (A) and of $[H+]/V_{sp}$ parameter(B) on yield to EOE with respect to DEC at 8h. T=150ºC, $R_{OcOH/DEC}$=2, $W_{cat}$=2 g, 500 rpm. ♦Macroreticular; ♦Gel-type.

Finally, a parameter that estimates the concentration of acid centers per volume unit in swollen polymer state is the $[H^+]/V_{sp}$ ratio (meq $H^+/cm^3$). Fig. 4.4B shows the influence of $[H^+]/V_{sp}$ on the synthesis of EOE. It is seen that measured EOE yield decreases on increasing $[H^+]/V_{sp}$. It is to be noted that neither Amberlyst 46 (with all acid sites in the polymer surface) nor Amberlyst 48 (the resin with the highest acid capacity but also the less swollen one) follow the general trend. It can be concluded that the higher EOE yields are given by resins with low density of acid centers in the swollen polymer volume (less than 3 meq $H^+/cm^3$) and acid capacities of about 5 meq $H^+/g$ or a bit higher. These requirements would be fulfilled by ion-exchange resins with high $V_{sp}$ values and preferably conventionally sulfonated. Between tested resins, Dowex 50Wx2, Amberlyst 121 and CT 224 show the higher EOE yields.

## 4.4. Conclusions

The catalyst screening revealed that EOE can be successfully produced in liquid-phase from DEC and OcOH over acidic catalysts at 150ºC. High DEC conversion and high EOE yield were achieved over acidic resins. A two-step pathway for EOE synthesis is proposed. Firstly, the transesterification of DEC to EOC takes place. Subsequently, EOC decomposes to EOE. Unfortunately, direct decomposition of DEC to DEE also occurs. Besides carbonate decomposition route, linear ethers are also produced from alcohols dehydration reactions.

The synthesis of EOE is highly related to morphological resins properties. The accessibility of large molecules to acid centers is favoured over resins with large space between polymer chains. Consequently, in order to synthesize large ethers such as EOE, a greatly expanded polymer network in swollen state is the most suitable resin property. It is also desirable that density of acid centers in the swollen resin would be low. These requirements can be found in low DVB content resins (e.g., gel-type resins as Dowex 50Wx2, Amberlyst 121 or CT 224).

Chapter 5

# Comparison between ethanol and diethyl carbonate as ethylating agents for ethyl octyl ether synthesis over acidic ion-exchange resins

A REVISED VERSION OF THIS CHAPTER HAS BEEN PUBLISHED IN:

J. Guilera, R. Bringué, E. Ramírez, M. Iborra and J. Tejero. Comparison between ethanol and diethyl carbonate as ethylating agents for ethyl octyl ether synthesis over acidic ion-exchange resins. **2012**. *Industrial & Engineering Chemistry Research.* 51 (50) 16525-16530.

## 5.1 Introduction

EOE can be synthesized successfully either by the dehydration reaction of OcOH and EtOH (Chapter 3) or by the transesterification reaction between OcOH and DEC to EOC and its subsequent decomposition to EOE (Chapter 4). However, to the best of our knowledge, comparison between EtOH and DEC as ethylating agents (EA) to give linear asymmetrical ethers is not found in the open literature.

EtOH and DEC are considered as environmentally friendly reactants. Still, since DEC is produced from EtOH [61], [62], [75], DEC use as ethylating agent would be justified only if higher selectivity and yield were obtained with respect to its counterpart, EtOH. Thus, the aim of this chapter is to compare the efficiency of EtOH and DEC as ethylating agents (EA) to produce EOE by the reaction with OcOH.

In former chapters it was revealed that highly swollen acidic resins are preferred on both reactions to catalyze efficiently EOE synthesis. Thus, the comparison between both EA was carried out over the low-crosslinked acidic PS-DVB resins Amberlyst 39 (macroreticular, with 8% crosslinking degree) and Amberlyst 121, Dowex50Wx2, CT 124, CT 224 and Dowex50Wx8 (gel-type with DVB% ranging from 2 to 8%). The two reaction pathways are compared and the influence of the initial reactants ratio and temperature are evaluated. By using low-crosslinked resins, the polymer expansion with a good liquid swelling is required to make acid sites accessible. Thus, the expansion of the polymer immersed in the reactants is checked.

## 5.2 Experimental procedure

The particle size of acidic ion-exchange resins were measured in several media. Dried samples were placed 2 days in different solvents to assure that the solvent was completely sorbed in the resin. Then, resins mean diameter was measured by means of a LS 13320 Laser Diffraction Particle Size Analyzer. Five solvents (DEC, EtOH, 1-pentanol, OcOH and water) and two mixtures ($R_{OcOH/DEC}$=2 and $R_{OcOH/EtOH}$=2) were used. Resin swelling which is the relative volume increase in the liquid media was calculated by eq. 5.1. V is the mean particle volume in the solvent or mixture, whereas the mean volume of reference, $V_0$, was obtained from measurements of dried resins in air. Volumes were calculated under the assumption that particles are spherical.

$$\text{Swelling} = \frac{V\text{-}V_0}{V_0} \times 100 \quad [\%] \qquad \text{eq. 5.1}$$

From swelling values**,** the amount of solvent moles into the polymer mass was estimated through equation 5.2, where $\rho_j$ and $M_j$ are the density and molecular weight of compound j, and $\rho_s$ the skeletal density of the resin [22]. This data permits estimating the number of molecules sorbed in each catalyst.

$$\text{Mole of solvent per gram of catalyst} = \frac{V\text{-}V_0}{V_0}\frac{\rho_j}{\rho_s}\frac{1}{M_j} \quad \left[\frac{\text{mole solvent}}{\text{g catalyst}}\right] \qquad \text{eq. 5.2}$$

Catalytic tests were performed in the batch reactor (described in section 2.3.1). Resins were dried at 110ºC for 3h at atmospheric pressure and subsequently under vacuum overnight. The reactor was loaded with 70 mL of OcOH / DEC or OcOH / EtOH mixture, heated up to the desired temperature and stirred at 500 rpm. Pressure was set at 25 bar with $N_2$ to maintain the liquid-phase. When the mixture reached the working temperature (130-150ºC), 2 g of dried acidic ion-exchange resin was injected into the reactor from an external cylinder by shifting with $N_2$. Catalyst injection was taken as zero time. It is worth mentioning that the experimental procedure, involving catalyst injection of 2 g of catalyst mass, is unified in this chapter for comparison purposes. Typical runs lasted 8h but long time experiments (48h) were also performed. Working conditions were selected to avoid external and internal mass transfer influence.

Experiments were replicated twice to ensure the reproducibility of experimental data. Conversion of the EA, selectivity, and yield to EOE with respect to EA was computed conventionally by means of eqs. 5.3, 5.4, and 5.5, respectively. Initial reaction rates of EOE synthesis were calculated from the experimental function of formed EOE moles versus time, by differentiating it at zero time (eq. 5.6).

$$X_{EA} = \frac{\text{mole of EA reacted}}{\text{mole of EA initially}} \times 100 \quad [\%\,,\,\text{mol/mol}] \qquad \text{eq. 5.3}$$

$$S_{EA}^{EOE} = \frac{\text{mole of EA reacted to form EOE}}{\text{mole of EA reacted}} \times 100 \quad [\%\,,\,\text{mol/mol}] \qquad \text{eq. 5.4}$$

$$Y_{EA}^{EOE} = \frac{\text{mole of EA reacted to form EOE}}{\text{mole of EA initially}} \times 100 = \frac{X_{EA} \cdot S_{EA}^{EOE}}{100} \quad [\%\,,\,\text{mol/mol}] \qquad \text{eq. 5.5}$$

$$r_{EOE}^{0} = \frac{1}{W_{cat}}\left(\frac{dn_{EOE}}{dt}\right)_{t=0} \quad \left[\frac{\text{mol}}{\text{h}\cdot\text{kg}_{cat}}\right] \qquad \text{eq. 5.6}$$

## 5.3 Results and discussion

### 5.3.1 Resin swelling

The increase of resin volumes in DEC, water and some alcohols is shown in Table 5.1. Resin swelling in each solvent was estimated by eq. 5.1. As seen, swelling in DEC is negative but that of Dowex 50Wx8. This fact can be explained because acidic resins are highly hygroscopic and quickly adsorb humidity from the air, masking in this way data measured in air. However, this fact also reveals that resins barely swell in DEC. On the contrary, resins greatly swell in alcohols and water, which agree with their high polarity.

Table 5.1: Resin swelling in different solvents measured by a Laser Diffraction Particle Size Analyzer.

| | | % swelling | | | | | | |
|---|---|---|---|---|---|---|---|---|
| **resin** | **$d_p$[a] (mm)** | **DEC** | **EtOH** | **1-pentanol** | **OcOH** | **water** | **OcOH/DEC[b]** | **OcOH/EtOH[b]** |
| Amberlyst 39 | 0.540 | -16 | 150 | 175 | 177 | 166 | 194 | 183 |
| Dowex 50Wx8 | 0.167 | 4 | 99 | 113 | 135 | 179 | 110 | 96 |
| Purolite CT 124 | 0.758 | -1 | 152 | 214 | 247 | 291 | 245 | 236 |
| Purolite CT 224 | 0.342 | -2 | 124 | 198 | 203 | 156 | 149 | 142 |
| Dowex 50Wx2 | 0.252 | -27 | 235 | 274 | 360 | 473 | 350 | 303 |
| Amberlyst 121 | 0.441 | -21 | 298 | 369 | 441 | 552 | 418 | 367 |

[a] Particle diameter in air in dry state. [b] $R_{OcOH/EtOH}$=2; $R_{OcOH/DEC}$=2.

In general, resins showed the highest swelling value in water. As for alcohols, the following swelling trend was observed: OcOH > 1-pentanol > EtOH, wherein measurements with 1-pentanol, an alcohol of molecular size intermediate between OcOH and EtOH, were carried out for the sake of comparison. Hence, the greater swelling corresponds to the bulkier alcohol, what suggests that interaction of the organic moiety of the alcohol with the polymer network also contributes significantly to resin swelling. As Table 5.1 shows, swelling of gel-type resins in the three alcohols increases as the DVB% of resins decreases. Thus, Amberlyst 121 and Dowex 50Wx2 (2% of DVB content) swell twice than CT 124 and CT 224 (4% of DVB), and between three and four-fold than Dowex 50Wx8 (8% of DVB) in the three alcohols. It is to be noted that swelling data for Amberlyst 39 is higher than those of Dowex 50Wx8 despite that both have 8% of DVB. It is likely due to the fact that gel-type resins develops only a porous structure by the swelling of the gel-phase, whereas the macroreticular resin also develops in the presence of solvents a non permanent pore structure in the mesopore range among the gel-type aggregates of the resin.

By comparing the pair CT 124 / CT 224 (gel-type resins with 4% of DVB) it is observed that the former (conventionally sulfonated) was able to swell around 1.5 times more than the latter (oversulfonated). This fact is a consequence of CT 224 has a slightly denser gel-phase (0.8 $nm^{-2}$) than that of CT 124 (1.5 $nm^{-2}$). Accordingly, from the swelling values it is also confirmed

that the effect of an oversulfonation treatment upgrades the polymer stiffness. As a result, despite the fact that oversulfonated PS-DVB resins have a higher number of acid centers, they have typically less accessibility to them (see chapter 3 and 4).

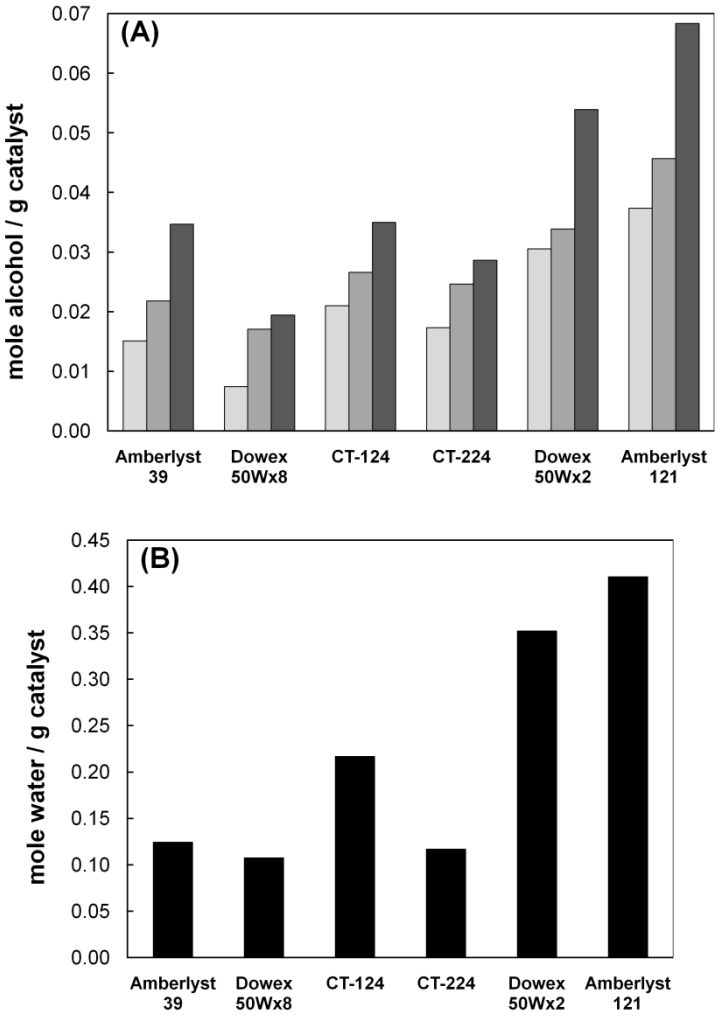


Fig. 5.1: Mole of sorbed alcohol (A) (■ OcOH; ■ 1-pentanol; ■ EtOH) and water (B) (■ water) per gram of dry catalyst.

On the other hand, the moles of solvent present in each resin in swollen state were estimated by eq. 5.2. Fig. 5.1 displays the solvent moles retained per gram of dried catalyst. As seen, it is retained much more water (Fig. 5.1B) than any alcohol (Fig. 5.1A) because of the higher polarity of water. Between alcohols, the number of moles retained in the resin follows this trend: EtOH > 1-pentanol > OcOH, in agreement with the alcohols polarity (dielectric constants: EtOH, 24.3 > 1-pentanol, 13.9 > OcOH, 10.9, respectively) [76]. On the contrary, as commented previously resin swelling showed the opposite trend: OcOH > 1-pentanol > EtOH. Consequently, the longest alcohol showed the highest swelling because of its molecular size, despite the amount of molecules sorbed is lower.

Moreover, particle size was measured in $R_{OcOH/EtOH}$=2 and $R_{OcOH/DEC}$=2 liquid mixtures (Table 5.1), representative of the mixture composition at the beginning of the EOE synthesis runs. Resin swelling in OcOH / DEC mixture shows similar values than those in pure OcOH what suggests that OcOH was preferably retained from the OcOH / DEC mixture. The little DEC-resin affinity aforementioned would be consistent with this observation. Thus, the concentration of DEC inside the swollen resin would be probably low. On the contrary, resin swelling in OcOH / EtOH mixture showed that into the polymer network could be a similar composition to the bulk solution.

### 5.3.2 Catalytic tests

As a function of the used ethylating agent, EtOH or DEC, two different pathways are displayed in Fig. 5.2. OcOH / EtOH system (Fig. 5.2A) consists in three competitive reactions (described in detail in chapter 3), while OcOH / DEC system (Fig. 5.2B) consists on a complex series-parallel one (described in detail in chapter 4).

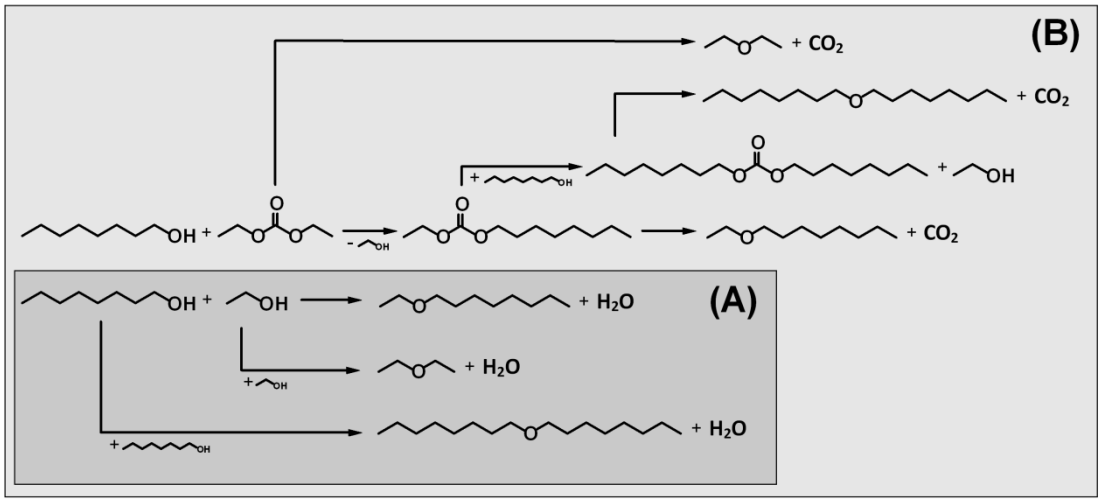


Fig. 5.2: Reaction scheme of EOE synthesis from OcOH and EtOH (A) and from OcOH and DEC (B).

Despite the differences in the two reaction networks, the efficiency as ethylating agents of EtOH or DEC to synthesize EOE is mainly affected by the loss of ethyl groups giving place to DEE formation. As a consequence, the initial molar ratio OcOH / EtOH ($R_{OcOH/EtOH}$) or OcOH / DEC ($R_{OcOH/DEC}$) might be an important factor to hinder DEE production, and at the same time favour that of EOE.

Experiments were carried out by varying the initial OcOH to EA molar ratio ($R_{OcOH/EA}$ = 0.5-2) at 150°C over Dowex50Wx2. Product distribution at 8h for OcOH / EtOH and OcOH / DEC systems is shown in Fig. 5.3A and 5.3B, respectively. It is to be noted that EtOH formed in OcOH / DEC runs was not plotted for the sake of clarity since it can be further dehydrated to DEE or else to EOE. As expected, EOE formation is highly influenced by the initial molar ratio OcOH / EA, and the production of the lower molecular weight ether was favoured (DEE > EOE > DNOE) for $R_{OcOH/EA} \leq 1$, DEE being the product formed in higher amount.

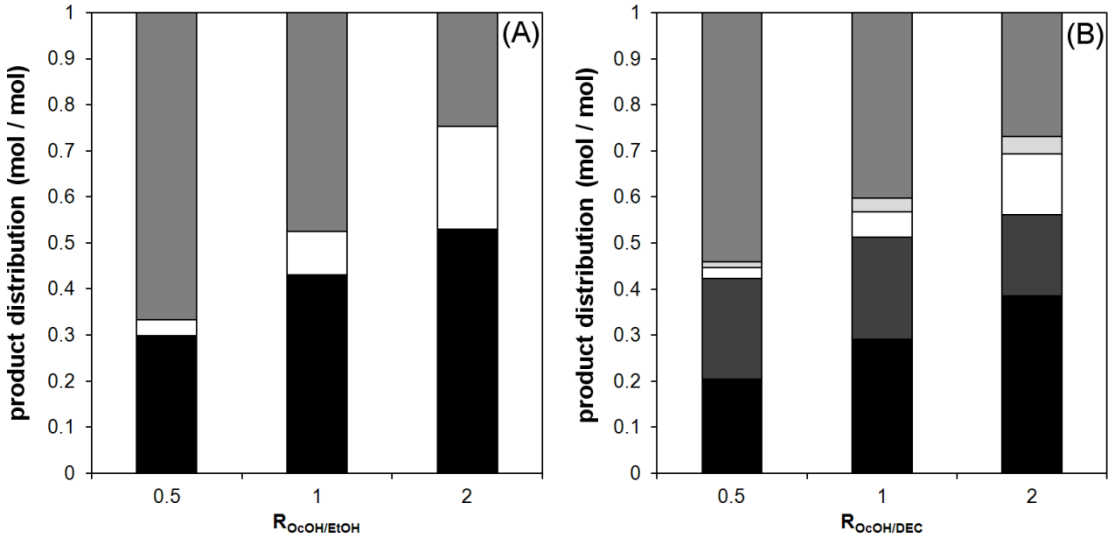


Fig. 5.3: Influence of $R_{OcOH/EtOH}$ (A) and $R_{OcOH/DEC}$ (B) on product distribution. Dowex 50Wx2, T=150ºC, $W_{cat}$=2g, t=8h. ■ EOE; ■ EOC; □ DNOE; ■ DOC; ■ DEE

As seen, the efficiency of EtOH or DEC as ethylating agents to synthesize EOE is mainly limited by the loss of ethyl groups giving place to DEE. At $R_{OcOH/EA}$ = 2, EOE is the main reaction product in the two systems, particularly in the OcOH / EtOH system. As a result, the loss of ethyl groups to form EOE is minimized when the limiting reactant is the ethylating agent, EtOH or DEC. Accordingly, further experiments were performed in OcOH initial excess ($R_{OcOH/EA}$ = 2).

Table 5.2: Yield to form EOE with respect to the ethylating agent. Dowex 50Wx2, T=150ºC, $R_{OcOH/EtOH}$= $R_{OcOH/DEC}$=2, $W_{cat}$ =2g, t=8h.

| catalyst | $Y^{EOE}_{EtOH}$ (%) | $Y^{EOE}_{DEC}$ (%) |
|---|---|---|
| Amberlyst 39 | 37.4 ± 0.8 | 30.5 ± 1.2 |
| Dowex 50Wx8 | 33.7 ± 0.2 | 30.2 ± 0.8 |
| Purolite CT124 | 37.0 ± 0.5 | 29.5 ± 1.3 |
| Purolite CT224 | 39.6 ± 1.4 | 33.1 ± 0.2 |
| Dowex 50Wx2 | 43.4 ± 0.4 | 33.2 ± 0.9 |
| Amberlyst 121 | 42.9 ± 0.9 | 33.2 ± 1.2 |

The six resins were tested in OcOH molar excess at 150°C (see Table 5.2). EOE yield was higher in the OcOH / EtOH system because the selectivity to EOE on all catalysts was always clearly higher in the OcOH / EtOH system than in the OcOH / DEC one. The products distribution at 8h is shown in Fig. 5.4A for the OcOH / EtOH system and in Fig. 5.4B for OcOH / DEC one. It is to be noted that for each reacting system selectivity to EOE was similar on the different catalysts. In this way, in the OcOH / DEC system EOE selectivity was a bit less than 40%, that of DNOE about 10%, and the DEE selectivity was close to 30%. EOC and DOC appeared in significant amounts particularly the first one. In the OcOH / EtOH system, EOE selectivity was about 50%, DEE selectivity was a bit higher than 25%, and that of DNOE was about 20%, but on Dowex 50Wx8, whose selectivity to DNOE was only about 15%, while selectivity to DEE rose to 35%.

Morphological analysis of ISEC data reveals that in the swollen gel-phase of Dowex 50Wx8 has a predominant zone of very high dense polymer (1.5 $mm^{-2}$). Amberlyst 39, CT 124, CT 224, Dowex 50Wx2, and Amberlyst 121 have zones of polymer density ≤ 0.8 $mm^{-2}$. From swelling data it is seen that OcOH and EtOH are present inside the resin from the start of the reaction, however some diffusion restriction could be advanced for OcOH. Moreover, steric restrictions would be higher for the long ethers EOE and DNOE than for shorter ether DEE. In the case of Dowex 50Wx8, this zone of higher polymer density probably causes more significant steric restrictions for bulky ether DNOE than the other resins, and would explain the distinct selectivity of this resin in the OcOH / EtOH system, as seen in Fig. 5.4A.

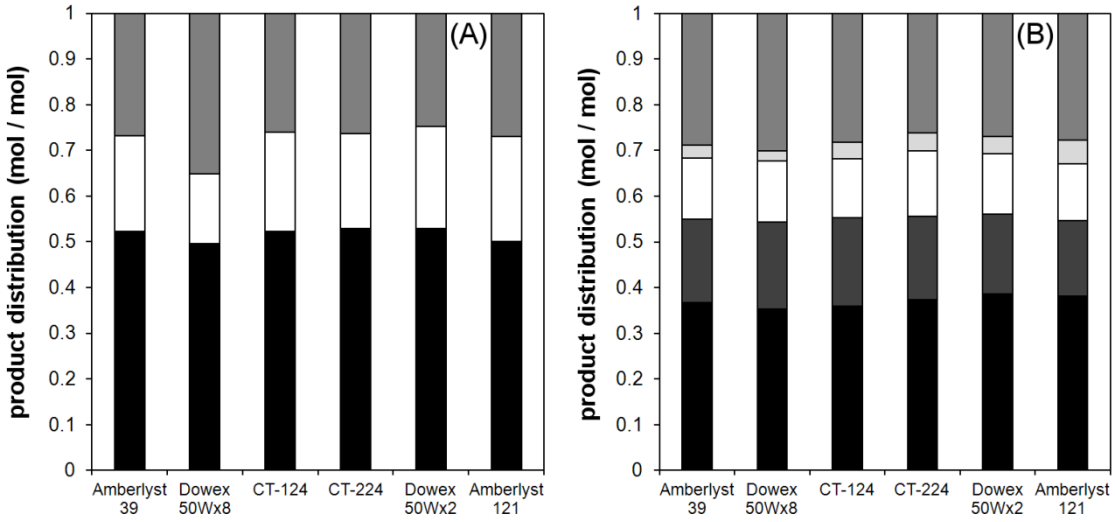


Fig. 5.4: Product distribution on tested catalysts from OcOH / EtOH (A) and from OcOH / DEC (B) feeds. Dowex 50Wx2, T=150ºC, $W_{cat}$=2g, t=8h. ■ EOE; ■ EOC; □ DNOE; ■ DOC; ■ DEE.

As for the OcOH / DEC system, swelling data point out that probably at short reaction times OcOH predominates inside the catalyst, however gel-phase morphology is flexible enough to allow OcOH and DEC to access more or less easily to acidic centers. As for reaction intermediates, EOC and DOC probable have similar steric restrictions than EOE and DNOE, respectively. Nevertheless, in the OcOH / DEC reaction system, morphology of the resins hardly influences their selectivity because, as seen in Fig. 5.4B, products distribution is very similar over all these catalysts although selectivity to EOE over Dowex 50Wx8 is something lower. As a consequence, to favour EOE production, ion-exchangers with polymer density ≤ 0.8 $mm^{-2}$ in the swollen state showed to be flexible enough to synthesize EOE in the two systems. Fig. 5.4 also shows that selectivity of Dowex 50Wx2 to EOE is slightly higher in both of them. In addition, Dowex 50Wx2 gives the best EOE yield after 8h reaction time (see Table 5.2).

Temperature influence on both reaction systems was checked in the range 130-150°C over Dowex 50Wx2, as it showed to be the most active catalyst. The products distribution shown in Fig. 5.5 suggests that selectivity to EOE in OcOH / EtOH reaction system was not significantly affected by the temperature (Fig. 5.5A), what indicates that the reaction rates of DEE, EOE, and DNOE formations have similar dependence on the temperature.

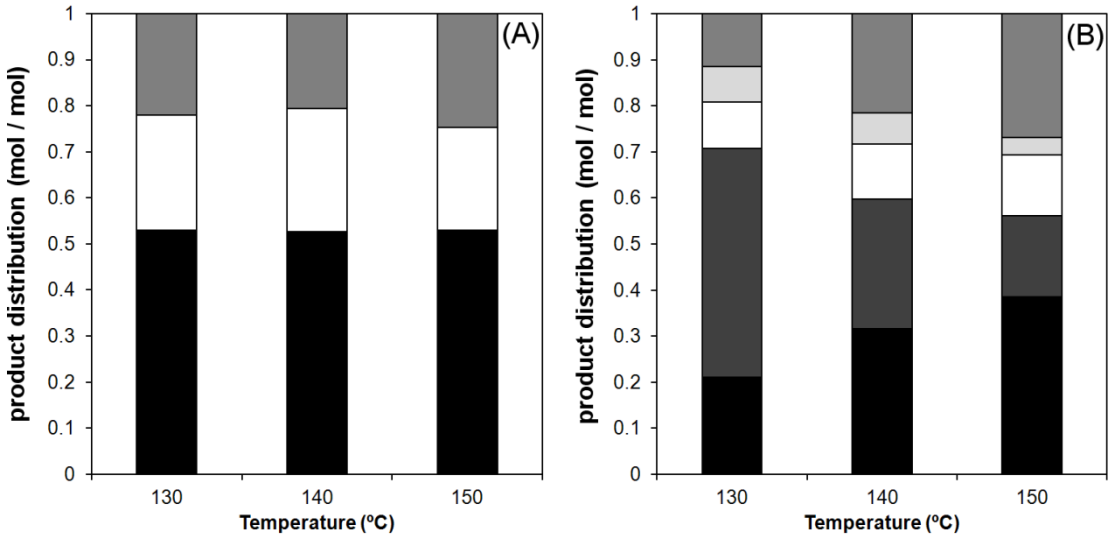


Fig. 5.5: Temperature influence on product distribution from OcOH / EtOH (A) and OcOH / DEC (B) feeds. Dowex 50Wx2, T=150ºC, $W_{cat}$=2g, t=8h. ■ EOE; ■ EOC; □ DNOE; ■ DOC; ■ DEE

On the contrary, in OcOH / DEC runs the products distribution changed drastically with temperature (Fig. 5.5B). Decomposition of carbonates (DEC, EOC, and DOC) to ethers (DEE, EOE, and DNOE, respectively) was more noticeable than the carboxylation of DEC to EOC on increasing temperature. As a result, DEC decomposition to DEE was more hindered at 130°C. However, a drawback to operate industrially at this relatively low temperature is that the reaction rate to form EOE would be around 5-fold lower than that at 150°C, as shown in Table 5.3. By comparing the behaviour of both ethylating agents, initial EOE reaction rates were always lower for OcOH / DEC system than for OcOH / EtOH one. This is probably due to the fact that

synthesis of EOE from DEC requires the formation and subsequently decomposition of EOC, whereas in the OcOH / EtOH system EOE synthesis is straightforward from the two alcohols.

Table 5.3. Initial reaction rates to form EOE. Dowex 50Wx2, T=150ºC, $R_{OcOH/EtOH}$= $R_{OcOH/DEC}$=2.

| | $r^0_{EOE}$ (mol / (h · $kg_{cat}$)) | |
|---|---|---|
| **T (ºC)** | **EtOH** | **DEC** |
| 130 | 1.91 ± 0.11 | 1.79 ± 0.10 |
| 140 | 4.74 ± 0.30 | 4.08 ± 0.15 |
| 150 | 9.94 ± 0.19 | 9.42 ± 0.61 |

### 5.3.2 Long time catalytic tests

Long time experiments were performed at $R_{OcOH/EA}$ = 2 to study the evolution versus time of DEC and EtOH conversion, EOE selectivity, and EOE yield with respect to ethylating agent of both reaction systems. DEC reacts faster than EtOH (Fig. 5.6A) in such a way that $X_{DEC}$ is about 97% at about 8h, whereas $X_{EtOH}$ is nearly 84%. However, at 48h both DEC and EtOH are almost depleted. In the OcOH / EtOH system, $S_{EtOH}^{EOE}$ increased quickly to 55% at 20 h; it further rises to 59% but very slowly (Fig. 5.6B). As for the OcOH / DEC system, probably because the EOC decomposition to EOE is slow, $S_{DEC}^{EOE}$ values lower than $S_{EtOH}^{EOE}$ ones were initially observed.

Nevertheless, when the intermediate EOC was almost entirely depleted (48h), similar selectivity and yield to EOE values were achieved in both reaction systems (Fig. 5.6B and 5.6C). Summarizing, similar potential selectivity and yields to EOE were obtained by using DEC or else by using EtOH in excess of OcOH at very large reaction times, but at a reaction time of a few hours the OcOH / EtOH system gave a higher EOE yield (Fig. 5.6C).

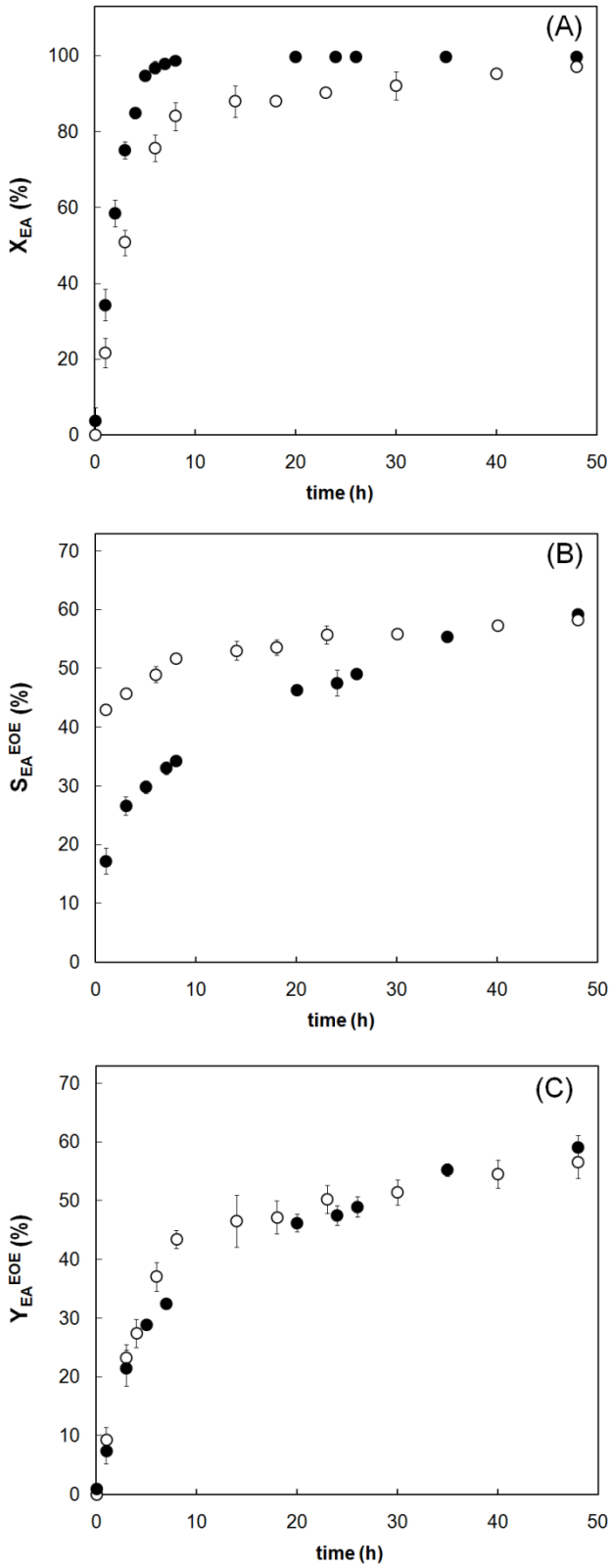


Fig. 5.6: Conversion (A), selectivity (B) and yield (C) to EOE with respect to the ethylating agent (○ EtOH; ● DEC). Dowex 50Wx2, T=150ºC, $R_{OcOH/EtOH}$= $R_{OcOH/DEC}$=2, $W_{cat}$=2g. The error bars indicate the confidence interval at a 95% probability level

## 5.4 Conclusions

EOE synthesis from OcOH / EtOH and OcOH / DEC mixtures over acidic ion-exchange resins is compared. The main secondary reaction in the two reaction schemes (and therefore the main drawback in industrial practice) is the loss of ethyl groups to produce DEE. As a consequence, selectivity to EOE with respect to ethylating agent (DEC or EtOH) is relatively low (40-50% at 8 h reaction time). The loss of ethyl groups by DEE formation is a serious problem since this ether cannot be blended straightforwardly in commercial diesel fuels.

Similar selectivities and yields to EOE were obtained at long reaction time (48h). Nevertheless, initial reaction rates to form EOE are slightly higher in the OcOH / EtOH system than in the OcOH / DEC one. Accordingly, EtOH was shown to be a more suitable ethylating agent to produce synthetic ethers biofuels such as EOE over acidic resins of low cross-linking degree. Otherwise, the EOE synthesis from OcOH and DEC is only competitive at long reaction times or, in continuous units, if oversized reactors are used.

Furthermore, the reaction between OcOH and EtOH gives water as a by-product, a nontoxic substance. It would be an environmentally friendly process, like the one based on the OcOH / DEC system (there is no net $CO_2$ production). In summary, the current availability of EtOH and the production of water as by-product suggest EtOH to be a suitable ethylating agent to produce long chained ethers such as EOE.

Chapter 6

# Thermal stability and water effect on ion-exchange resins in ethyl octyl ether production at high temperature

A REVISED VERSION OF THIS CHAPTER HAS BEEN REVISED AND RESUBMITTED IN:

J. Guilera, E. Ramírez, C. Fité, M. Iborra, J. Tejero. Thermal stability and water effect on ion-exchange resins in ethyl octyl ether production. *Applied Catalysis A-General*.

## 6.1 Introduction

A drawback of using sulfonic PS-DVB resins is their low thermal stability [40], [41]. In general, thermal deactivation by sulfonic groups leaching hinders their application at high temperature. With respect to EOE formation from EtOH and OcOH, the increase of the reactor temperature would not involve a loss of selectivity to EOE (chapter 5). Thus, the operating temperature of the reaction between EtOH and OcOH can be increased to obtain higher reaction rates, and therefore, a more competitive reaction unit. In contrast, when temperature is increased on the OcOH / DEC mixture higher amount of DEC is decomposed to DEE, involving a loss of selectivity (chapter 5).

Most PS-DVB resins are stable up to 150ºC, but the maximum operating temperature of some resins such as Amberlyst 15 is even lower (120ºC) [41]. In contrast, fluorinated polystyrene sulfonic resins like Nafion® can operate up to 210ºC, because fluorine atoms upgrade their thermal stability. In addition, they confer a higher acid strength that could contribute positively to the catalytic activity [26], [77]. Nevertheless, compared to PS-DVB resins, Nafion® has lower acid capacity and is more expensive (500-800 $/m$^2$), which are great disadvantages for industrial use [5]. New thermally stable PS-DVB resins Amberlyst 70 and Purolite CT482 have been recently commercialized to catalyze processes such as esterification, aromatic alkylation and olefin hydration at temperatures higher than 150ºC [40], [41]. In these resins, some hydrogen atoms have been substituted by chlorine. These additional electron withdrawing atoms increase the acid strength of ion exchangers and minimize the cleavage of the sulphur bond to aromatic carbon atoms up to 190ºC [30], [57], [79].

Besides, it is well-known that acidic resins suffer different morphological changes, and therefore catalytic performance varies, depending on the nature of reaction medium. Consequently, their catalytic activity is highly related to the properties of the reaction mixture [80]. In the presence of polar substances such as alcohols and water, non-permanent pores appear and diffusion of reactants towards the acid centres is enhanced [22], [26], [32]. However, in some reaction systems interactions between water and PS-DVB resin matrix have opposite effects: on one hand, water competes with reactants as it adsorbs strongly on the sulfonic groups [81]–[85]; on the other hand, as water is a polar compound, it contributes to open the resin backbone, what enhances the accessibility of reactants to acid centres. In addition, depending on the water amount, the catalytic mechanism can change from concerted to ionic which are slower. In industrial reaction units, the best resin performance takes place at low water contents (0.1-3 mol water/L) where sulfonic groups are partially dissociated [86].

The aim of this chapter is to evaluate the thermal stability of chlorinated resins, as well as the effect of water on their catalytic performance, in the temperature range 150-190ºC. Besides, their properties are examined and compared to those of conventional ones. The chlorinated PS-DVB resins Amberlyst 70, Amberlyst XE804, and Purolite CT482 have been used as catalysts. The PS-DVB resin Dowex 50Wx2 has also been used for the sake of comparison.

## 6.2 Experimental procedure

The experiments were performed in the fixed-bed reactor (described in section 2.3.2). Catalysts were dried overnight at 110ºC under vacuum (0.01 bar). Dry samples (0.1-0.7 g) were diluted in quartz (12-15 g). Reactor feed consisted of an OcOH-EtOH mixture ($R_{OcOH/EtOH}$ = 10). The large excess of 1-octanol was selected to promote the formation of 1-octenes, and in this way, to study the possible catalyst deactivation by carbon deposition. Water (1 w/w %) was added to the reactant mixture in some runs to stress its effect on the reaction rate without the liquid splitting off in two phases. The feed was preheated in a hot box at 80ºC and then fed to reactor at a flow rate of 0.25 mL/min. The reactor operated isothermally at 25 bars in the temperature range 150-190ºC to assure that the reaction took place in the liquid phase.

An additional series of experiments was performed to test the catalyst reusability. After 48 h on-stream, the reactor was cooled at room temperature. EtOH was fed at a flow rate of 2 mL/min were fed for 1 h to remove water and OcOH present in the resins. Subsequently, the catalysts were dried for 2 h in a 50 mL/min $N_2$ stream to remove EtOH. Catalysts dried in this way in the reactor were re-used in two times. It is to be noted that water content of fresh catalysts (2-4 w/w %) was some higher than the residual water content after the reactivating process (< 1 w/w % [87]).

Due to the small catalyst mass in the reactor bed, conversions were low ($X_{OcOH}$<10%, $X_{EtOH}$<25 %). Reaction rates to form EOE, DEE and DNOE were calculated by means of the following equations where it is assumed that the reactor operated in the differential regime:

$$r_1 = r_{EOE} = \frac{F_{OcOH}\, X_{OcOH}}{W_{cat}} S_{OcOH}^{EOE} = \frac{F_{EtOH}\, X_{EtOH}}{W_{cat}} S_{EtOH}^{EOE} \quad \left[\frac{mol}{h \cdot kg_{cat}}\right] \qquad \text{eq. 6.1}$$

$$r_2 = r_{DEE} = \frac{1}{2}\frac{F_{EtOH}\, X_{EtOH}}{W_{cat}} S_{EtOH}^{DEE} \quad \left[\frac{mol}{h \cdot kg_{cat}}\right] \qquad \text{eq. 6.2}$$

$$r_3 = r_{DNOE} = \frac{1}{2}\frac{F_{OcOH}\, X_{OcOH}}{W_{cat}} S_{OcOH}^{DNOE} \quad \left[\frac{mol}{h \cdot kg_{cat}}\right] \qquad \text{eq. 6.3}$$

$$S_j^k = \frac{\text{mole of j reacted to form k}}{\text{mole of j reacted}} \quad [\%\,, mol/mol] \qquad \text{eq. 6.4}$$

In these equations, $W_{cat}$ is the dry catalyst mass, $F_j$ the molar flow rate of species j fed into the reactor, $X_j$ the conversion of species j, and $S_j^k$ the selectivity of reactant j towards product k at the reactor outlet. The relative error by assuming differential behaviour of the fixed-bed reactor in eq. 6.1 was estimated to be lower than 5%, within the limits of the experimental analysis error.

Catalyst activity, $a_i$, for reaction i was defined as the ratio of the reaction rate at time t to the reaction rate for fresh catalyst, $r_i^0$ by means of Eq. 6.

$$a_i = \frac{r_i}{r_i^0} \qquad \text{eq. 6.5}$$

## 6.3 Results and discussion

The catalytic performance has been studied in the liquid-phase reaction between 1-octanol and ethanol. Experiments were carried out at 150°C and 190°C in the fixed bed reactor at a flow rate of 0.25 mL/min (WHSV = 17-120 $h^{-1}$), representative of the industrial case. They lasted 70 h to evaluate possible catalytic activity variation. Besides EOE, DEE and DNOE were formed. $C_8$ alkenes from 1-octanol dehydration were also detected, but in very small amounts (<1 w/w % at 190ºC; <0.25 w/w % at 150ºC). Results are gathered in Table 6.1.

Table 6.1: Reaction rates and activity at t=0 (fresh catalyst) and after 70 h on-stream $R_{OcOH/EtOH}$=10, q=0.25 mL/min, P=25 bar.

| T=150ºC | | | | | | | |
|---|---|---|---|---|---|---|---|
| catalyst | t (h) | $r_1 = r_{EOE}$ mol/(h·kg) | $r_2 = r_{DEE}$ mol/(h·kg) | $r_3 = r_{DNOE}$ mol/(h·kg) | $a_1$ | $a_2$ | $a_3$ |
| Purolite CT 482 | 0 | 2.89 | 0.442 | 3.08 | | | |
| | 70 | 2.55 | 0.328 | 2.88 | 0.89 | 0.74 | 0.94 |
| Amberlyst XE804 | 0 | 2.11 | 0.380 | 2.50 | | | |
| | 70 | 1.78 | 0.285 | 2.12 | 0.84 | 0.67 | 0.85 |
| Amberlyst 70 | 0 | 1.88 | 0.228 | 2.89 | | | |
| | 70 | 1.54 | 0.155 | 2.50 | 0.82 | 0.68 | 0.86 |
| Dowex 50Wx2 | 0 | 2.60 | 0.251 | 6.40 | | | |
| | 70 | 2.30 | 0.200 | 5.90 | 0.89 | 0.74 | 0.92 |
| T=190ºC | | | | | | | |
| catalyst | t (h) | $r_1 = r_{EOE}$ mol/(h·kg) | $r_2 = r_{DEE}$ mol/(h·kg) | $r_3 = r_{DNOE}$ mol/(h·kg) | $a_1$ | $a_2$ | $a_3$ |
| Purolite CT 482 | 0 | 28.2 | 4.58 | 35.8 | | | |
| | 70 | 23.0 | 3.31 | 33.0 | 0.82 | 0.73 | 0.89 |
| Amberlyst XE804 | 0 | 24.8 | 3.60 | 26.1 | | | |
| | 70 | 17.5 | 2.53 | 20.2 | 0.71 | 0.70 | 0.77 |
| Amberlyst 70 | 0 | 18.5 | 2.20 | 32.0 | | | |
| | 70 | 15.2 | 1.77 | 28.4 | 0.82 | 0.80 | 0.89 |
| Dowex 50Wx2 | 0 | 24.0 | 1.83 | 49.1 | | | |
| | 70 | 15.9 | 0.865 | 33.4 | 0.66 | 0.72 | 0.68 |

As Table 6.1 shows, although 1-octanol was in large excess in the reactor feed ($R_{OcOH/EtOH}$=10), reaction rates of EOE and DNOE syntheses were of the same order of magnitude on the macroreticular resins at 150ºC, whereas that of DEE was much lower. On gel-type resin Dowex 50Wx2, results are qualitatively similar, but the reaction rate of DNOE synthesis was about 3-fold higher than that of EOE, which is about 10-fold higher than reaction rate of DEE synthesis. For EOE synthesis, Purolite CT482 showed the highest reaction rate, followed by Dowex 50Wx2, Amberlyst XE804 and 70. As seen in Fig. 6.1, reaction rate of EOE synthesis decreased continuously with time; the same effect was observed for DNOE and DEE formation reactions. Activity decay for EOE synthesis was of the same order on all resins, by 12-18% with regard to the fresh catalyst. Decay for DNOE synthesis was of 6-15%, and for DEE synthesis it was of 25-35%.

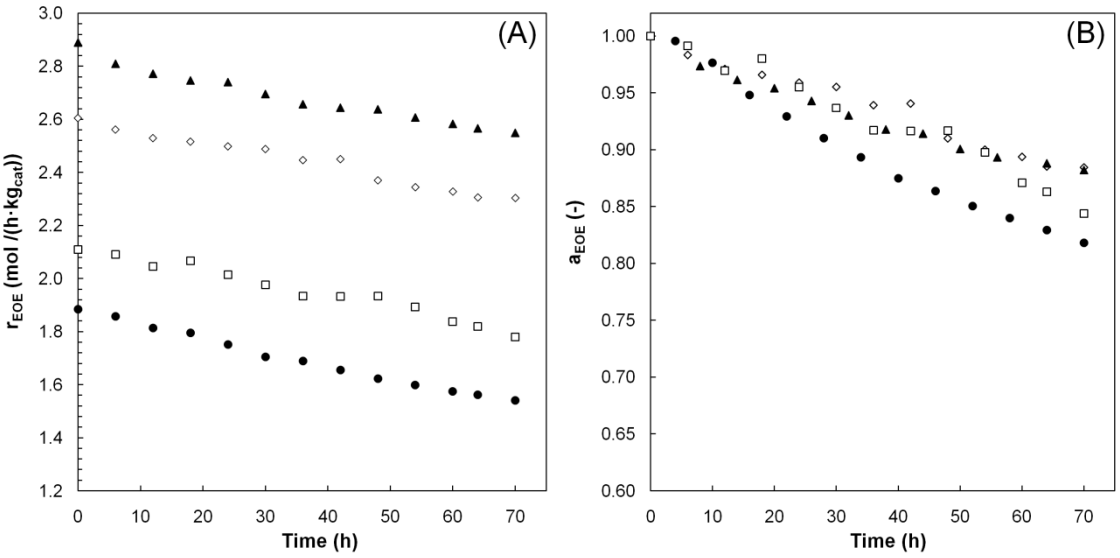


Fig. 6.1: Reaction rates (A) and activity (B) for EOE synthesis vs. time over tested resins at 150ºC. $R_{OcOH/EtOH}$=10, q=0.25 mL/min, P=25 bar. (▲CT482 ●Amberlyst 70 ◊ Dowex 50Wx2 □ XE804).

At 190ºC, Purolite CT482 was the most active resin for both EOE and DEE formation, followed by Amberlyst XE804, Dowex 50Wx2 and Amberlyst 70. Dowex 50Wx2 was the most active to DNOE formation. Among macroreticular resins, reaction rate of DNOE synthesis decreased in the order CT482, Amberlyst 70 and Amberlyst XE804. Activity decay for the three reactions also occurs and it is more noticeable on Amberlyst XE804 and Dowex 50Wx2. It is to be noted that a short period of constant activity was seen before decay starts (Fig. 6.2). As shown in Table 6.1, activity decay of EOE synthesis ranges from 18 to 34%, from 10 to 32% in DNOE formation and from 20 to 30% in DEE synthesis. In general, selectivity hardly changes with time.

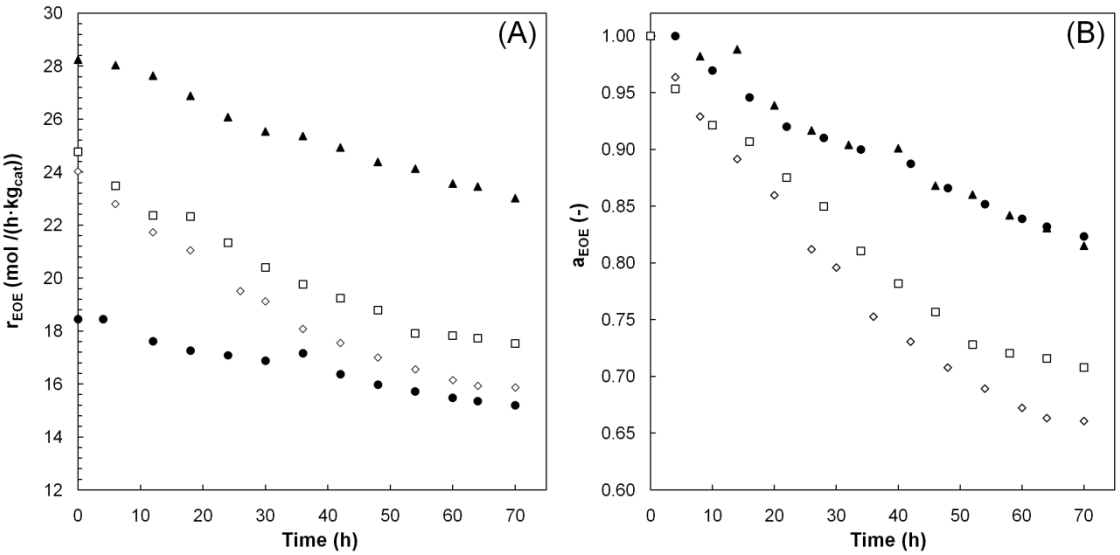


Fig. 6.2: Reaction rates (A) and activity (B) for EOE synthesis vs. time over tested resins at 190ºC. $R_{OcOH/EtOH}$=10, q=0.25 mL/min, P=25 bar. (▲CT482 ●Amberlyst 70 ◊ Dowex 50Wx2 □ XE804).

Apparent activation energies can be estimated by Arrhenius relationship from reaction rates at the two temperatures both on fresh catalysts and after 70h on-stream (Table 6.2). Apparent activation energies for the three reactions of ether formation are in the range 90-100 kJ/mol, what shows a high sensitivity to temperature. Apparent activation energies obtained for CT482 and Amberlyst 70 do not change with time, that of Amberlyst XE482 decreased moderately, and for Dowex 50Wx2 decreased by 10-15% with respect to the values found over fresh catalysts.

Table 6.2: Apparent activation energies for the reactions of ether formation at t=0 (fresh catalyst) and after 70 h on-stream. $R_{OcOH/EtOH}$=10, q=0.25 mL/min, P=25 bar.

| catalyst | t (h) | $E_{EOE}$ (kJ/mol) | $E_{DEE}$ (kJ/mol) | $E_{DNOE}$ (kJ/mol) |
|---|---|---|---|---|
| Purolite CT482 | 0 | 93 | 95 | 100 |
| | 70 | 90 | 94 | 99 |
| Amberlyst XE804 | 0 | 100 | 92 | 96 |
| | 70 | 93 | 89 | 92 |
| Amberlyst 70 | 0 | 93 | 92 | 98 |
| | 70 | 93 | 97 | 99 |
| Dowex 50Wx2 | 0 | 91 | 81 | 83 |
| | 70 | 79 | 74 | 71 |

Observed activity decays could be ascribed to several causes: 1) thermal instability of resins, 2) changes of activity caused by the interaction of the polymeric matrix with the water formed as byproduct, and/or 3) deposition of alkene oligomers on the resin surface.

### 6.3.1 Hydrothermal stability

Hydrothermal stability tests were carried out by adding bidistilled water to the reactor feed for 24h at the selected temperature. Afterwards, acid capacity was measured by titration and compared to that of fresh catalyst. The difference correspond to the lost of acid sites (Table 6.3). The conventional PS-DVB resin Dowex 50Wx2 retained acid capacity fully at 150ºC, but it greatly decreased at 190ºC, which is far above its maximum operating temperature. Amberlyst 70 and Purolite CT482 showed negligible desulfonation at 150°C and 190ºC, in agreement with the manufacturer's tests [40], [41]. These data confirm that introduction of chlorine atoms into the resin backbone improves its thermal stability. Finally, Amberlyst XE804 lost sulfonic groups at both temperatures, what indicates that it is not as suitable as the other two chlorinated resins for catalyzing high temperature processes.

Table 6.3: Acid sites loss by hydrothermal treatment at 24h. $q_{water}$=0.25 mL/min, P=25 bar.

| catalyst | T (ºC) | acid sites lost (%) |
|---|---|---|
| Dowex 50Wx2 | 150 | negligible |
| | 190 | 36.3 ± 8.5 |
| Amberlyst 70 | 150 | negligible |
| | 190 | negligible |
| XE804 | 150 | 4.0 ± 1.9 |
| | 190 | 16.2 ± 3.6 |
| CT482 | 150 | negligible |
| | 190 | negligible |

Since hydrothermal tests showed that resins retained the acid capacity at 150ºC, except for the slight desulfonation of Amberlyst XE804, the activity decay observed at this temperature cannot be ascribed to the loss of sulfonic groups by thermal instability. As a result, interaction with the reaction medium has to be considered. Activity drop at 190ºC after 70h on-stream agrees well with the higher leaching of acid groups found in hydrothermal experiments. Some differences in the activity decay of catalysts have been observed at this temperature which could be partly ascribed to their thermal stability. After 70h on-stream, the non-chlorinated resin Dowex 50Wx2 showed higher activity decay at 190ºC (34%) than at 150ºC (12%) for EOE synthesis. Similar decays have been found in DNOE synthesis (32% at 190ºC, and 8% at 150ºC). The decay found at 190ºC is of the same order of sulfonic group leaching and could be explained because its low maximum operating temperature is 150ºC. Similarly, activity decay of Amberlyst XE804 at 190ºC (29%) was almost twice that observed at 150ºC (16%) for EOE synthesis, whereas for DNOE synthesis decays are 23% at 190ºC and 15% at 150ºC. For both catalysts, activity decay in DEE synthesis is of the same order at both temperatures

Some inferences about the water influence on the leaching of sulfonic groups can be drawn by comparing acid capacity loss in hydrothermal experiments and activity decay. Sulfonic group leaching rate in PS-DVB resins is not uniform; the most active sites are lost faster [56]. As a result, the early loss of a small number of acid sites should cause a high drop on the catalytic activity. Data show that the active sites loss after 24 h in water stream was equivalent to the activity drop after 70 h in the alcohol stream for Dowex 50Wx2 and Amberlyst XE804. As a result, sulfonic group hydrolysis seems to be faster in water than in alcohols, in agreement with the open literature [88]. However, since activity decay is much higher than acid sites leaching on the two catalysts at the low temperature of explored range, other causes than desulfonation have to be taken into account to explain activity drop.

Over Purolite CT482 and Amberlyst 70, catalytic activity decay at 150°C and 190°C is similar for the three reactions, especially on Amberlyst 70. As desulfonation was not observed in the hydrothermal stability experiments with these resins, activity decay cannot be accounted for sulfonic groups leaching. Instead, it could be attributed to carbon deposition by chemical species present in the reaction medium, particularly $C_8$-alkene oligomers. $C_8$ alkenes formation rose by 6-fold from 150ºC to 190ºC, but the catalytic activity decay was of the same order at both temperatures, what excludes such relationship. On the other hand, it can be assumed that the formed ethers (DEE, EOE and DNOE) do not deactivate the catalyst as their effect on the reaction rate was found to be negligible in ether syntheses as in that of di-n-pentyl ether from 1-pentanol previously studied [89].

### 6.3.2 Reusability tests

Accordingly to literature, activity decay of thermally stable resins in alcohol dehydration reactions can be ascribed to the preferred adsorption of the water formed in the reaction on active sites [57], [81], [82], [84], [86]. In order to confirm the inhibitory effect of water, Purolite CT482 and Amberlyst 70 were washed and dried in the reactor at room temperature after 48 h on-stream and reused twice. Fig. 6.3A and 6.3B display the activity evolution of Purolite CT482 and Amberlyst 70, respectively, in EOE synthesis during the three cycles at 190ºC. Fresh ($1^{st}$ cycle) and reused catalyst ($2^{nd}$ and $3^{rd}$ cycle) showed the same pattern. After two cycles using reused catalyst, both resins show a very similar behaviour to the fresh catalyst. As a result, it can be concluded that Purolite CT482 and Amberlyst 70 could be recovered after 48h on-stream and reused without any noticeable activity loss. This fact confirmed that catalyst decay on these two resins was caused mainly by the inhibitory effect of water formed in the EOE formation.

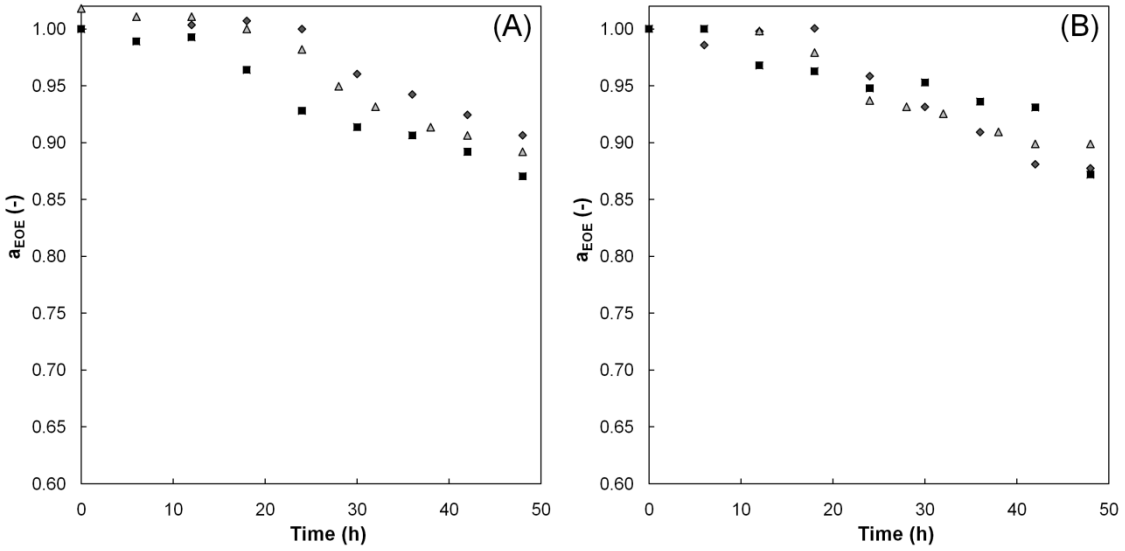


Fig. 6.3: Evolution of activity to EOE formation along the time on CT482 (A) and on Amberlyst 70 (B) at T=190ºC, $R_{OcOH/EtOH}$=10, q=0.25 mL/min, P=25 bar.
(■ 1st cycle; ♦ 2nd cycle; ▲ 3rd cycle).

### 6.3.3 Catalytic tests with alcohol-water feed

A set of experiments was performed on Amberlyst 70 and Purolite CT482 by adding water to the alcohol mixture feed. Fig. 6.4 and Fig. 6.5 show the activity of Amberlyst 70 and that of Purolite CT482, respectively, with ethanol-octanol and ethanol-octanol-water feeds. The reaction rate of fresh catalyst in ethanol-octanol mixtures was taken as the reference for catalysts activity. As seen, activity to EOE was lower in the presence of water. Unlike experiments with ethanol-octanol feed, the activity to EOE formation was almost constant along time on Purolite CT482 but it decreased slightly on Amberlyst 70. The water content of resins was determined after each experiment by titration. As Table 6.4 shows, water content within the resin increased with time-on-stream, which could be related to the continuous decrease of the catalytic activity to EOE with ethanol-octanol feed. It is also seen that higher water contents were found in resins when feeds contained water. Purolite CT482 retained higher water amounts than Amberlyst 70. However, the number of water molecules per sulfonic group is similar on the two resins (2.78-2.98 mol $H_2O$/mol sulfonic group). These water contents are far from those of a resin saturated by water (4.2 mol $H_2O$/mol sulfonic group) [87]. This fact can be due to the high affinity of alcohols, which compete with water, for the acid sites.

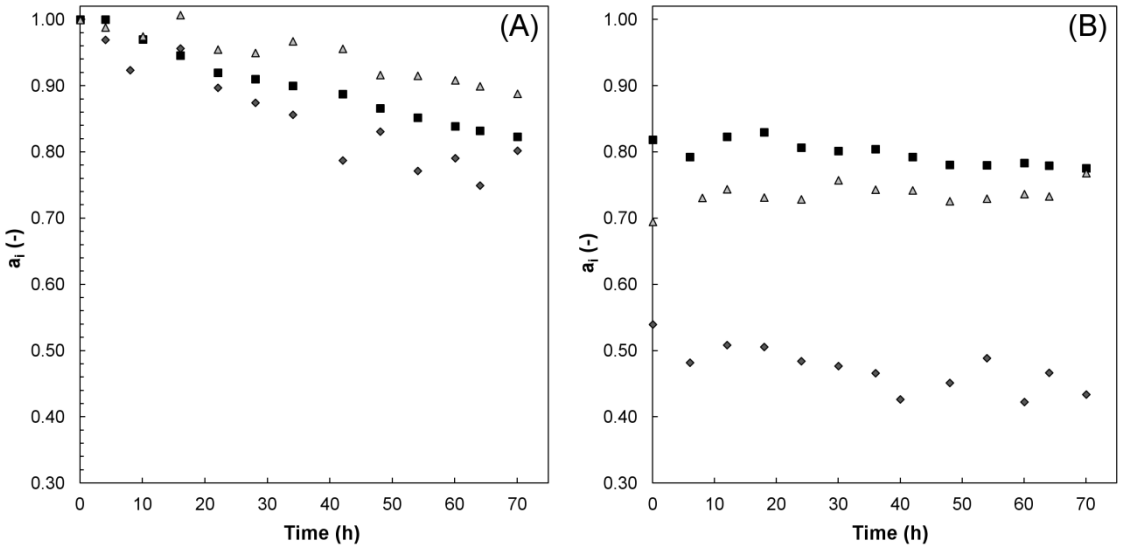


Fig. 6.4: Activity to DEE (♦), EOE (■) and DNOE (▲) formation vs. time on Amberlyst 70 at T=190ºC, q=0.25 mL/min, P=25 bar, $R_{OcOH/EtOH}$=10. (A) pure alcohols fed and (B) 1% (w/w) water fed.

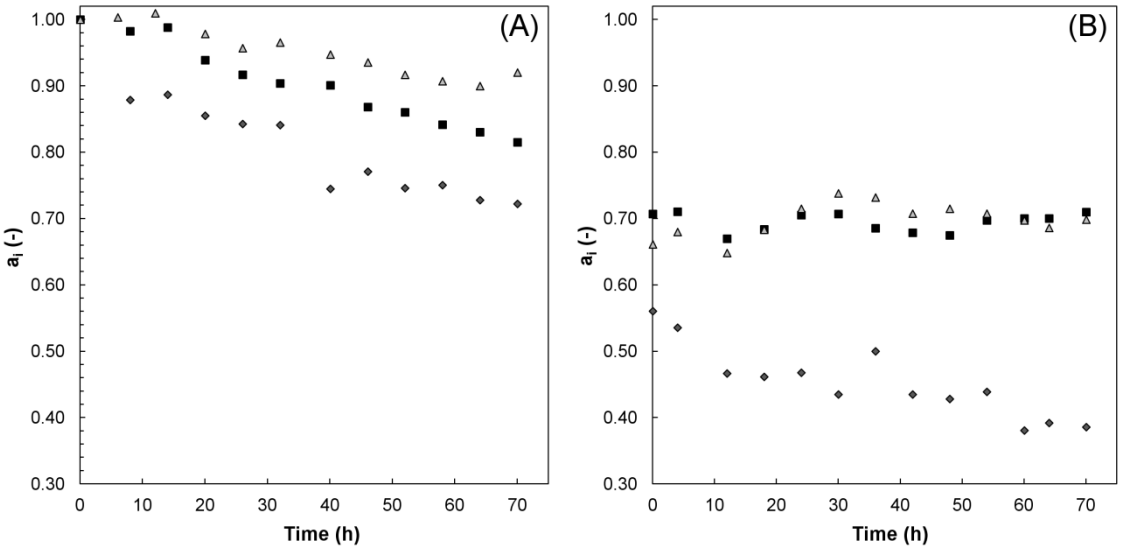


Fig. 6.5: Activity to DEE (♦), EOE (■) and DNOE (▲) formation vs. time on CT482 at T=190ºC, q=0.25 mL/min, P=25 bar, $R_{OcOH/EtOH}$=10. (A) pure alcohols fed and (B) 1% (w/w) water fed.

As Table 6.4 shows, turnover frequency (TOF) is similar at the beginning of ethanol-octanol fed experiments; however TOF of Purolite CT482 is a bit lower after 70h, and with ethanol-octanol-water feed it is lower by 20% than activity at the same time on stream with ethanol-octanol feed. Thus, the effect of water on the activity drop of Purolite CT482 was stronger than on Amberlyst 70. This pattern can be attributed to the higher acid site density in the gel-phase of Purolite CT482. With respect to activity of Amberlyst 70, a short initial flat period is observed (4h) and

afterwards a continuous decay, whereas for CT482 the flat period is longer (16h) and the decay rate is higher, so that after 70 h the activity level of Amberlyst 70 is slightly higher than that of Purolite CT482. In experiments where water was fed, the activity level of Purolite CT482 is always clearly lower.

Table 6.4: Water content inside resin and TOFs as a function of time on stream. T=190ºC, $R_{OcOH/EtOH}$=10, q=0.25 mL/min, P=25 bar.

| catalyst | time on-stream (h) | water content (w/w,%) | mol $H_20$ per sulfonic group | TOF ($h^{-1}$) |
|---|---|---|---|---|
| Amberlyst 70 | 0 | 2.1 | 0.45 | 6.98 |
| | 24 | 7.2 | 1.62 | |
| | 70 | 9.5 | 2.19 | 5.74 |
| | 70[a] | 12.5 | 2.98 | 5.40 |
| Purolite CT482 | 0 | 3.6 | 0.49 | 6.94 |
| | 24 | 10.6 | 1.55 | |
| | 70 | 13.2 | 1.98 | 5.41 |
| | 70[a] | 17.5 | 2.78 | 4.71 |

[a] 1% (w/w) water in the feed

Without water in the feed, both OcOH and EtOH swell the resins and compete for adsorbing on acid centres and the highest reaction rate is achieved with fresh catalyst. Then, a part of formed water adsorbs gradually on the resin and the reaction rate starts to decrease. The phase-equilibrium between water in the liquid phase and adsorbed on acid sites is not likely to be reached during the experiments without feeding water. On the contrary, when water was fed, the water amount in the liquid phase was enough to reach water-resin quasi-equilibrium, and the reaction rate to form EOE is nearly independent on time on-stream. As Table 6.4 shows, the amount of adsorbed water is similar in both resins. The different TOF could be explained by the fact that water probably acts as a solvent inside pores even at small quantities, and a transition takes place from concerted to ionic catalytic mechanism (slower) where the hydrated proton is the true catalytic agent takes place [82]. The effect of the mechanism change on the rate would be more noticeable on the three dimensional networks of sulfonic groups in the denser gel-phase of Purolite CT482 as a result of their proximity [90].

### 6.3.4 Catalytic activity for DEE, EOE and DNOE syntheses

Morphological changes that take place in the resins with time-on-stream by the action of water can modify their catalytic behaviour. As the amount of water adsorbed on resins increases with time-on-stream, accessibility of OcOH and EtOH to acid sites is also modified. It is observed that activity drop present different pattern depending on the ether (see Fig. 6.4 and 6.5). As a rule, activity decay was higher as the ether is less bulky: DEE>EOE>DNOE. When water is fed together with the alcohol mixture, it is seen that EOE and DNOE syntheses tend to similar activity levels, but DEE formation continues decreasing.

In ethanol-octanol feed, fresh ion-exchange resins were not fully swollen and the accessibility to acid centres was in some extent hindered. It is expected that steric restrictions play a major role for larger ether formation (DNOE>EOE>DEE). Resins swelled progressively with reaction time and the void spaces appearing between polymer chains favoured the diffusion of OcOH and bulky ethers EOE and DNOE. Thus, activity drop was less pronounced as the size of the ether increased. The effect of water was especially stressed in ethanol-octanol-water experiments. The adsorption of water caused remarkable activity decay for DEE synthesis, but in the case of EOE and DNOE it was partially balanced by the higher accessibility to acid centres of 1-octanol. Accordingly, the activity after 70 h time-on-stream was reduced by 30-35% in EOE and DNOE syntheses, and 57% in DEE formation, in relation to activity of fresh catalysts in ethanol-octanol feed.

Summarizing, water effects on the reaction between OcOH and EtOH are complex as this study shows. It is seen that the period of time necessary to get a steady activity in this case is extremely long. On Purolite CT482 and Amberlyst 70, which show very good hydrothermal stability at 190ºC, released water acts as a solvent and increased the accessibility of bulky molecules to the active centres. Consequently, catalytic activity to produce long chain ethers is less hindered in the presence of water than to short ones. In the particular case of Dowex 50Wx2 and Amberlyst XE804 the presence of significant desulfonation at 190ºC makes the situation more complicated.

Finally, activity decay patterns were modelled for Amberlyst 70 and Purolite CT482 in runs with ethanol-octanol feed. Activity drop in Dowex 50Wx2 and Amberlyst XE804 was not modelled since it was partly due to leaching of sulfonic groups. Literature supplies relationships between resin activity and the amount of water in the liquid-phase. Some are essentially empirical, but equations based on exponential, or Langmuir and Freundlich equilibrium approaches have been also used [90], [91]. Still, in our experiments the water amount in the liquid phase was always small and often around the threshold of chromatographic detection. So that, activity as a function of time was fitted to first and second order activation decays functions. Best results were found by assuming a first order decay with terminal activity (eq. 6.6):

$$-\frac{da_i}{dt} = k_{d,i}\left(a - a_\infty\right) \qquad \text{eq. 6.6}$$

whose integrated form is

$$a_i = a_{\infty,i} + \left(1 - a_{\infty,i}\right)\exp\left(-k_{d,i}\left(t - t_0\right)\right) \qquad \text{eq. 6.7}$$

where $a_{\infty,I}$ is the terminal activity, $k_{d,i}$ is the rate constant of decay, and $t_0$ the time when decay starts. The parameters of eq. 6.7 for EOE, DNOE and DEE syntheses on both catalysts are shown in Table 6.5. As seen, terminal activities roughly agree with the values found at large

time-on-stream in alcohol-water experiments. Therefore, it can be assumed that activity stabilizes after a long period of time at lower reaction rates than fresh catalyst. Rate decay constants are of the same order of magnitude on both resins and increase in the order DEE, EOE, DNOE syntheses on Purolite CT482, and DNOE, DEE, EOE syntheses on Amberlyst 70. As apparent activation energies show, temperature dependence of rate decay constant is low except for DEE synthesis. Finally, it is to be noted that $t_0$ appear for EOE and DNOE syntheses, being higher at 190ºC. On the contrary for DEE synthesis decay starts as soon as the reaction begins.

Table 6.5: Parameters of first-order activity decay function for Amberlyst 70 and CT482. $R_{OcOH/EtOH}$=10, q=0.25 mL/min, P=25 bar.

| | reaction | T(ºC) | $k_{d,i}$ ($h^{-1}$) | $a_\infty$ | $t_0$ (h) | $E_{d,i}$ (kJ/mol) |
|---|---|---|---|---|---|---|
| Amberlyst 70 | EOE | 150 | $5.17 \cdot 10^{-2}$ | 0.71 | 4 | 3.0 |
| | | 190 | $5.56 \cdot 10^{-2}$ | 0.72 | 6 | |
| | DEE | 150 | $3.38 \cdot 10^{-2}$ | 0.50 | 0 | 20 |
| | | 190 | $5.31 \cdot 10^{-2}$ | 0.65 | 0 | |
| | DNOE | 150 | $2.53 \cdot 10^{-2}$ | 0.67 | 6 | 4.6 |
| | | 190 | $2.81 \cdot 10^{-2}$ | 0.69 | 12 | |
| Purolite CT482 | EOE | 150 | $1.89 \cdot 10^{-1}$ | 0.87 | 2 | 6.4 |
| | | 190 | $2.21 \cdot 10^{-1}$ | 0.81 | 14 | |
| | DEE | 150 | $5.22 \cdot 10^{-2}$ | 0.63 | 0 | 28 |
| | | 190 | $1.04 \cdot 10^{-1}$ | 0.70 | 0 | |
| | DNOE | 150 | $4.90 \cdot 10^{-1}$ | 0.93 | 0 | 7.8 |
| | | 190 | $5.95 \cdot 10^{-1}$ | 0.91 | 12 | |

## 6.4 Conclusions

The thermal stability study of acidic PS-DVB resins shows that Dowex 50Wx2 and XE804 lose a relevant quantity of acid centres at 190ºC. Leaching of active sites appears to be enhanced by the action of the water formed in the reaction between OcOH and EtOH to form EOE

On the contrary, desulfonation is not significant for Amberlyst 70 and Purolite CT482 at 190ºC. As a consequence of the adsorption of water which competes with ethanol and 1-octanol for sulfonic groups, reaction rate on thermally stable resins Amberlyst 70 and Purolite CT482 decreases with time-on-stream up to a constant activity level lower than that of fresh resins. Both resins recover completely their activity as soon as water is removed from the reaction medium and therefore they could be reused. Reused resins showed a similar kinetic behaviour in the reaction system of EOE formation.

Ion-exchange resins are not completely swollen in the absence of water. As a consequence, diffusion of OcOH and bulky ethers are hindered. However, with time on-stream, released water acts as solvent and swells partially the resin. Thus, the catalytic activity drop is less pronounced for the ethers with more steric restrictions (EOE and DNOE) than for the smallest one (DEE).

Chapter 7

# Kinetic and equilibrium study of ethyl octyl ether formation from ethanol and 1-octanol dehydration on Amberlyst 70

THE EQUILIBRIUM SECTION OF THIS CHAPTER HAS BEEN REVISED AND RESUBMITTED IN:

J. Guilera, E. Ramírez, M. Iborra, J. Tejero, F. Cunill. Experimental study of chemical equilibria of the liquid-phase alcohol dehydration to 1-ethoxy-octane and to ethoxyethane. *Journal of Chemical & Engineering Data*.

THE KINETIC SECTION OF THIS CHAPTER HAS BEEN ACCEPTED AS A POSTER IN:

J. Guilera, R. Bringué, E. Ramírez, J. Tejero, F. Cunill. Kinetics of 1-octanol and ethanol dehydration to ethyl octyl ether over Amberlyst 70. **September 2013**. To be presented at XI EUROPACAT (European Congress on Catalysis), Lyon, France.

## 7.1 Introduction

Former chapters revealed that a feasible way to produce EOE is by means of EtOH and OcOH dehydration catalyzed by acidic ion-exchange resins. The main drawback of EOE production is the loss of EtOH molecules to form DEE. In poorly swollen resins such as Amberlyst 15 or 35 (macroreticular, high and medium divinylbenzene content), OcOH permeation is hindered whereas EtOH reach most of acid sites. As a result, DEE is preferably obtained in these macroreticular resins (selectivity to EOE 15-20% and to DEE 15-83%, with respect to EtOH). However, low-crosslinked resins such as Amberlyst 121, Amberlyst 70 or Purolite CT224 have wide enough spaces between polymer chains to allow OcOH access more easily to acid centers, and in this way to compete efficiently with EtOH for the acid sites. Therefore, low-crossliked resins maximized the production of EOE and reduced the amount of DEE formed (selectivity to EOE 41-46% and to DEE 43-53%).

As concerns to low-crosslinked resins, the chlorinated Amberlyst 70 showed a negligible desulfonation on EOE formation up to 190ºC (chapter 6), whereas common ion-exchange resins are only stable up to 120-150ºC [40], [41]. Another commercial thermally stable resin is Purolite CT482. Such catalyst showed a higher activity to EOE due to its higher acid capacity (4.25 mmol $H^+$/g) in comparison to Amberlyst 70 (2.65 mmol $H^+$/g). However, Purolite CT482 has a stiffer morphology than Amberlyst 70 favouring the production of the less sterically demanding ether, DEE (chapter 6). Therefore, Amberlyst 70 was chosen as the best acidic ion-exchange catalyst to produce EOE at relatively high temperature range (up to 190ºC).

Preferential adsorption of polar species on ion-exchangers is a key factor to evaluate the kinetics on alcohol dehydrations [89]. With respect to EOE formation, water preferably adsorbs on acid centers of exchangers excluding OcOH and EtOH, and as a result, the reaction to form EOE is inhibited (chapter 6). In order to obtain reaction rate models based on reaction mechanisms, LHHW and ER formalisms have been used successfully for the treatment of alcohol dehydration experimental data [54], [89], [92]–[94]. However, to the best of our knowledge, the liquid-phase kinetics of the synthesis of EOE from EtOH and OcOH, necessary for design reactor purposes, is not reported in the open literature.

On the other hand, to the best of our knowledge, equilibrium data for EOE synthesis has not been reported in the open literature up-to-date. As for the main side reaction, DEE formation, liquid-phase equilibrium data of DEE synthesis up to 190ºC is still unknown. To cover this gap, in the present chapter, experimental values of the equilibrium constant of the dehydration reaction between EtOH and OcOH to EOE and water, and the dehydration reaction of two EtOH molecules to DEE and water; have been determined at the temperature range 137-190ºC by direct measurement of the mixture composition at equilibrium state. Besides, standard enthalpy, entropy and free Gibbs energy changes were computed for both EOE and DEE synthesis reactions

In this chapter, the dehydration between EtOH and OcOH to form EOE on Amberlyst 70 is studied from a kinetic and equilibrium standpoint. Experiments were carried out in a fixed-bed reactor and in a batch reactor to find the parameters of a kinetic model able to predict reaction rates to EOE in a wide range of alcohols, ether and water concentrations. Besides, a kinetic model for the main side product, DEE, is also proposed.

## 7.2 Experimental procedure

### 7.2.1 Equilibrium experiments

Equilibrium experiments were performed in the batch reactor (described in chapter 2.3.1). Resins were dried at 110ºC under vacuum overnight. Then, the reactor was loaded with 70 mL of OcOH / EtOH / 1,4-dioxane mixture and 10 g of dry Amberlyst 70. OcOH and EtOH were used as reactants (30% w/w) in equimolar ratio. 1,4-dioxane was used as solvent (70% w/w) to avoid the immiscibility between organic and aqueous phases, and as a result of its suitable physical and chemical stability. Literature works showed that this solvent do not alter the equilibrium position [95]–[98].

The mixture liquid-catalyst was pressurized at 25 bar, heated up to the working temperature (137-190ºC) and stirred at 300 rpm. This low value of stirring speed was selected to avoid attrition of the catalyst during the long-term equilibrium runs. Experiments were finished when the measured equilibrium constant had the same value along time, within the limits of the experimental error, typically after 24 h (at 190ºC) - 150 h (at 137ºC). Duplicate runs were carried out at each temperature but 150ºC. Associated error of the linear fits presented in this work corresponds to 0.95 level of confidence.

### 7.2.2 Kinetic experiments

Experiments were performed in a fixed-bed and in a batch reactor.

**Fixed-bed reactor**

The major set of experiments was performed in the fixed-bed reactor (described in section 2.3.2). The reactor bed consisted of a mixture of Amberlyst 70 and inert SiC particles. As it can be observed in Fig. 7.1, the catalytic bed was formed by catalyst ($d_p$=0.49 ± 0.05mm, 95% confidence interval) and inert particles ($d_p$=0.48 ± 0.17mm, 95% confidence interval) of similar size. The reactant liquid mixture, OcOH and EtOH, was pumped by two HPLC pumps at q=4-6.7 mL/min. Otherwise, one pump at q=5 mL/min was used when products, DEE and EOE, were added to the reaction mixture. Liquid samples were taken on-line from the reactor inlet and outlet and injected directly into the GLC apparatus.

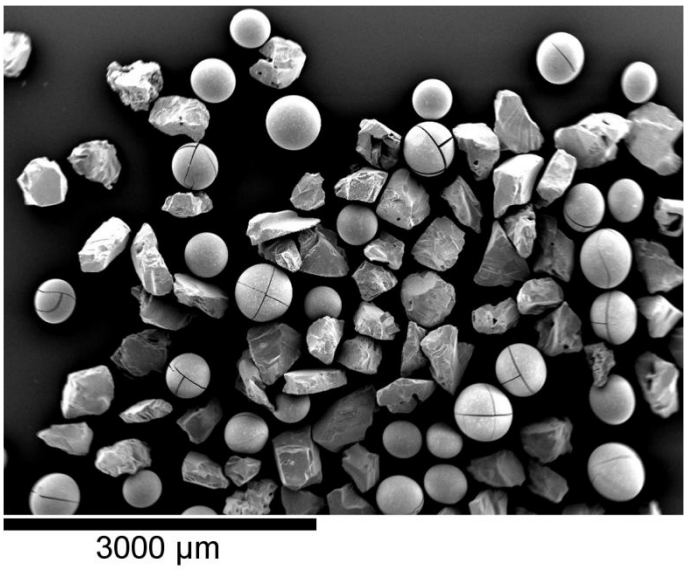


Fig. 7.1: SEM microphotography of the catalytic bed (Amberlyst 70 and SiC).

Previous to its use in the reactor, the catalyst was dried in an atmospheric oven at 110ºC overnight. The catalyst water content (≤2.25 w/w %) was determined by means of an Orion AF8 Karl Fisher titrator. Then, dried catalyst samples (0.1-2 g) were diluted in inert SiC (12-15 g). After filling and placing the reactor in the experimental set-up, the water content of the catalyst was reduced to 1.23 w/w % by EtOH percolation (q=5 mL/min, t=5 min), and then, the catalyst water content was reduced to less than 1 w/w % by the action of $N_2$ stream (q=300 mL/min, t=5 min) [87]. Subsequently, reactants were mixed and preheated into a hot box at 80ºC and introduced to the reactor.

The reactor operated in the temperature range 150-190ºC and the pressure was kept to 25 bar to ensure that the reaction medium was in the liquid-phase. OcOH / EtOH molar ratio in the feed ($R_{OcOH/EtOH}$) ranged between 0.25 and 4. 20 Experiments were performed from pure reactants (OcOH/EtOH mixture) and 15 additional experiments were performed by adding DEE and EOE to the reactant mixture (0-17 w/w % and 0-33 w/w %, respectively).

Experiments performed in the fixed-bed reactor were conducted in differential regime, experimentally assured for $X_{EtOH}$<14% (which corresponded to $X_{OcOH}$=6% at $R_{OcOH/EtOH}$=1, T=190ºC), discussed further. Reaction rates to form EOE and DEE were computed assuming a differential behaviour as follows;

$$r_{EOE} = \frac{F_{OcOH} \cdot X_{OcOH}}{W_{cat}} \; S_{OcOH}^{EOE} = \frac{F_{EtOH} \cdot X_{EtOH}}{W_{cat}} \; S_{EtOH}^{EOE} \quad \left[\frac{mol}{h \cdot g_{cat}}\right] \qquad \text{eq. 7.1}$$

$$r_{DEE} = \frac{1}{2}\frac{F_{EtOH} \cdot X_{EtOH}}{W_{cat}} \; S_{EtOH}^{DEE} \quad \left[\frac{mol}{h \cdot g_{cat}}\right] \qquad \text{eq. 7.2}$$

$W_{cat}$ is the dry catalyst mass, $F_j$ the molar flow rate of species j entering the reactor, $X_j$ the conversion of species j and $S_j^k$ the selectivity of reactant j towards product k at the reactor outlet as follows,

$$S_j^k = \frac{\{\text{mole of j reacted to form k}\}}{\{\text{mole of j reacted}\}} \times 100 \left[\%, \text{mol/mol}\right] \qquad \text{eq. 7.3}$$

**Batch reactor**

A series of 6 experiments was carried out in the batch reactor (described in section 2.3.1). The reactor operated in the temperature range 150-190ºC, OcOH / EtOH initial molar ratio ($R_{OcOH/EtOH}$) ranged between 0.5 and 2 and the pressure was kept to 25 bar with $N_2$ ensuring, in this way that the reaction medium was in the liquid-phase. Amberlyst 70 was previously dried at 110ºC under vacuum overnight (water content ≤ 2.25 wt%). Then, the reactor was loaded with 70 mL of OcOH / EtOH mixture, stirred at 500 rpm and heated up to the working temperature. When the mixture reached the desired temperature, dried catalyst (1-3 g) was injected into the reactor. Catalyst injection was taken as zero time. Experiments lasted 6h and the liquid composition was analyzed hourly. Working conditions were selected since, as quoted in literature, similar reactions take place at these conditions free of external and internal mass transfer resistances [22], [54]

Batch reactor experiments were performed operating in an integral regime. Reaction rates to DEE, EOE were calculated by differentiating the experimental function of the formed moles versus time (eq. 7.4).

$$r_j = \frac{1}{W_{cat}}\left(\frac{dn_j}{dt}\right) \quad \left[\frac{mol}{h \cdot g_{cat}}\right] \qquad \text{eq. 7.4}$$

## 7.3 Results and discussion

The equilibrium and kinetic analysis was made as a function of activities rather than concentrations in order to take into account the non-ideality of the alcohol-ether mixture. Activity coefficients were computed by the UNIFAC-DORTMUND predictive method [99].

### 7.3.1 Equilibrium study

Experiments were finished when both EOE and DEE synthesis reactions reached a pseudo-equilibrium state. The assessment of the equilibrium state was done by checking the constancy of the calculated equilibrium constants, within the limits of the experimental error. However, the reaction rates to form DNOE were lower, and at the end of the run, DNOE synthesis reaction did not reach the equilibrium state yet [98].

The thermodynamic equilibrium constant, $K_a$, for a liquid-phase nonideal system is given by

$$K_a = \prod_{j=1}^{S} (a'_j)_e^{v_j} = \prod_{j=1}^{S} (\gamma_j)_e^{v_j} (x_j)_e^{v_j} = K_\gamma \cdot K_x \qquad \text{eq. 7.5}$$

$K_\gamma$ values were computed by

$$K_\gamma^{DEE} = \frac{\gamma_{DEE} \cdot \gamma_{water}}{\gamma_{EtOH}^{2}} \qquad \text{eq. 7.6}$$

$$K_\gamma^{EOE} = \frac{\gamma_{EOE} \cdot \gamma_{water}}{\gamma_{EtOH} \cdot \gamma_{OcOH}} \qquad \text{eq. 7.7}$$

where superscripts DEE and EOE refer to EtOH dehydration to DEE and water (hereinafter referred to as DEE synthesis reaction); and EOE refer to OcOH and EtOH dehydration to EOE and water (EOE synthesis reaction). $K_x$ was calculated by the use of molar fractions,

$$K_x^{DEE} = \frac{x_{DEE} \cdot x_{water}}{x_{EtOH}^{2}} \qquad \text{eq. 7.8}$$

$$K_x^{EOE} = \frac{x_{EOE} \cdot x_{water}}{x_{EtOH} \cdot x_{OcOH}} \qquad \text{eq. 7.9}$$

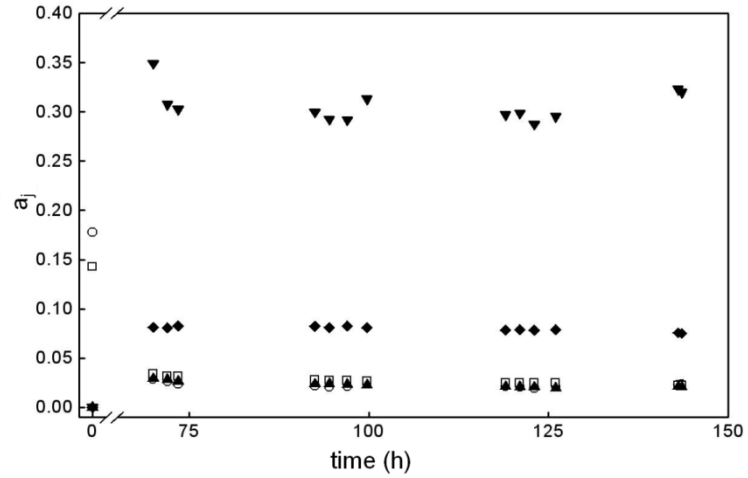


Fig. 7.2: Evolution of activities with time at 137ºC. ○EtOH; □OcOH; ♦EOE;▲DEE; ▼water.

As an example, Fig. 7.2 shows the activities evolution of the compounds involved in the DEE and EOE synthesis reactions at 137ºC. As it is seen, activities of all the compounds involved in both reactions were relatively low as a consequence of the use of 1,4-dioxane as solvent ($a_{1,4\text{-}Dioxane} \approx 0.74$). Reactant activities ($a_{EtOH}$ and $a_{OcOH}$) decreased and product activities ($a_{DEE}$, $a_{EOE}$ and $a_{water}$) increased to reach constant $K_a^{DEE}$ and $K_a^{DEE}$ values with time. As mentioned above, the intermolecular dehydration between two 1-octanol molecules to form 1-octoxyoctane and water had not reach the chemical equilibrium during the experiments. As a result of the advance of this reaction to chemical equilibrium, it was observed a fast readjustment of the mixture composition in such a way that $a_{water}$ showed a slight trend to increase, while $a_{DEE}$, $a_{EOE}$ and $a_{OcOH}$ showed a slight trend to decrease. However, computed values of $K_a^{DEE}$ and $K_a^{DEE}$ were random and constant within the limits of the experimental error.Table 7.1: Experimental equilibrium constants for the dehydration of EtOH to DEE and water, and dehydration of EtOH and OcOH to EOE and water.

| T (ºC) | $K_x^{DEE}$ | $K_y^{DEE}$ | $K_a^{DEE}$ | $K_x^{EOE}$ | $K_y^{EOE}$ | $K_a^{EOE}$ |
|---|---|---|---|---|---|---|
| 137 | 6.5 ± 0.7 | 2.1 ± 0.1 | 13.9 ± 1.5 | 16.8 ± 0.6 | 2.7 ± 0.1 | 46.0 ± 1.4 |
| | 7.1 ± 0.3 | 2.1 ± 0.1 | 15.2 ± 0.7 | 17.4 ± 0.3 | 2.7 ± 0.1 | 47.8 ± 0.7 |
| 150 | 5.7 ± 0.9 | 2.3 ± 0.1 | 13.0 ± 2.3 | 13.8 ± 1.2 | 2.6 ± 0.1 | 36.2 ± 3.1 |
| | 5.8 ± 0.4 | 2.2 ± 0.1 | 13.0 ± 0.9 | 14.9 ± 0.4 | 2.6 ± 0.1 | 39.4 ± 0.9 |
| 164 | 5.2 ± 0.6 | 2.2 ± 0.1 | 11.6 ± 1.3 | 12.5 ± 0.6 | 2.5 ± 0.1 | 30.8 ± 1.5 |
| 177 | 4.2 ± 0.2 | 2.3 ± 0.1 | 9.7 ± 0.4 | 9.9 ± 0.5 | 2.4 ± 0.1 | 23.4 ± 1.2 |
| | 4.5 ± 0.3 | 2.3 ± 0.1 | 10.6 ± 0.7 | 11.0 ± 0.6 | 2.4 ± 0.1 | 25.9 ± 1.3 |
| 190 | 3.6 ± 0.5 | 2.5 ± 0.1 | 8.8 ± 1.6 | 8.5 ± 0.4 | 2.3 ± 0.1 | 19.3 ± 0.9 |
| | 3.9 ± 0.4 | 2.4 ± 0.1 | 9.3 ± 1.1 | 8.8 ± 0.3 | 2.3 ± 0.1 | 19.9 ± 0.6 |

Table 7.1 presents the equilibrium constants for the DEE and EOE synthesis reaction found experimentally. Equilibrium constant values showed are the average of those calculated during each experiment. As it can be seen, both $K_\gamma^{EOE}$ and $K_\gamma^{DEE}$ values differed significantly from unity, mainly due to the presence of water, what confirm the non-ideality of the mixture.

Table 7.2: Dependence of the mean experimental values of the equilibrium constants with the temperature.

| T (ºC) | $K_a^{DEE}$ | $K_a^{EOE}$ |
|---|---|---|
| 137 | 14.5 ± 0.9 | 46.9 ± 1.3 |
| 150 | 13.0 ± 0.1 | 37.8 ± 2.3 |
| 164 | 11.6 | 30.8 |
| 177 | 10.2 ± 0.6 | 24.7 ± 1.8 |
| 190 | 9.1 ± 0.4 | 19.6 ± 0.5 |

Mean values of the equilibrium constant at each temperature are presented in Table 7.2. As it can be observed, the reproducibility of experiments was found to be reliable, with experimental uncertainties of less than 7% of relative error. $K_a^{DEE}$ and $K_a^{EOE}$ relatively large values indicate that both reactions are shifted to the products at the equilibrium state, what assures high conversion levels in an industrial etherification process. By comparing both reactions, EOE synthesis reaction is more shifted to products than DEE one. In agreement with that fact, at a given temperature higher equilibrium constant values were found as longer was the linear ether formed [96]–[98]. Comparing the equilibrium values obtained in this work for EOE synthesis reaction with those obtained for 1,1'-oxybis-pentane [96], the symmetrical $C_{10}$ linear ether; it can be inferred that the equilibrium to the symmetrical ether was more shifted towards products than for the asymmetrical EOE.

Regarding the dependence of the equilibrium constants with the temperature, both $K_a^{DEE}$ and $K_a^{EOE}$ values clearly decreased with the temperature. Therefore, DEE and EOE syntheses are exothermic reactions, as other n-alkyl ether syntheses [5], [6], [9], [12]–[14]. As it is well-known, the temperature dependence of the thermodynamic equilibrium constant can be related to other thermodynamic variables of the reaction system by

$$\ln K_a = \frac{-\Delta_r G^0_{(l)}}{RT} = \frac{-\Delta_r H^0_{(l)}}{RT} + \frac{\Delta_r S^0_{(l)}}{R} \qquad \text{eq. 7.10}$$

If the enthalpy change of reaction is assumed to be constant over the temperature range (137-190ºC), the thermodynamic variables, $\Delta_r H_{(l)}^0$ and $\Delta_r S_{(l)}^0$ can be obtained by fitting eq. 7.10 to values of the equilibrium constant at different temperatures (see Fig. 7.3). The temperature dependence of $K_a^{DEE}$ and $K_a^{EOE}$ is given by the following expressions

$$\ln K_a^{DEE} = \frac{(1691 \pm 205)}{T} + (-1.4 \pm 0.5) \qquad \text{eq. 7.11}$$

$$\ln K_a^{EOE} = \frac{(3097 \pm 360)}{T} + (-3.7 \pm 0.8) \qquad \text{eq. 7.12}$$

where T is expressed in K.

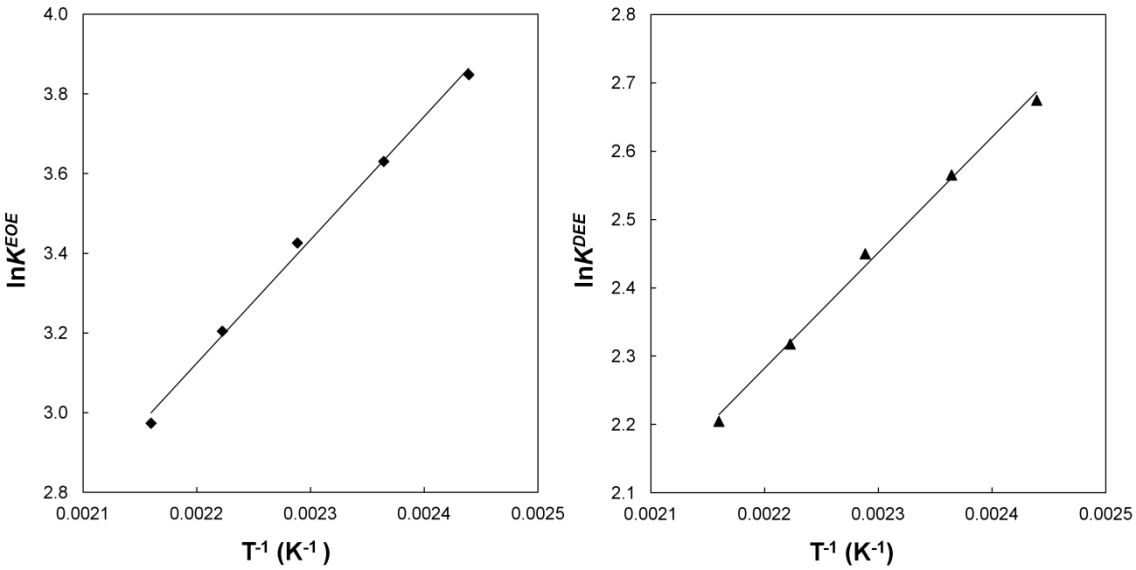


Fig. 7.3: ln K versus 1/T considering $\Delta_r H_{(l)}^0$ constant over the temperature range. (A) EOE synthesis reaction; (B) DEE synthesis reaction.

Considering that the standard enthalpy of reaction changes significantly over the temperature range, its dependence on temperature can be computed by the Kirchhoff and van't Hoff equations,

$$\frac{d\Delta_r H_{(l)}^0}{dT} = \sum_{j=1}^{S} \nu_j \cdot C_{p(l),j} \qquad \text{eq. 7.13}$$

$$\frac{d\ln K_a}{dT} = \frac{\Delta_r H^0}{RT^2} \qquad \text{eq. 7.14}$$

where $C_{p,(l)}$ are the molar heat capacities in the liquid-phase of the compounds j that take part in the reaction. If $C_{p,(l)}$ polynomial dependence on temperature is introduced into Kirchhoff and van't Hoff equations, the dependence of $\Delta_r H_{(l)}^0$, $\Delta_r S_{(l)}^0$, $\Delta_r G_{(l)}^0$ and $K_a$ on the temperature can be computed by integrating the Kirchhoff and the van't Hoff equations, thus:

$$\Delta_r H^0_{(l)} = I_K + aT + \frac{b}{2}T^2 + \frac{c}{3}T^3 + \frac{d}{4}T^4 \qquad \text{eq. 7.15}$$

$$\Delta_r S^0_{(l)} = I_H R + a + a\ln T + bT + \frac{c}{2}T^2 + \frac{d}{3}T^3 \qquad \text{eq. 7.16}$$

$$\Delta_r G^0_{(l)} = I_K - RI_H T - aT\ln T - \frac{b}{2}T^2 - \frac{c}{6}T^3 - \frac{d}{12}T^4 \qquad \text{eq. 7.17}$$

$$\ln K_a = I_H - \frac{I_K}{RT} + \frac{a}{R}\ln T + \frac{b}{2R}T + \frac{c}{6R}T^2 + \frac{d}{12R}T^3 \qquad \text{eq. 7.18}$$

where

$$a = \sum_{j=1}^{S} \nu_j a_j \qquad b = \sum_{j=1}^{S} \nu_j b_j \qquad c = \sum_{j=1}^{S} \nu_j c_j \qquad d = \sum_{j=1}^{S} \nu_j d_j \qquad \text{eq. 7.19}$$

and $a_j$, $b_j$, $c_j$ and $d_j$ are the coefficients of $C_{p,(l),j}$ polynomial equations. Thermochemical data of the compounds involved in the DEE and EOE synthesis reactions are shown in Table 7.3. Gathering the second term of eq. 18 containing a, b, c and d as f(T),

$$f(T) = -\left(\frac{a}{R}\ln T + \frac{b}{2R}T + \frac{c}{6R}T^2 + \frac{d}{12R}T^3\right) \qquad \text{eq. 7.20}$$

$I_K$ and $I_H$ were obtained from the slope and the intercept of eq. 7.18.

Table 7.3: Thermochemical data of EtOH, OcOH, water, DEE and EOE.

| property | units | EtOH | OcOH | water | DEE | EOE |
|---|---|---|---|---|---|---|
| $C_{p,j}=a_j+b_jT+c_jT^2+d_jT^3$ | J/(mol·K) | | | | | |
| $a_j$ | J/(mol·K) | 29.01[a] | 43.38[c] | 106.61[e] | 155.58[f] | 383.09[g] |
| $b_j$ | J/(mol·K$^2$) | 0.2697[a] | -1.3132[c] | -0.2062[e] | -0.0856[f] | 0.1439[g] |
| $c_j$ | J/(mol·K$^3$) | $-5.658\cdot10^{-4}$[a] | $-1.654\cdot10^{-3}$[c] | $3.770\cdot10^{-4}$[e] | $3.193\cdot10^{-4}$[f] | $-5.225\cdot10^{-4}$[g] |
| $d_j$ | J/(mol·K$^4$) | $2.079\cdot10^{-6}$[a] | $-1.325\cdot10^{-6}$[c] | $-1.226\cdot10^{-7}$[e] | $4.148\cdot10^{-7}$[f] | $6.646\cdot10^{-7}$[g] |
| $\Delta_fH^0_{(l)}$ (25ºC) | kJ/mol | -276 ± 2[b] | -429 ± 4[b] | -285.8[b] | -271 ± 2[b] | -430.2[h] |
| $S^0_{(l)}$ (25ºC) | J/(mol·K) | 165 ± 8[b] | 357.1[d] | 70.0[b] | 253 ± 1[b] | 394.4[h] |

[a] Kitchaiya et al. [102]. [b] NIST average of values [103]. [c] Obtained from Naziev et al. [104] and fitted to a third-order equation. [d] Miltenburg et al. [105]. [e] Calculated from Shomate equation and fitted to a third-order equation [106]. [f] Obtained from Gallant et al.[107] and fitted to a third-order equation. [g] Estimated by Rowlinson-Bondi method [108] and fitted to a third-order equation. [h] Estimated by a modified Benson method [109].

Furthermore, deviation in $K_a$ values as a result of the difference between the working pressure (25 bar) and the pressure at the standard state (1 bar), was evaluated by means of the Poynting correction factor $K_\Gamma$ by the following expression [110]

$$K_{a,P=1bar}=K_{a,P}\cdot K_\Gamma=K_{a,P}\cdot\exp\left(\frac{P-1}{RT}\sum_{j=1}^{S}\nu_j V_j\right) \qquad \text{eq. 7.21}$$

where $V_j$ is the molar volume of compound j. Molar volumes and $K_\Gamma$ for DEE and EOE synthesis reactions are shown in Table 7.4.

Table 7.4: Molar volumes of EtOH, OcOH, water, DEE and EOE; and $K_\Gamma$ correlation factors of DEE and EOE synthesis reactions, calculated by Hawkinson-Brobst-Thomson (HBT) method [108].

| T (ºC) | $V_{EtOH}$ (L/mol) | $V_{OcOH}$ (L/mol) | $V_{water}$ (L/mol) | $V_{DEE}$ (L/mol) | $V_{EOE}$ (L/mol) | $K_\Gamma^{DEE}$ | $K_\Gamma^{EOE}$ |
|---|---|---|---|---|---|---|---|
| 137 | 0.072 | 0.154 | 0.019 | 0.136 | 0.209 | 1.007 | 1.001 |
| 150 | 0.075 | 0.156 | 0.019 | 0.143 | 0.213 | 1.009 | 1.001 |
| 164 | 0.078 | 0.159 | 0.020 | 0.154 | 0.217 | 1.013 | 1.000 |
| 177 | 0.081 | 0.162 | 0.020 | 0.174 | 0.222 | 1.021 | 0.999 |
| 190 | 0.085 | 0.165 | 0.021 | 0.188 | 0.227 | 1.025 | 0.998 |

Values of the standard molar enthalpy, entropy and free energy changes of DEE and EOE at 25ºC determined for the described methods are gathered in Table 7.5. Concerning the experimental values obtained in this work for DEE synthesis, the best linear fits, and as a result, the lowest associated standard errors were obtained by taking into account both the pressure deviation from the standard state and the enthalpy changes over the temperature range. As for

EOE synthesis, the improvement of considering the pressure deviation from the standard state was not significant. Accordingly, the standard enthalpy, entropy and free Giggs energy changes proposed are presented in row 4 of Table 7.5 ($\Delta_rH^0_{(l)}$ as f(T) with P deviation).

Table 7.5: Standard Gibbs energy, enthalpy and entropy changes of EOE and DEE synthesis reaction in liquid-phase at 25ºC.

| | DEE | | | EOE | | |
|---|---|---|---|---|---|---|
| | $\Delta_rH^0_{(l),25ºC}$ | $\Delta_rS^0_{(l),25ºC}$ | $\Delta_rG^0_{(l),25ºC}$ | $\Delta_rH^0_{(l),25ºC}$ | $\Delta_rS^0_{(l),25ºC}$ | $\Delta_rG^0_{(l),25ºC}$ |
| | kJ/mol | J/(K·mol) | kJ/mol | kJ/mol | J/(K·mol) | kJ/mol |
| $\Delta_rH^0_{(l)}$ constant | -14.1 ± 1.7 | -12.0 ± 3.9 | -10.5 ± 2.9 | -25.8 ± 3.0 | - 30.7 ± 7.9 | -16.6 ± 5.0 |
| $\Delta_rH^0_{(l)}$ with P deviation | -13.5 ± 1.5 | -10.6 ± 3.3 | -10.4 ± 2.5 | -25.8 ± 3.0 | -30.9 ± 7.9 | -16.6 ± 5.1 |
| $\Delta_rH^0_{(l)}$ as f(T) | -12.7 ± 1.2 | -8.9 ± 2.7 | -10.0 ± 2.0 | -18.8 ± 1.3 | -13.4 ± 3.0 | -14.8 ± 2.2 |
| $\Delta_rH^0_{(l)}$ as f(T) with P deviation | -12.1 ± 0.9 | -7.6 ± 2.1 | -9.9 ± 1.5 | -18.9 ± 1.3 | -13.6 ± 3.0 | -14.8 ± 2.2 |
| literature[29] | -12.2 ± 0.2 | 0.5 ± 0.5 | -12.2 ± 0.3 | | | |
| theoretical | -5 ± 8 | -6 ± 9 | -3 ± 11 | | -11 ± 6 | -53 ± 8 |

Enthalpy change values proposed for EtOH dehydration to DEE and water are in completely agreement with those estimated by Kiviranta-Pääkkönen at lower temperature range 50-90ºC [45]. With respect to EOE synthesis, no thermochemical data was found in bibliography. Comparing the reaction enthalpy change proposed for EOE synthesis with other symmetrical dialkyl ethers, such as DNOE, di-n-hexyl ether, di-n-pentyl ether, di-n-butyl ether, di-n-propyl ether, DEE and dimethyl ether [45], [98], [100], [101], [111], the dehydration between EtOH and OcOH to form EOE and water showed slightly lower enthalpy change values, and as a result, the most exothermic reaction.

In addition, theoretical thermochemical data were computed from enthalpy and entropy of formation of the compounds involved in both reactions. If possible, thermochemical data were obtained from NIST database (Table 7.3). As it can be observed in Table 7.5, the proposed enthalpy change value of DEE synthesis, $\Delta_rH^0_{(l)}$ = (-12.1 ± 0.9) kJ·mol$^{-1}$, was lower than that obtained from the enthalpy of formation of the compounds involved. From the enthalpy change value for DEE synthesis proposed in this work and $\Delta_fH^0_{(l)}$ values of EtOH and water in Table 7.3, $\Delta_fH^0_{(l)}$ value for DEE at 298 K can be obtained: (-279 ± 5) kJ·mol$^{-1}$. This value is in agreement with that estimated by the improved Benson group additive method [109], $\Delta_{f,DEE}H^0_{(l)}$ = -277.2 kJ/mol, or that obtained by Pihlaja and Heikkil [112], $\Delta_{f,DEE}H^0_{(l)}$ = -(276.9 ± 1.8) kJ/mol, but 2.5% lower than that obtained by Murrin and Goldhagen [113], $\Delta_{f,DEE}H^0_{(l)}$ = -(271.2 ± 1.9) kJ/mol. As for the entropy change value for DEE synthesis, they are in agreement with that estimated by the molar entropy of the compounds involved.

To the best of our knowledge, the thermochemical data of EOE formation is not quoted in the open literature. Again, from the thermochemical reaction data obtained in this work and that experimentally found in literature of the compounds involved, $\Delta_{f,EOE}H^0_{(l)}$ = (-436 ± 7) kJ·mol$^{-1}$ and

$\Delta S^0_{(l)}$ (EOE) = (434.0 ± 11) J·mol$^{-1}$·K$^{-1}$ values are obtained. Enthalpy of EOE formation obtained is only 1% lower than that predicted by the improved Benson group additive method [109], while molar entropy of EOE obtained is 9% higher or 8% (considering the effect of pressure [97], [109]). Eventually, Table 7.6 compares the thermochemical values predicted by the modified Benson group additivity method of EOE and its symmetrical linear ether homologue, DNPE. It is inferred that the Benson method is very useful in predicting the enthalpy of formation; however, it seems that it underestimate the standard molar entropy of $C_{10}$ linear ethers.

Table 7.6: Comparison between predicted standard formation enthalpy and standard molar entropy values by the modified Benson method for linear $C_{10}$ ethers and the experimental ones.

| | $\Delta_f H^0_{(l)}$ (25ºC) (kJ/mol) | | $\Delta S^0_{(l)}$ (25ºC) (kJ/mol) | |
|---|---|---|---|---|
| | EOE | DNPE | EOE | DNPE |
| predicted by modified Benson[a] | -430.2 | -430.2 | 399.4 | 399.4 |
| experimental | -436 ± 7[b] | 430 ± 8[c] | 434 ± 11[b] | 474 ± 4[d] |

[a] Verevkin [109]. [b] this work. [c] average of Bringué et al. [96] and Murrin et al. [113] . [d] Bringué et al. [96].

### 7.3.2 Kinetic study

#### Fixed-bed reactor experiments

Preliminary experiments were performed at the highest temperature of the range explored (190ºC) in order to evaluate the influence of external mass transfer, EMT, and internal mass transfer, IMT, on reaction rates in the fixed-bed reactor. Additionally, preliminary experimental data was used to assess the effect of the inert dilution ratio and to ensure that experiments were carried out in differential regime.

Firstly, a blank experiment confirmed that SiC particles did not catalyze the reactions. Thus, Amberlyst 70 beads were diluted in SiC inert particles to obtain an isothermal bed and good contact pattern between reactants and catalyst. Nonetheless, bed dilution can enhance bypassing of catalyst particles due to channelling, and additionally, some activity distribution could occur along the bed. However, it was confirmed that the used dilution ratios ($RD=W_{inert}/W_{cat}<300$) did not influence on reaction rates (Fig. 7.4A). Simultaneously, it was observed that the liquid flow was drastically blocked if no inert particles were used, as a consequence of the high capacity of Amberlyst 70 to swell in polar media. On the other hand, the linear fit of the EtOH conversion versus the contact time confirmed that the reactor operated in differential regime (Fig. 7.4B).

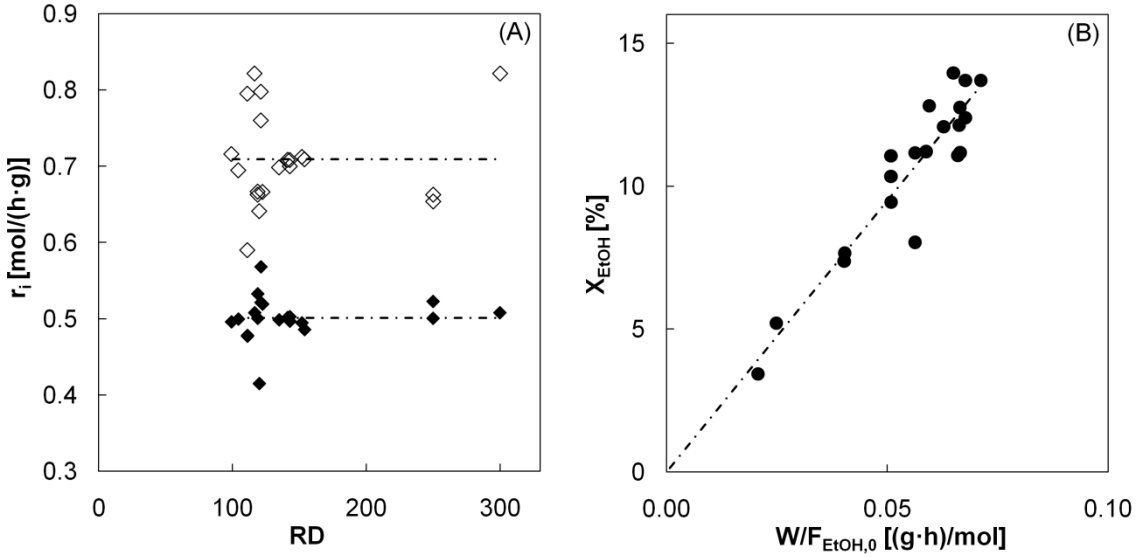


Fig. 7.4: Effects of the dilution ration on reaction rates (A) and the contact time on EtOH conversion (B). T=190ºC, P=25 bar, q=6.7 mL/min, $R_{OcOH/EtOH}$=1.

As far as EMT is concerned, runs were performed by changing the flow rate (LHSV=20-33.5 $h^{-1}$) at fixed conditions ($R_{OcOH/EtOH}$=1 and 190ºC). The used catalyst particle size was 0.16-0.25 mm to avoid internal mass influence, as further discussed. Commercial samples were previously crushed and sieved as the particle diameter distribution of commercial Amberlyst 70 ranges between 0.40-0.80 mm. Fig. 7.5A shows that reaction rates of DEE and EOE formations remained constant in the whole range of flow rates explored (q=4-6.7 ml/min, which correspond to surface velocity $v_s$=0.105-0.176 cm/s. Hence, it is assured that reaction rates do not depend on volumetric flow rate over 0.105 cm/s at 190ºC.

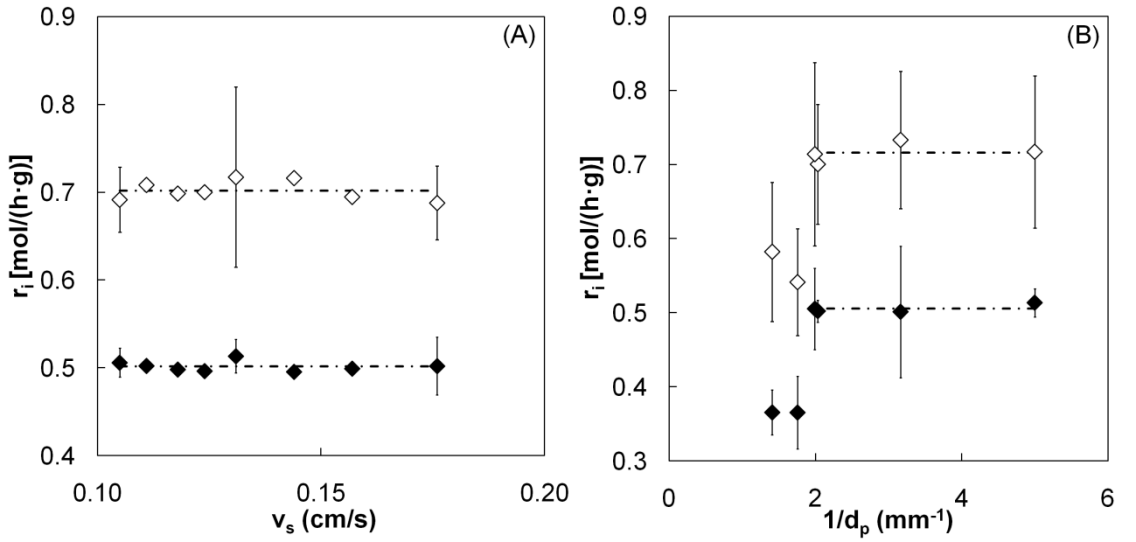


Fig. 7.5: Effects of $v_s$ ($d_p$=0.16-0.25 mm) (A) and of $1/d_p$ ($v_s$=0.176 cm/s) (B) on reaction rate of DEE (◊) and EOE (♦) formations. T=190ºC, P=25 bar, $R_{OcOH/EtOH}$=1. The error bars indicate the confidence interval at a 95% probability level.

As for IMT, experiments were carried out to delimit the operation conditions in which catalyst particle size has no influence on the measured reaction rates. IMT influence was checked by varying catalyst particle diameter at the operation conditions where EMT has no influence (T=190ºC, $R_{OcOH/EtOH}$=1, Q=6.7 ml/min). Catalyst batches with particle diameter 0.16-0.25 mm, 0.25-0.40 mm, 0.40-0.63 mm and 0.63-0.80 mm were tested. In addition, commercial distribution of particle sizes of Amberlyst 70 ($d_p$=0.57 ± 0.05 mm, 95 % confidence interval) and commercial fraction with the $d_p \geq 0.63$ mm particles excluded ($d_p$=0.49 ± 0.05 mm, 95 % confidence interval) were also tested.

Fig. 7.5B plots reaction rates of DEE and EOE synthesis by varying the catalyst particle size ($1/d_p$). It is shown that above $1/d_p$=2 $mm^{-1}$ reaction rates do not change, within the limits of the experimental error. Accordingly, it can be considered that the influence of IMT on the measured reaction rates was avoided by using Amberlyst 70 particles with $d_p \leq 0.63$ mm. As commercial particle distribution of Amberlyst 70 has a significant amount of larger particles than 0.63 mm, they were affected by internal diffusion restrictions. Thus, the measured reaction rates by using commercial Amberlyst 70 at 190ºC were 38% lower than those observed without IMT resistances. Accordingly, further experiments were performed over sieved but non-crushed commercial Amberlyst 70 ($d_p$=0.49 ± 0.05mm, 95 % confidence interval).

Preliminary experiments allowed setting the conditions at which measured reaction rates were free of mass transfer resistences ($q \geq 4$ mL/min and $d_p \leq 0.63$ mm). Different sets of experiments were carried out to outline the form of the rate equations and to endorse the suitability of the expressions. The first set of experiments was carried out using OcOH / EtOH mixtures. Tested temperatures were 150, 164, 177 and 190ºC, and explored OcOH / EtOH molar ratios ($R_{OcOH/EtOH}$) were 0.25, 0.5, 1, 2 and 4. Fig. 7.6 gathers the reaction rates obtained in the fixed-bed reactor from pure reactants. Reaction rates to DEE and EOE are plotted as a function of EtOH activity (A and B, respectively) and as a function of OcOH activity (C and D, respectively). It has to keep in mind that in the present case $a_{EtOH}$ and $a_{OcOH}$ are mutually dependents as no diluents were added to the mixture.

As observed, the maximum reaction rates to form DEE were achieved in the runs with EtOH excess, where $a_{EtOH}$ is the highest and $a_{OcOH}$ the lowest. (Fig. 7.6A). As concerns to EOE formation, it clearly shows an reaction rate maximum in equimolar runs, $a_{EtOH}=a_{OcOH}$~0.5 (Fig. 7.6B). The driving force of the surface reaction step of EOE formation, $a_{EtOH}a_{OcOH}$, also has the maximum values in equimolar conditions, while it decreases in excess of EtOH or OcOH. This fact is in agreement with the hypothesis that the rate-limiting step of the EOE formation is the surface reaction step; thereby, the adsorptive equilibrium of all the participants is maintained.

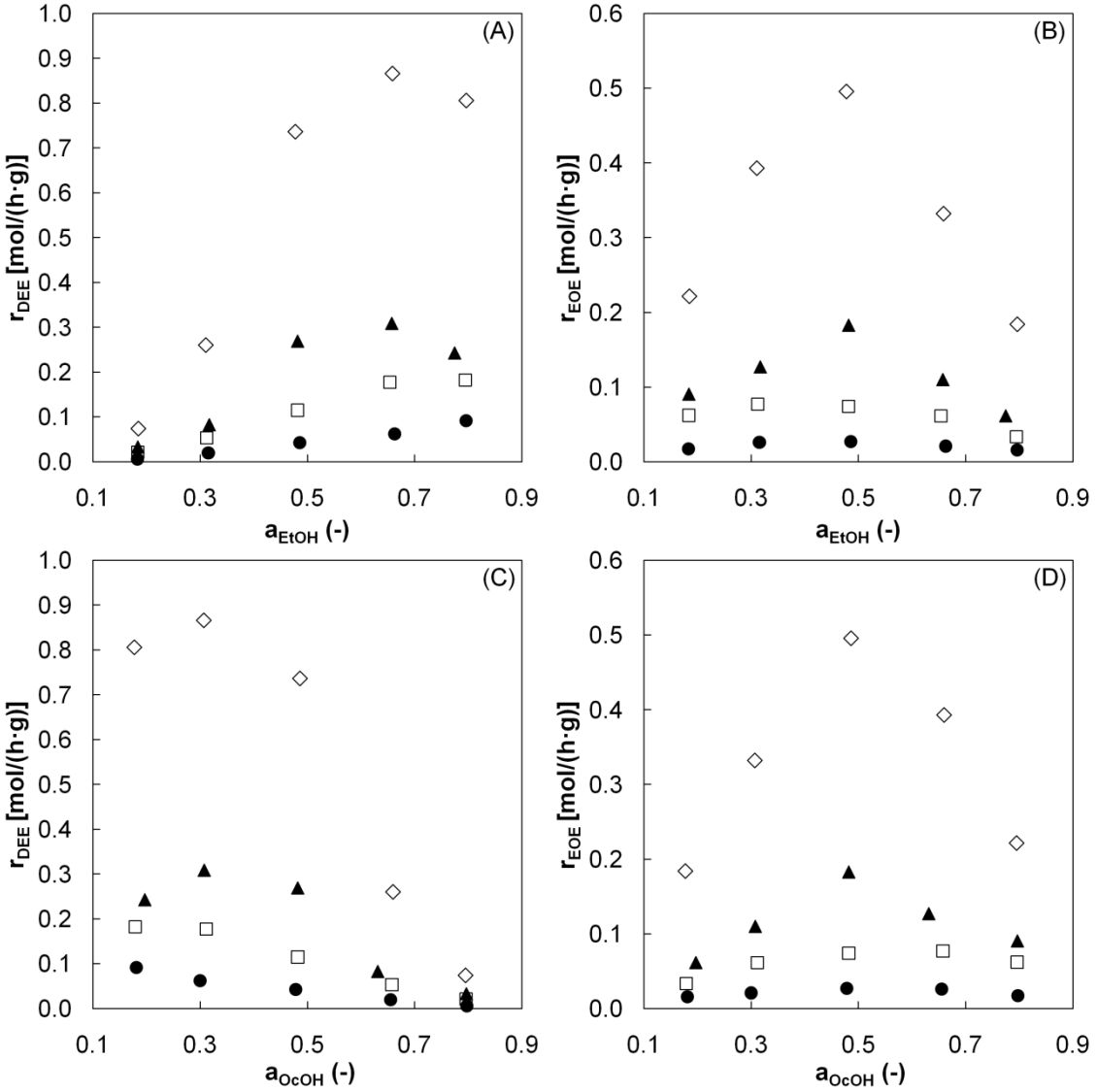


Fig. 7.6: Reaction rates of DEE (A) and EOE (B) formation from pure reactants as a function of EtOH activity and reaction rates of DEE (C) and EOE (D) formation as a function of OcOH activity. ◊ 190ºC; ▲177ºC; □ 164ºC; ● 150ºC.

A second set of experiments were performed by adding DEE and EOE to the reactant mixture (≤17 w/w %, ≤33 w/w %, respectively) in the feed of the fixed-bed reactor to evaluate the effect of $a_{DEE}$ and $a_{EOE}$ on the reaction rates. From a kinetic point of view, the presence of an additional compound in the feed lowers the driving force of the reaction but they can also compete with reactants for the adsorption on the sulfonic groups. As it can be observed in Fig. 7.7A for DEE formation and Fig. 7.7B for EOE formation, the decrease of the reaction rates can be successfully explained by the decrease of the driving force of the surface reaction step to form DEE ($a_{EtOH}^2$-$a_{DEE}a_w/K_{eq,DEE}$) and to form EOE ($a_{EtOH}a_{OcOH}$-$a_{DEE}a_w/K_{eq,EOE}$). Accordingly, the inhibiting effect of the presence of DEE and EOE in the feed on the reaction rates seems to be negligible. This fact is most probably due to the DEE and EOE adsorption on acid sites is low, and therefore, they do not compete with EtOH and OcOH, what agrees with their low polarity [76].

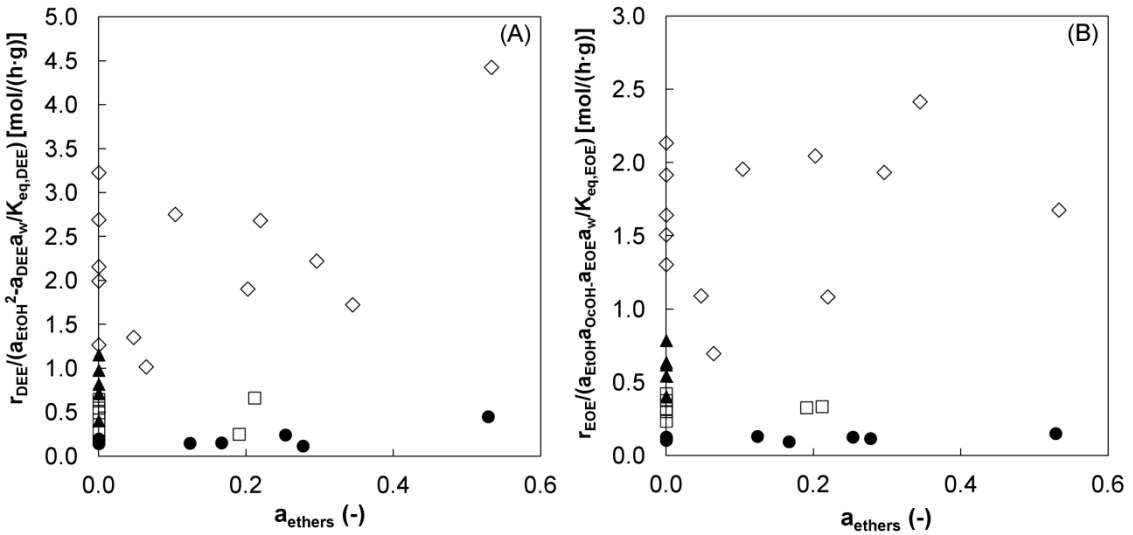


Fig. 7.7: Reaction rates divided per the driving force of the surface reaction of DEE (A) and EOE (B) formation as a function of the $a_{ethers}$. ◊ 190ºC; ▲177ºC; □ 164ºC; ● 150ºC.

Besides the formation of DEE and EOE, the dehydration of EtOH and OcOH forms stoichiometric quantities of water. The effects of water on the reaction between OcOH and EtOH in the fixed-bed are complex, as discussed in the former chapter. Using a fixed-bed reactor, an excessively long period of time was necessary to get a steady activity to EOE. As for DEE, after 70 h of experiment reaction rates of DEE formation were still decreasing. Accordingly, the effect of $a_{water}$ on the reaction rates to form DEE and EOE was evaluated in the batch reactor.

**Batch reactor experiments**

A third set of experiments were performed to evaluated the effect of water on the reaction rates. Tested temperatures were 150, 164, 177 and 190ºC; examined OcOH / EtOH molar ratios ($R_{OcOH/EtOH}$) were 0.5, 1, and 2; and explored conversions $0 < X_{EtOH}$ (%) < 84 and $0 < X_{OcOH}$ (%) < 65. Reaction rates to form DEE and EOE decreased with the presence of reaction products in the mixture; as a result of the equilibrium approach. Nevertheless, Fig. 7.8A for DEE formation and Fig. 7.8B for EOE formation shows a high sensitivity of the reaction rates towards water activity, and as a result, the rate-decreasing cannot be explained only by the decrease of the driving force. This behaviour was not observed by the presence of ethers in the reaction mixture (Fig. 7.7). As expected, the inhibiting effect of water must play a relevant role on the reaction rates expressions.

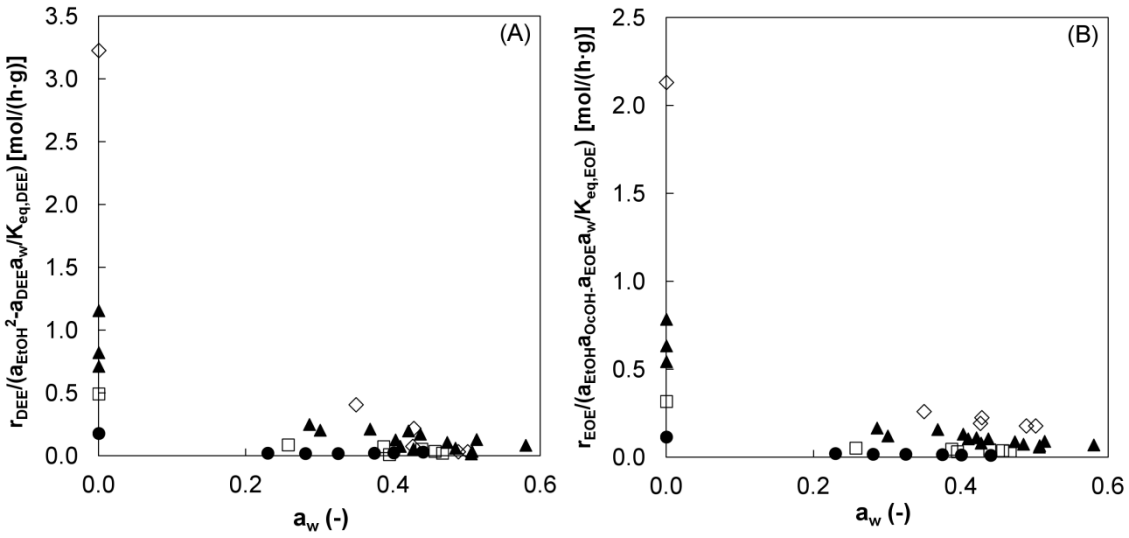


Fig. 7.8: Reaction rates divided per the driving force of the surface reaction of DEE (A) and EOE (B) formation as a function of the $a_w$. ◊ 190ºC; ▲177ºC; □ 164ºC; ● 150ºC.

**Modelling of kinetic data**

Based on the reaction rate dependence, and considering the LHHW or ER formalisms by assuming that surface reaction is the rate-limiting step [54], [89], [92]–[94], [114], [115], [116] the basic kinetic models are;

$$r_{DEE} = \frac{k_{DEE} \cdot \left( a_{EtOH}^2 - a_{DEE} a_w \Big/ K_{eq,DEE} \right)}{(1 + K_{EtOH} a_{EtOH} + K_{OcOH} a_{OcOH} + K_w a_w)^n} \qquad \text{eq. 7.22}$$

$$r_{EOE} = \frac{k_{EOE} \cdot \left( a_{EtOH} a_{OcOH} - a_{EOE} a_w \Big/ K_{eq,EOE} \right)}{(1 + K_{EtOH} a_{EtOH} + K_{OcOH} a_{OcOH} + K_w a_w)^n} \qquad \text{eq. 7.23}$$

Three parts can be distinguished in the kinetic expressions (eq. 7.22 and 7.23): the kinetic term, the driving force and the adsorption term. The kinetic terms, $k_{DEE}$ and $k_{EOE}$, are the product of the surface rate constants and the adsorption equilibrium constants. The particular form how constants are grouped depends on the formalism (LHHW or ER) [44], [89]. The kinetic terms are expected to be only temperature dependent according to Arrhenius law. The driving force accounts for the distance to the equilibrium position. The values of the thermodynamic equilibrium constants, $K_{eq,i}$, were found experimentally in the previous section (see eq. 7.11 and eq. 7.12). The adsorption term of the general expression accounts for the adsorption of each species on the active sites of the catalysts. Simplified models can be obtained by assuming the adsorption of some substances to be negligible in front of that of the others. Likewise, simplified

models are doubled if the fraction of unoccupied sites in the catalyst is considered significant or not (by taking values of 0 if it is assumed the number of unoccupied sites to be negligible, or 1 if this assumption is neglected). Finally, one of the parameters to be determined is the exponent of the adsorption term related to the number of active centers that participates in the surface reaction step. In this work, the exponent of the adsorption term has been varied from 1 to 3.

Table 7.7 shows all the possible kinetic expressions for DEE and EOE formation, derived from eq. 7.21 and 7.22, which were fitted to the experimental data (36 models). Optimal values of the parameters have been obtained by minimization of the sum of squared relative errors (SSRR), based on Levenberg-Marquardt algorithm (eq. 7.24). Relative errors were used instead of the absolute ones as relative error is assumed to be similar in whole temperature range.

$$SSRR=\sum\left(\frac{r_{exp}-r_{calc}}{r_{exp}}\right)^2 \qquad \text{eq. 7.24}$$

Table 7.7: Kinetic models tested with n values ranging from 1 to 3.

| model | $r_{DEE}$ | $r_{EOE}$ |
|---|---|---|
| 1 | $\frac{k_{DEE}\left(a_{EtOH}^2-a_{DEE}a_w/K_{eq,DEE}\right)}{\left(a_{EtOH}+\left(K_w/K_{EtOH}\right)a_w\right)^n}$ | $\frac{k_{EOE}\left(a_{EtOH}a_{OcOH}-a_{EOE}a_w/K_{eq,EOE}\right)}{\left(a_{EtOH}+\left(K_w/K_{EtOH}\right)a_w\right)^n}$ |
| 2 | $\frac{k_{DEE}\left(a_{EtOH}^2-a_{DEE}a_w/K_{eq,DEE}\right)}{\left(a_{OcOH}+\left(K_w/K_{EtOH}\right)a_w\right)^n}$ | $\frac{k_{EOE}\left(a_{EtOH}a_{OcOH}-a_{EOE}a_w/K_{eq,EOE}\right)}{\left(a_{OcOH}+\left(K_w/K_{EtOH}\right)a_w\right)^n}$ |
| 3 | $\frac{k_{DEE}\left(a_{EtOH}^2-a_{DEE}a_w/K_{eq,DEE}\right)}{\left(a_{EtOH}+\left(K_{OcOH}/K_{EtOH}\right)a_{OcOH}+\left(K_w/K_{EtOH}\right)a_w\right)^n}$ | $\frac{k_{EOE}\left(a_{EtOH}a_{OcOH}-a_{EOE}a_w/K_{eq,EOE}\right)}{\left(a_{EtOH}+\left(K_{OcOH}/K_{EtOH}\right)a_{OcOH}+\left(K_w/K_{EtOH}\right)a_w\right)^n}$ |
| 4 | $\frac{k_{DEE}\left(a_{EtOH}^2-a_{DEE}a_w/K_{eq,DEE}\right)}{\left(1+K_{EtOH}a_{EtOH}+K_wa_w\right)^n}$ | $\frac{k_{EOE}\left(a_{EtOH}a_{OcOH}-a_{EOE}a_w/K_{eq,EOE}\right)}{\left(1+K_{EtOH}a_{EtOH}+K_wa_w\right)^n}$ |
| 5 | $\frac{k_{DEE}\left(a_{EtOH}^2-a_{DEE}a_w/K_{eq,DEE}\right)}{\left(1+K_{OcOH}a_{OcOH}+K_wa_w\right)^n}$ | $\frac{k_{EOE}\left(a_{EtOH}a_{OcOH}-a_{EOE}a_w/K_{eq,EOE}\right)}{\left(1+K_{OcOH}a_{OcOH}+K_wa_w\right)^n}$ |
| 6 | $\frac{k_{DEE}\left(a_{EtOH}^2-a_{DEE}a_w/K_{eq,DEE}\right)}{\left(1+K_{EtOH}a_{EtOH}+K_{OcOH}a_{OcOH}+K_wa_w\right)^n}$ | $\frac{k_{EOE}\left(a_{EtOH}a_{OcOH}-a_{EOE}a_w/K_{eq,EOE}\right)}{\left(1+K_{EtOH}a_{EtOH}+K_{OcOH}a_{OcOH}+K_wa_w\right)^n}$ |

The kinetic fit was performed at each temperature separately. It was observed that kinetic constants were highly temperature dependent, as expected. On the contrary, the adsorption equilibrium constants (models 4-6), or else, the adsorption constant ratios (models 1-3) were low sensitive to the temperature. As a consequence, a satisfactory description of the reaction rates of EOE and DEE formations were obtained by using values of the adsorption coefficients which are independent of the temperature.

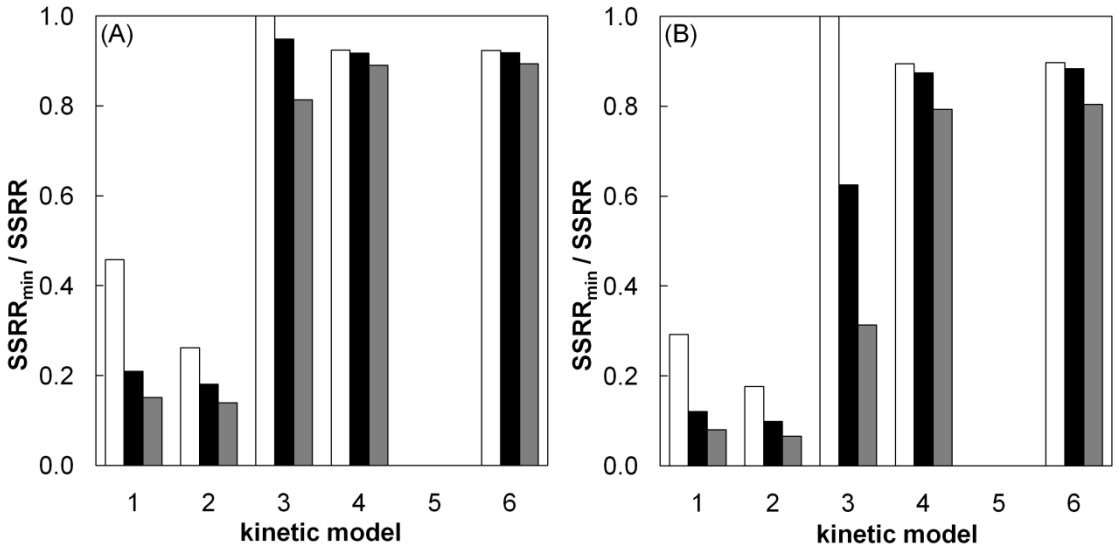


Fig. 7.9: Comparison of goodness of fit in terms of $SSRR_{min}/SSRR$ of DEE (A) and EOE (B) formations. □n=1 ■ n=2 ■ n=3.

Fig. 7.9 gathers the goodness of the fitted for the different kinetic models. A value of 1 corresponds to the minimum of squares, and as a result, the best fit. As observed in Fig. 7.9, models 5.1, 5.2 and 5.3 were rejected, as a consequence that they presented negative adsorption constants. A closer look at those models leads to infer that in both reactions

a) The best models are explained by the participation of 1 sulfonic group in the surface-reaction step.
b) The number of unoccupied active centers in the catalyst during the reaction is not significant, what seems reliable in alcohol liquid-phase dehydrations.
c) The best kinetic models of DEE and EOE formations are those where adsorption of both EtOH and OcOH is present. This fact is in agreement with chapter 5 that states that both OcOH and EtOH are present into the acidic ion-exchange resins, possibly in a similar composition to the bulk solution.

Accordingly, the best models with the optimal fitted parameters appeared to be

$$r_{DEE}\left[\frac{mol}{h\cdot g}\right]=\frac{2.10\cdot10^{11}\exp\left(-11983/RT\right)\left(a_{EtOH}^{2}-a_{DEE}a_{water}/K_{eq,DEE}\right)}{a_{EtOH}+0.5a_{OcOH}+11.7a_{water}};\quad K_{eq,DEE}=\exp\left(\frac{1691}{T}-1.4\right)\qquad \text{eq. 7.25}$$

$$r_{EOE}\left[\frac{mol}{h\cdot g}\right]=\frac{7.04\cdot10^{11}\exp\left(-12620/RT\right)\left(a_{EtOH}a_{OcOH}-a_{EOE}a_{water}/K_{eq,EOE}\right)}{a_{EtOH}+0.5a_{OcOH}+11.7a_{water}};\quad K_{eq,EOE}=\exp\left(\frac{3374.8}{T}-4.3\right)\qquad \text{eq. 7.26}$$

where T is expressed in K.

In Fig. 7.10 is compared the calculated reaction rates to DEE from eq. 7.25 (A) and to EOE from eq. 7.26 (B) versus experimental reaction rates. Proposed models are able to predict the experimental data with similar deviations, independently of the reactor used, what enhances the reliability of both expressions. In addition, residuals of the fitted equations proved to be randomly distributed in the whole range of reaction rates explored (Fig. 7.11).

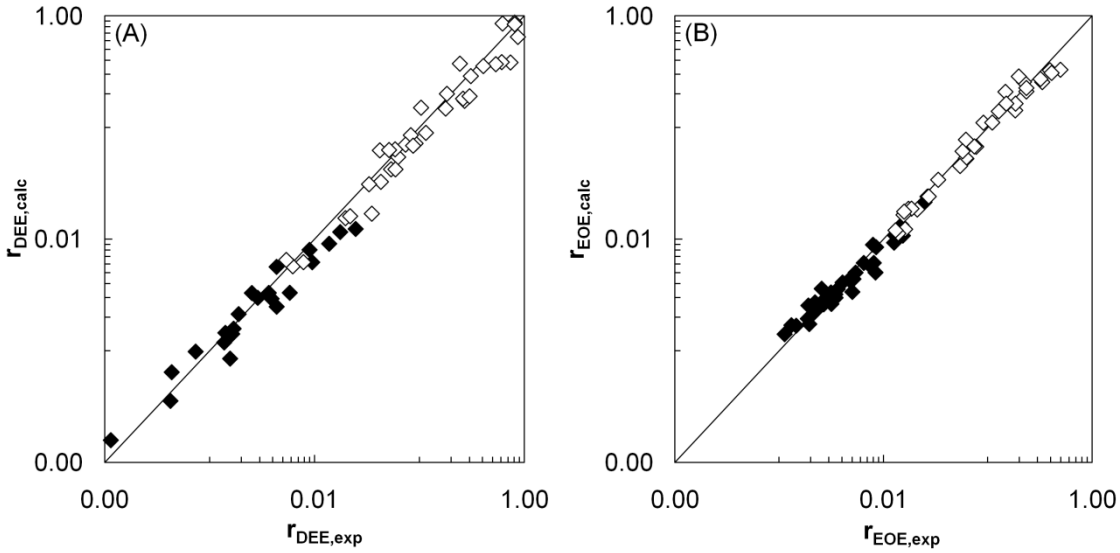


Fig. 7.10: Calculated reaction rates by eq. 7.25 (A) and by eq. 7.26 (B) versus experimental rates. Open symbols represent the experimental data by using the fixed-bed reactor and closed symbols by using the batch reactor.

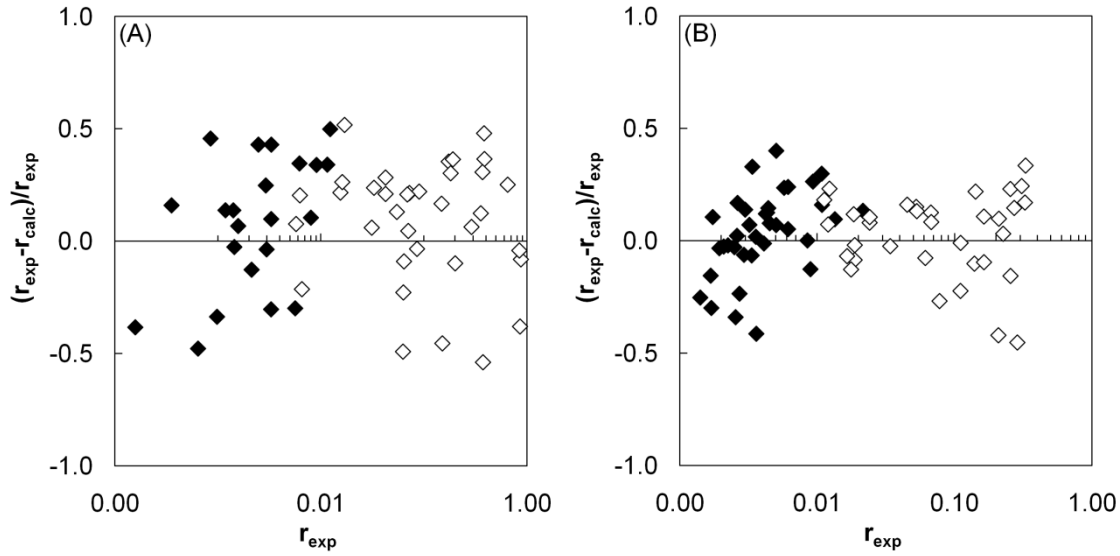


Fig. 7.11: Residuals distribution for eq. 7.25 (A) and by eq. 7.26 (B). Open symbols represent the experimental data by using the fixed-bed reactor and closed symbols by using the batch reactor.

With respect to the parameter values, $E_a$ values are obtained from the kinetic term of eqs. 7.25 and 7.26. In Fig. 7.12 shows that the apparent rate constant of eqs. 4 and 5 follows an Arrhenius temperature dependence (7.12A and 7.12B, respectively). Similar dependence on the temperature was observed for EOE formation, $E_{a,EOE}$=105 ± 4 kJ/mol, than for DEE formation, $E_{a,DEE}$=100 ± 5 kJ/mol. It is to be noted that the obtained $E_a$ value of EOE formation from OcOH and EtOH on Amberlyst 70 is slightly lower than that obtained on a preliminary study over Dowex 50Wx2 (117 ± 5 kJ/mol) and in the range of the dehydration reactions of 1-pentanol to di-n-pentyl ether and 1-hexanol to di-n-hexyl ether (115 ± 5 and 108 ± 5 kJ/mol, respectively) [26], [27].

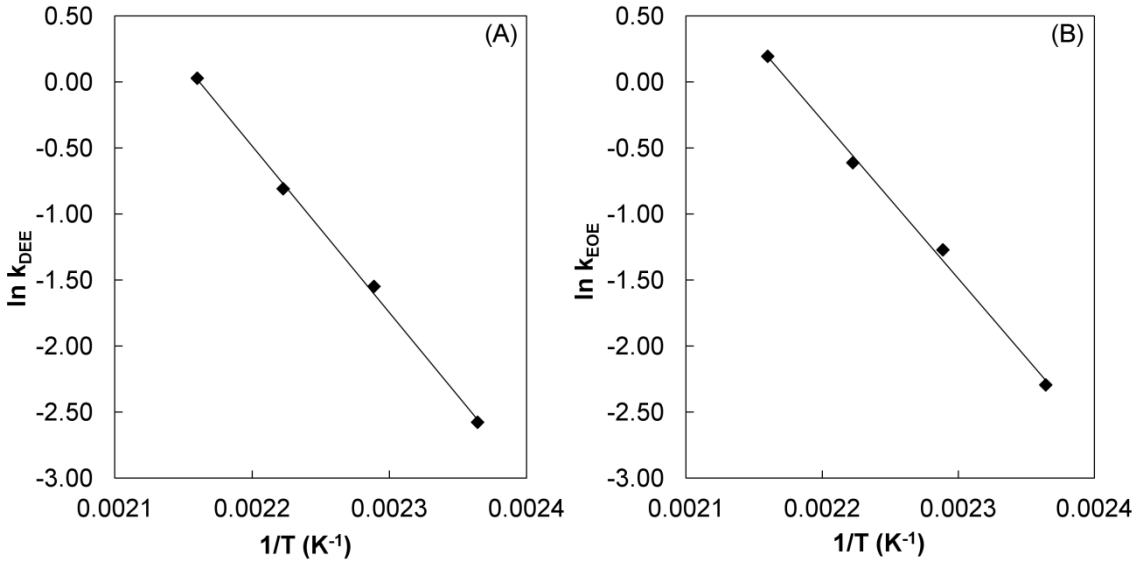


Fig. 7.12: Arrhenius plot of the kinetic term of DEE (A) and of EOE (B) formations.

As concerns to adsorption constants, $K_w$ / $K_{EtOH}$=11.7 ± 1.0 and $K_{OcOH}$ / $K_{EtOH}$=0.5 ± 0.1 values were obtained. Thus, the following trend is inferred: $K_{water}$ >> $K_{EtOH}$ > $K_{OcOH}$, in agreement with reported literature [5]. The role attributed to water in the proposed expressions assumes a strong competitive adsorption by competing with EtOH and OcOH for acid centers, being the $K_w$ 12-fold than that of EtOH and 23-fold than that of OcOH. Therefore, reaction rates to DEE and to EOE are greatly affected by the presence of water in the liquid-phase.

The strong inhibitor effects of water on EOE formation by using an acid resin are still much lower than those observed in the synthesis of bisphenol A, being $K_w$ two orders of magnitude higher than those of acetone and phenol [115]. This fact is most probably a result of the also greater affinity of EtOH and OcOH for acid sites, which competes with water, than those of acetone and phenol that have less affinity for acid sites.

## 7.4 Conclusions

From the larger equilibrium values obtained from EOE synthesis reaction, it can be concluded that EOE synthesis is more shifted to products than DEE reaction. Such observation is in agreement with the literature data on linear ethers formation, where as a general rule, the longer the ether chain formed, the higher the experimental equilibrium values are.

Both alcohol dehydration reactions proved to be exothermic, with a reaction enthalpy change (at 25ºC) of -(18.9 ± 1.3) kJ/mol for EOE synthesis, and -(12.1 ± 0.9) kJ/mol for DEE synthesis, in the same magnitude order than other dialkyl ethers. Concerning reaction entropy changes, both reaction showed negative values, being -(13.6 ± 4.2) J/(K·mol) for EOE synthesis and -(7.6 ± 2.1) J/(K·mol) for DEE synthesis. Standard formation enthalpy and molar entropy of EOE were computed to be -(436 ± 7) kJ/mol and -(434 ± 11) J/(mol·K), respectively.

A kinetic model in terms of compound activities to describe the formation of ethyl octyl ether from ethanol and 1-octanol is proposed. From the proposed model it is inferred that the fraction of free actives sites is negligible and only one acid site seems to take part in the surface reaction step, which is considered as the rate-limiting step of the mechanism.

The adsorption equilibrium constants of the formed ethers are negligible compared with that of alcohols and water. Thus, it is considered that diethyl ether and ethyl octyl ether are released directly to the liquid-phase. On the contrary, reaction rates were highly sensitive to water content, by clearly showing strong inhibiting effects. Eventually, the apparent activation energy for the ethyl octyl ether reaction is about 105 ± 4 kJ/mol, a similar dependence on the temperature to that of the main side product diethyl ether, 100 ± 5 kJ/mol.

Chapter 8

# Influence of the functionalization degree of acidic ion-exchange resins on ethyl octyl ether formation

A SUMMARY OF THIS CHAPTER HAS BEEN PRESENTED AS AN ORAL COMMUNICATION IN:

J. Guilera, L. Hankova, K. Jerabek, E. Ramírez, J. Tejero. Influence of the sulfonation degree of acidic ion-exchange resins on ethyl octyl ether formation. **June 2013**. Presented at CAFC10 (Congress on Catalysis Applied to Fine Chemicals), Turku, Finland.

## 8.1 Introduction

EOE production has to compete with the less steric demanding DEE formation, obtained from the ethylating agent, EtOH or DEC. Thus, the loss of bioethanol molecules by DEE formation is a serious industrial trouble as this ether cannot be blended straightforwardly in commercial diesel fuels. Steric hindrances within the catalyst play a determinant role on the selectivity to EOE or to DEE. A greatly expanded polymer in the reaction medium favours the diffusion of bulky reactants molecules, such as OcOH, inside the catalysts and EOE production is maximized (Chapter 3 and 4). In general, this desired flexible structure can be achieved by decreasing the crosslinking degree of the resin. Nevertheless, it is worth mentioning that an extensive catalyst swelling reduces the efficiency per unit of volume of the catalyst bed [37].

Another tailoring technique to reduce steric limitations could be achieved by controlling the location of acid centers. This concept was patented by Chevron Research Company in 1972 and attempts to reduce the amount of by-products by using resins with less amount of acid groups, but more accessible ones. Such invention reduced the extent of isobutene polymerization process by partially neutralizing the resin capacity [117]. Instead of neutralizing acid groups, McMaster and Gilliland limited the sulfonation time with the aim of limiting location of the sulfonic groups to the pellicular layer at the surface of the polymer beads [118], [119]. Further step was then partial sulfonation of porous (macroreticular) polymer beads gradually advancing in the whole volume of the polymer beads from pore wall surface into deeper layers of polymer matrix. In 1995, Rohm and Haas Company patented the use of such partially functionalized resins for esterification process, favoring in this way the formation of esters over the formation of ethers [120]. Eventually, the partially sulfonated macroreticular resin Amberlyst 46 (hereinafter termed surface sulfonated) has been commercialized [41].

The term surface sulfonated refers to a functionalization near to the surface of the polymer gel-phase and it is not restricted to only the surface layer. As a result, Amberlyst 46 has a heterogeneous distribution of the sulfonic groups, with a sulfonated shell enveloping an inner non-sulfonated polymer core. Thus, the polymer has great morphological differences depending on the polymer depth. The external layers posses an strong hydrophilic character, whereas the inner part has an hydrophobic one [9], [42]. Nowadays, specific acid site distribution in Amberlyst 46 has been used to study the influence of the acid sites location on many reaction processes, as well, to optimize the selectivity to the desired products [121]–[126].

In previous chapters, a relationship between the resin crosslinking degree and the EOE yield was found. In the present work, the influence of the resin functionalization degree on EOE formation is explored.

## 8.2 Experimental procedure

A series of partially sulfonated resins were prepared from a macroreticular PS-DVB copolymer (DVB content about 20 %) originally manufactured as an intermediate for production of ion exchanger Ostion KSPC (Spolchemie, Ústí nad Labem, Czech Republic). For to achieve low to intermediate sulfonation degrees, 15 g of the polymer was placed in 100 mL of concentrated sulphuric acid and afterwards, the mixture was stirred and heated for 6 hours at a temperature selected for to achieve the desired degree of sulfonation (T=30-80ºC). These conditions (long reaction time and control of the conversion by reaction temperature) were chosen with the aim of limiting differences in the sulfonation degree at the periphery and center of the polymer beads. Then, the mixture was cooled down slowly and slowly diluted by percolation with sulphuric acid solution of gradually diminishing concentration (90, 70, 50, 30 and 10 v/v %). Eventually, the product was washed with deionized water till neutral pH of the eluent. Additionally, two samples with higher sulfonation degree were prepared by sulfonation of polymer pre-swollen in DCE overnight.

The performance of a series of partially sulfonated resins was tested over two reaction pathways for obtaining EOE: the dehydration of OcOH and EtOH; and the transesterification reaction between OcOH and DEC to EOC, and its subsequent decomposition to EOE.

Catalytic tests were performed in the batch reactor (described in section 2.3.1). Resins were previously dried at 110ºC under vacuum overnight. Then, the reactor was loaded with 70 mL of OcOH / DEC mixture (molar ratio, $R_{OcOH/DEC}$=2) or OcOH / EtOH mixture (molar ratio, $R_{OcOH/EtOH}$=1), stirred at 500 rpm and heated up to 150ºC. Pressure was set at 25 bar with $N_2$ to maintain the liquid-phase. When the mixture reached the working temperature, dried catalyst (1g) was injected into the reactor. Catalyst injection was taken as zero time. Experiments lasted 6h.

Conversion ($X_j$) and selectivity ($S_j^k$) were computed by eqs 8.1 and 8.2, respectively.

$$X_j = \frac{\text{mole of j reacted}}{\text{mole of j initially}} \times 100 \left[\%, \text{mol/mol}\right] \qquad \text{eq. 8.1}$$

$$S_j^k = \frac{\text{mole of j reacted to form k}}{\text{mole of j reacted}} \times 100 \left[\%, \text{mol/mol}\right] \qquad \text{eq. 8.2}$$

Relative turnover frequency ($TOF_{rel}$) of each catalyst with respect to the least sulfonated catalyst, 306, was computed by eq 8.3. Initial turnover frequency (TOF) of EtOH and OcOH reaction to form EOE and that of DEC and OcOH reaction to form EOC; were computed from the functions of formed moles vs. time, as described in former chapters.

$$TOF_{rel} = \frac{TOF_i}{TOF_{306}} [-] \qquad \text{eq. 8.3}$$

## 8.3 Results and discussion

### 8.3.1 Catalyst preparation

A series of partially functionalized catalysts were prepared by the procedure described in the previous section. As Table 8.1 shows, resins prepared without adding a pre-swelling solvent presented acid capacity ranging from 0.81 to 3.10 mmol $H^+$/g. The functionalization degree on those polymers was clearly controlled by the reaction temperature. Additionally, it was checked that the acid capacity was not increased by enlarging the reaction time from 6 to 12 h at 80ºC (3.10 ± 0.02 and 3.02 ± 0.13, respectively). Thus, it can be considered that after 6 h at 80ºC, the sulfonation reaction did not proceed. Accordingly, without the use of a swelling solvent a maximum of 3.10 mmol $H^+$/g of acid capacity were achieved, as a result of diffusion restrictions of acid sulphuric within the gel-phase.

Table 8.1: Description of the sulfonation procedure and the acid capacity of synthesized catalysts. Sulfonation time=6h.

| catalyst | solvent | T (ºC) | meq $H^+$/g[a] |
|---|---|---|---|
| 306 | no | 30 | 0.81 |
| 406 | no | 40 | 0.99 |
| 606 | no | 60 | 1.89 |
| 806 | no | 80 | 3.10 |
| D806A | DCE | 80 | 4.02 |
| D806B | DCE | 80 | 4.37 |

[a] titration against standard base

On the other hand, higher acid capacities were achieved (4.02-4.37 mmol $H^+$/g) at the same temperature by using DCE as solvent. It was used to pre-swell initially the PS-DVB sample (lipophilic character), and in this way, to make easier the permeation of sulphuric acid from the bead surface to the least accessible zones of the polymer skeleton. The resin D806B is a repetition sample of D806A with a slight modification of the preparation conditions. In the synthesis of D806B, it was diminished the DCE amount to bare minimum for the polymer swelling (50 mL), instead of the 100 mL of DCE used in the synthesis of D806A.

### 8.3.2 Catalyst characterization

The morphological properties of the prepared catalysts and those of the commercial ones were evaluated in dry and swollen state. Fig. 8.1 displays the surface areas in dry state as a function of the acid capacity of catalysts. It is observed that the higher the functionalization degree, the lower the surface area in dry state. The same pattern could be observed on the commercial

catalysts. These results can be explained by the fact that as higher the hydrophilic character of the polymer is, higher the pore collapse after the drying procedure was.

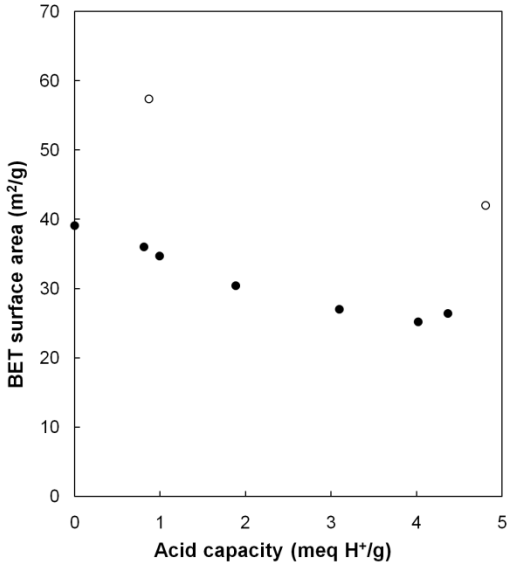


Fig. 8.1: BET surface area of the resins versus the acid capacity. ●prepared ○ commercial.

As seen in former chapters, resins swell in contact with liquids and their morphology is drastically changed. Accordingly, the surface area in dry state is only an indication of the polymeric structure and the measurements are not likely to be far from their working-state morphology. A suitable picture of such morphological modifications is provided by the resin swelling degree in the desired medium. As the catalytic tests were performed essentially in a polar environment, water was selected as representative solvent.

The swelling results are presented in Fig. 8.2. The bead swelling increased as higher was the acid capacity of catalysts. The results show that the least sulfonated polymers have negligible swelling in water as a result of the lipophilic character of the unsulfonated polymer. As for the medium sulfonated catalysts, the functionalized parts are surrounded by too much of the unsulfonated ones that prevents their fully expansion. Then, the presence of sulfonic groups in the whole gel-phase changed the initial lipophilic character of the polymer to a hydrophilic one. Consequently, the bead expansion was greatly enhanced in the most sulfonated polymers.

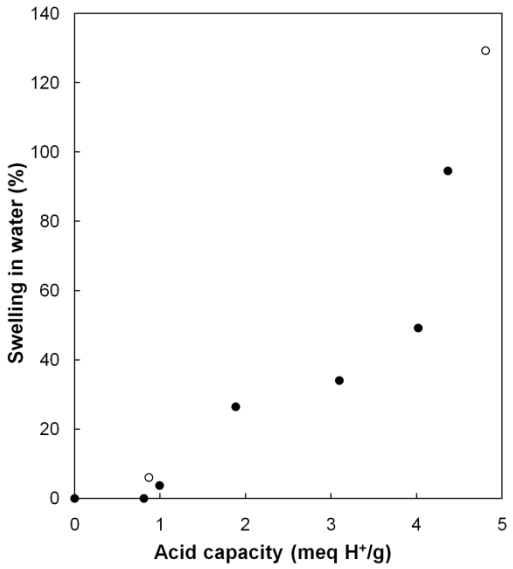


Fig. 8.2: Volume resin swelling versus the acid capacity of the resins. ●prepared; ○ commercial.

In addition to quantify the bead swelling, an extensive description of nature and characteristics of the polymeric pores can be obtained from ISEC technique. ISEC measurements provide information about the true pores and the gel-phase spaces in swollen state. The morphology of the starting polymer was assessed both in aqueous and in organic solvent. As Table 8.2 shows, the starting polymer showed in the two solvents a highly dense gel-phase structure in the 1.5 $nm^{-2}$ zone and large pores in the 30-60 µm range. Differences between organic and aqueous environment were found in the total porosity detected. Organic measurements showed twice volume of true pores than in water. However, the divergences were especially high in the gel-phase. In aqueous environment, the volume detected in the gel-phase was almost negligible, whereas it was 12-fold higher in organic solvent. Alternative ISEC measurements confirmed the lipophilic character of the starting polymer.

Table 8.2: Volumes of different density zones ($cm^3/g$) of the starting polymer provided from ISEC measurements.

| | $d_{pore}$ (nm) | tetrahydrofuran | water |
|---|---|---|---|
| macropores | 60 | 0.52 | 0.08 |
| | 30 | 0.35 | 0.42 |
| | 20 | | |
| | 15 | | |
| | 12 | | |
| | 8 | | |
| | polymer fraction density ($nm^{-2}$) | tetrahydrofuran | water |
| gel-phase | 0.1 | | |
| | 0.2 | | |
| | 0.4 | | |
| | 0.8 | | |
| | 1.5 | 0.60 | 0.05 |

With respect to the functionalized resins, ISEC experiments were performed in aqueous environment. The volume contribution of each true pore diameter is shown in Fig. 8.3. As concerns to the prepared catalysts, the least sulfonated catalyst showed very narrow true pores (in the 8-12 nm zone). In contrast, the true pore diameter ranged in the 30-60 nm zone in the most sulfonated ones. Accordingly, the diameter of true pores increased as more functionalized was the resin. By taking into account that the total true pore volume was not increased, results suggests that some true pores increased their original size and others disappeared as a result of the gel-phase expansion. The commercial catalysts presented a similar trend. The low sulfonated catalyst Amberlyst 46 only showed narrow pores (12 nm); while the fully sulfonated Amberlyst 15 presented a wide range of pore diameters, including large pores (12-60 nm).

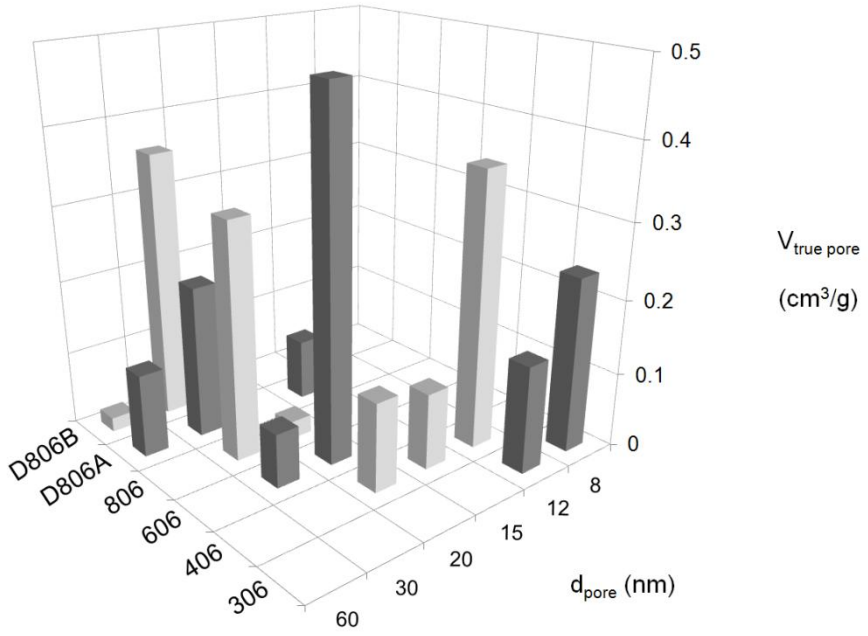


Fig. 8.3: ISEC pattern of the true pores.

With respect to the gel-phase morphology, Fig. 8.4 shows the volume contribution of each polymer chain fraction. As a general rule, the $V_{sp}$ was increased as more sulfonic groups were attached in the polymer skeleton. In agreement with the swelling measurements, the presence of sulfonic groups changed the initial lipophilic character of polymer phase to a partially or fully hydrophilic one. As for the quality of the gel-phase of the prepared catalysts, it appeared residual volumes in the least dense fractions in the most sulfonated resins. Nevertheless, the compact and poorly swollen polymer domain predominated in the entire series of sulfonated resins. As for the commercial catalysts, the gel-phase was even more rigid than the prepared ones by only showing the densest gel-phase fraction (1.5 $nm^{-2}$). This fact can be a consequence of a slightly higher crosslinking degree in the PS-DVB copolymers of Amberlyst 15 and Amberlyst 46 than that of the prepared catalysts.

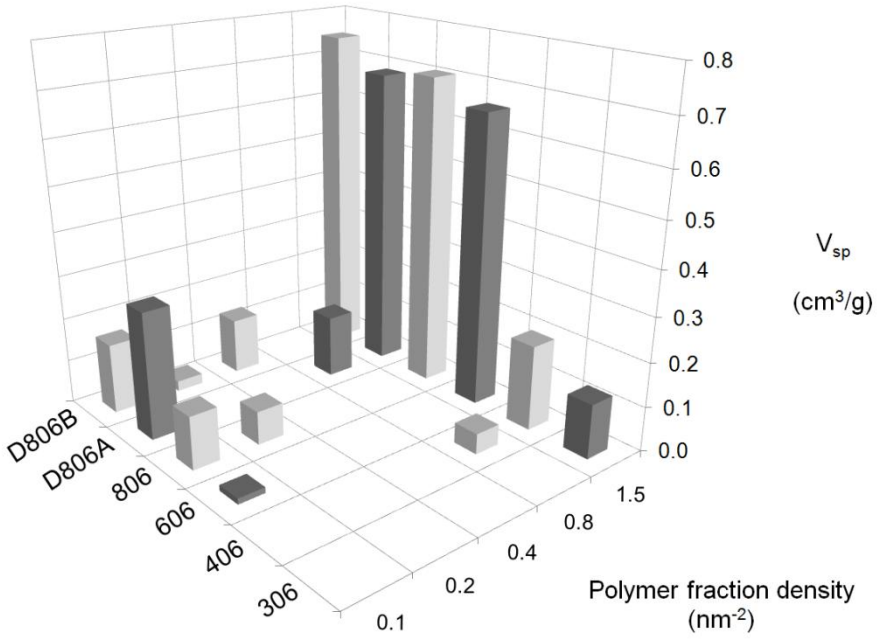


Fig. 8.4: ISEC pattern of the gel-phase.

After discussing the ISEC and swelling results, a schematic representation of the sulfonation process is proposed in Fig. 8.5. At the first sulfonation stage, the sulphonic groups were presumably located in the surface of microspheres, whereas the internal part remained unsulfonated. In these catalysts, interstitial volumes among gel-phase agglomerates were observed. Then, the progressive presence of sulfonic groups changed the lipophilic character of the gel-phase to hydrophilic, allowing water to swell it. In this procedure, gel-phase was progressively expanded and narrow true pores disappeared.

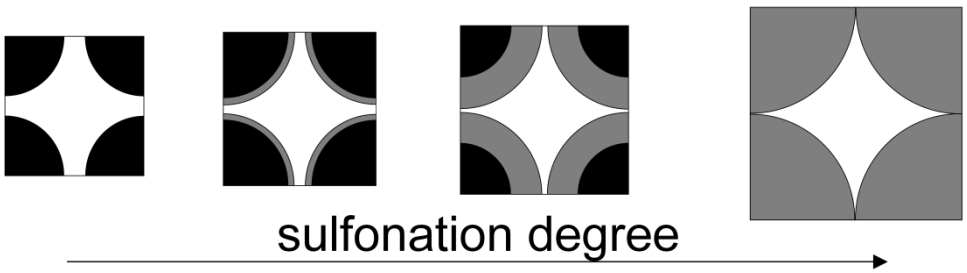


Fig. 8.5: Proposed morphological scheme of the sulfonation process.
●non sulfonated domain ●sulfonated domain; ○ true pores.

### 8.3.3 Catalytic tests

**OcOH / EtOH reaction system**

Table 8.3: Conversions (%) and selectivities (%) by using OcOH and EtOH as reactants. T=150ºC, P=25 bar, $R_{OcOH/EtOH}$=1, $W_{cat}$=1g, t=6h.

| catalyst | $X_{EtOH}$ | $X_{OcOH}$ | $S_{EtOH}^{EOE}$ | $S_{EtOH}^{DEE}$ | $S_{OcOH}^{EOE}$ | $S_{OcOH}^{DNOE}$ |
|---|---|---|---|---|---|---|
| 306 | 6.1 | 2.5 | 32.4 | 67.6 | 70.1 | 29.9 |
| Amberlyst 46 | 8.7 | 2.6 | 31.9 | 68.1 | 80.7 | 19.3 |
| 406 | 7.7 | 2.7 | 32.7 | 67.3 | 79.4 | 20.6 |
| 606 | 17.5 | 4.6 | 26.1 | 73.9 | 79.6 | 20.4 |
| 806 | 31.1 | 4.8 | 16.3 | 83.7 | 85.3 | 14.7 |
| D806A | 40.1 | 4.9 | 13.6 | 86.4 | 86.7 | 13.3 |
| D806B | 41.9 | 5.0 | 13.6 | 86.4 | 83.5 | 16.5 |
| Amberlyst 15 | 46.9 | 4.7 | 11.0 | 89.0 | 84.3 | 15.7 |

Table 8.3 summarizes the catalytic performance of the prepared sulfonated resins and the two commercial ones, Amberlyst 15 and 46, on the reaction of EOE formation from OcOH and EtOH. Conversion data show that EtOH reacts always faster ($X_{EtOH}$=6.1-46.9%) than OcOH ($X_{OcOH}$=2.5-5.0%). The difference between $X_{EtOH}$ and $X_{OcOH}$ were increased clearly with functionalization degree of the resin. As observed, they were especially pronounced in the more sulfonated catalysts. Fig. 8.6 displays the OcOH and EtOH conversions as the relative values, compared always to the most active catalyst, Amberlyst 15. Relative conversions of EtOH increased proportionally as the number of acid centers of the catalysts increased. Thus, it can be assumed from Fig. 8.6 that all the acid sites were accessible to EtOH molecules. Much less marked was the dependence of the sterically more demanding OcOH conversion on the acid capacity. The OcOH conversion pattern suggests that the acidic groups introduced in the latest stages of the sulfonation were attached to the least accessible zone of polymer skeleton, where OcOH accessibility was very poor.

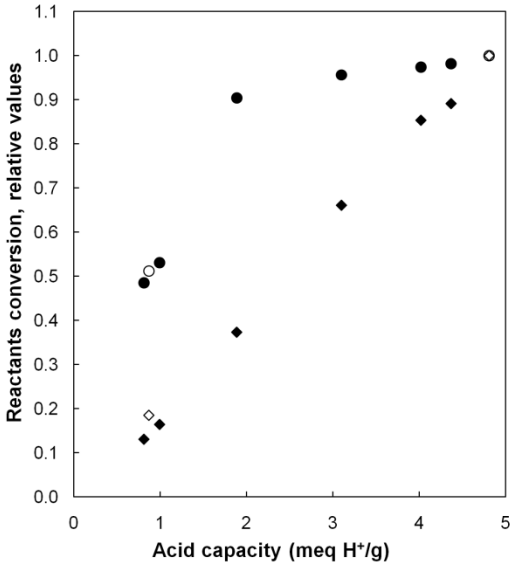


Fig. 8.6: OcOH (●) and EtOH (♦) conversion as a function of acid capacity of catalysts. T=150ºC, P=25 bar, $R_{OcOH/EtOH}$=1, W=1g, t=6h. Filled symbols represent prepared catalysts and open symbols represent commercial resins.

As for the selectivities, Table 8.3 reveals that for each alcohol the production of the ether with lower molecular weight, less sterically demanding ($S_{EtOH}^{DEE} > S_{EtOH}^{EOE}$ and $S_{OcOH}^{EOE} > S_{OcOH}^{DNOE}$) was the most favoured reaction. Such behaviour was more noticeable in the more sulfonated catalysts, what confirms that the reaction was sterically hindered within those sulfonated resins. On a fully sulfonated resin (Amberlyst 15), only 11% of the reacted EtOH was converted to EOE, whereas it was raised to 32% by using the least sulfonated resin (306). Similar behaviour was observed for OcOH. Fig. 8.7 shows the number of moles of DEE, EOE and DNOE formed over the acidic resins in the OcOH and EtOH reaction, where catalysts are ordered as a function of their acid capacity. It can be observed that the production of DEE was maximized in the most sulfonated catalysts. In contrast, such pattern was not observed for the ethers that require OcOH as reactant (EOE and DNOE). The product distribution profile suggests that the last acid centers added to the polymer skeleton were not as efficient as the first ones to catalyze the EOE and DNOE formations.

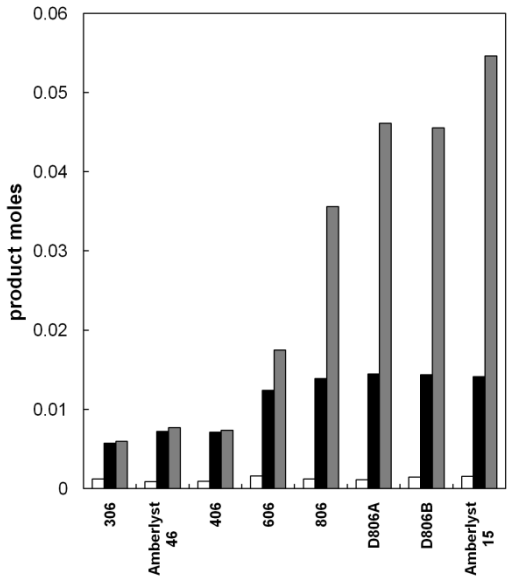


Fig. 8.7: Moles of DEE (■), EOE (■) and DNOE (□) formed from OcOH and EtOH on the sulfonated catalysts. T=150ºC, P=25 bar, $R_{OcOH/OcOH}$=1, $W_{cat}$=1g, t=6h.

**OcOH / DEC reaction system**

Table 8.4. Conversions (%) and selectivities (%) by using OcOH and DEC as reactants. T=150ºC, P=25 bar, $R_{OcOH/DEC}$=2, $W_{cat}$=1g, t=6h.

| catalyst | $X_{DEC}$ | $X_{OcOH}$ | $S_{DEC}^{EOE}$ | $S_{DEC}^{EOC}$ | $S_{DEC}^{DEE}$ | $S_{OcOH}^{EOE}$ | $S_{OcOH}^{EOC}$ | $S_{OcOH}^{DNOE}$ | $S_{OcOH}^{DOC}$ |
|---|---|---|---|---|---|---|---|---|---|
| 306 | 13.4 | 11.2 | 10.8 | 83.8 | 5.3 | 9.3 | 71.8 | 14.8 | 4.2 |
| Amberlyst 46 | 13.3 | 13.3 | 13.4 | 81.4 | 5.2 | 10.0 | 61.1 | 26.2 | 2.6 |
| 406 | 14.3 | 14.4 | 13.5 | 81.0 | 5.6 | 10.7 | 64.3 | 19.3 | 5.6 |
| 606 | 19.2 | 19.8 | 20.6 | 72.5 | 6.9 | 15.6 | 55.0 | 24.8 | 4.6 |
| 806 | 25.0 | 23.1 | 29.9 | 52.3 | 17.8 | 25.5 | 44.5 | 27.0 | 3.0 |
| D806A | 31.2 | 26.6 | 30.9 | 37.4 | 31.7 | 28.9 | 35.0 | 22.9 | 2.1 |
| D806B | 34.1 | 28.4 | 28.9 | 36.3 | 34.7 | 28.1 | 35.3 | 20.0 | 1.7 |
| Amberlyst 15 | 37.0 | 28.7 | 27.3 | 32.2 | 40.5 | 28.1 | 33.1 | 25.9 | 2.0 |

The catalytic behaviour of the sulfonated resins in the reaction between OcOH and DEC to form EOE is gathered in Table 8.4. After 6h, DEC conversions ranged from 13.3 to 37.0% and OcOH conversions from 11.2 to 28.7%. It is observed that OcOH conversions were higher in the reaction with DEC than with EtOH. Such behaviour can be explained by the affinity of reactants with sulfonated resins. The number of moles retained in the swollen resin follows this trend: EtOH > OcOH >> DEC, in agreement with their polarity [76]. In the OcOH / EtOH mixture, there is a higher amount EtOH than OcOH inside the resin, which favours EtOH conversion. On the contrary, in the OcOH / DEC mixture the liquid inside the resin is predominantly OcOH, which expedites the OcOH conversion.

Fig. 8.8 shows the OcOH and DEC conversions as the relative values, compared again to the most active catalyst, Amberlyst 15. With respect to DEC relative conversion, it increased linearly as a function of the acid capacity of the catalyst. DEC conversion pattern is similar to that previously observed for EtOH. Thus, it can be concluded that all the acid centers were accessible for both ethylating agents, DEC and EtOH. With respect to OcOH conversions, they were highly increased over the least sulfonated polymers, acid capacity less than 2 mmol $H^+$/g. Nevertheless, it is observed again a saturation region, in which the increase of OcOH conversion is low at the higher sulfonated degrees.

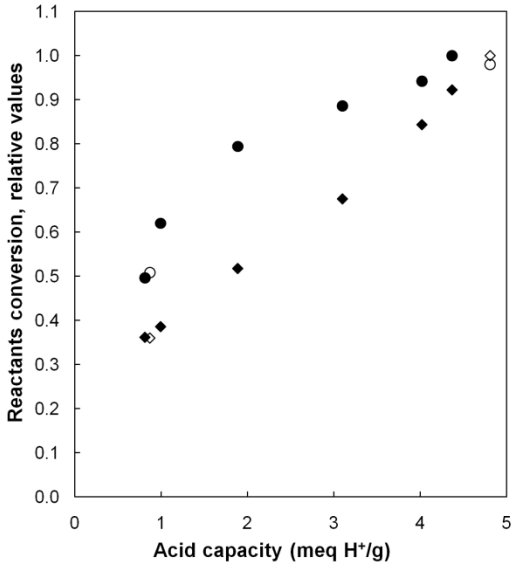


Fig. 8.8: OcOH (●) and DEC (♦) conversion as a function of acid capacity of catalysts. T=150ºC, P=25 bar, $R_{OcOH/DEC}$=2, W=1g, t=6h. Filled symbols are the prepared catalysts. Open symbols are the commercial ones.

In terms of selectivity, the formation of ethers from carbonates proceeds in two consecutive steps and intermediate compounds are involved (Table 8.4). Selectivity to DEE increased as the acid capacity of the catalysts increased. At the same time, the selectivity to EOE reaction pathway (EOC+EOE) diminished. It should be mentioned that at longer reaction time all EOC would be consumed to form EOE, and in the same way, DOC to form DNOE (described in detail in chapter 4). Fig. 8.9 displays the moles of products formed in the OcOH / DEC reaction system. For the sake of clarity, the intermediate compounds were plotted together with their corresponding ether. Thus, EOC, which would decompose to EOE at longer reaction time, was plotted together with EOE. Likewise, DOC and DNOE were plotted together. In this way, the formation of DEE, EOE and DNOE were displayed as competitive reactions, analogously as the first reaction system studied. As it is seen, the EOE reaction pathway was more favoured than the DEE formation. Nonetheless, DEE formation was highly increased in the more sulfonated catalysts, as a result of steric hindrances of EOE formation. With respect to DNOE formation, the ether with the highest molecular weight, its formation was low over all the tested catalysts

due to the highest sterically hindrances. However, selectivity to DNOE pathway (DOC+DNOE) was also decreased at the highest sulfonation degrees.

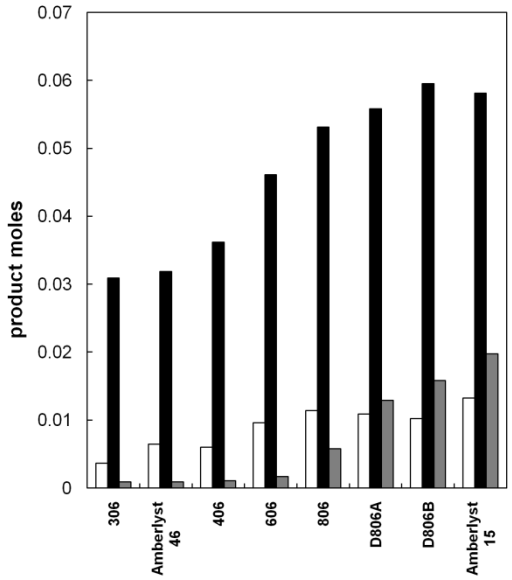


Fig. 8.9: Moles of DEE (■), EOE+EOC (■) and DNOE+DOC (□) formed from OcOH and DEC reaction on the catalysts. T=150ºC, P=25 bar, $R_{OcOH/DEC}$=1, W=1g, t=6h.

### 8.3.4 Relationship between resin morphology and catalytic activity

The degree of active site participation in the different resins can be estimated by assuming that all the acid groups of the least sulfonated catalyst, 306, are accessible and participating on the desired reaction (eq 8.3). Fig. 8.10 plots the $TOF_{rel}$ of EtOH and OcOH reaction to form EOE and DEC and OcOH reaction to form EOC (that would decompose to EOE) as a function of the acid capacity. Similar trend was observed on both reactions; the number of active sites that take part in the reaction dramatically decrease with the acid capacity. Surprisingly, the $TOF_{rel}$ values decrease from the very beginning of the sulfonation degree of catalysts. Thus, only a half of the 606 active sites (1.89 mmol $H^+$/g) would be involved in the dehydration of EtOH with OcOH and the transesterification of DEC with OcOH. With respect to the most sulfonated catalysts, only a third of active sites would be participating in such desired reactions. $TOF_{rel}$ values disclose that in the tested catalysts there is a relevant fraction of sulfonic groups, located in very dense polymer zones, unavailable for the EOE formation.

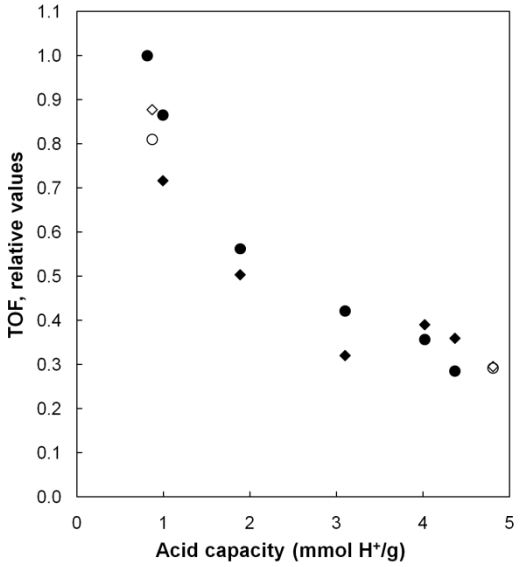


Fig. 8.10: $TOF_{rel}$ of EtOH and OcOH reaction to form EOE (♦) and $TOF_{rel}$ of DEC and OcOH reaction to form EOC (●) as a function of acid capacity of catalysts. T=150ºC, P=25 bar, $R_{OcOH/EtOH}$=1, W=1g, t=6h. Filled symbols represent prepared catalysts and open symbols represent commercial resins.

Analysis of ISEC data in aqueous media gives valuable qualitative information on the resin morphology in the reaction medium. In previous works, a successful correlation between the morphology depicted from ISEC data of fully sulfonated resins and catalytic activity were obtained for EOE synthesis. Apparently, EOE formation proceeds predominantly inside the swollen polymer gel matrix. This fact is assumed as a consequence of the fact that catalytic activity was much higher in gel-type polymers than macroreticular ones. Besides, steric restrictions were minimized over the resins that presented a highly swollen gel-phase in water ISEC measurements (chapter 3 and 4).

However, ISEC characterization technique was not able to predict the catalytic results in the present work. As quoted in the literature, the morphological description deduced from aqueous ISEC measurements is more complex on partially sulfonated resins [42]. This fact is a result of the presence of both lipophilic and hydrophilic domains. As it was revealed, the initial sulfonation stage influenced predominantly the more accessible, least dense, domains of the polymer mass. In the OcOH / EtOH and OcOH / DEC mixtures, the interaction of the organic moiety of OcOH with the unsulfonated polymer domains of the polymer skeleton most probably swelled it. By means of swelling of the unfunctionalized domains, the steric conditions were also improved in the sulfonated regions, as similarly observed by the presence of toluene in the phenol alkylation [42].

Nevertheless, the sulfonated form of these potentially low dense domains (0.1-0.4 $nm^{-2}$) cannot freely swell in ISEC measurements using water as solvent, due to hydrophobic surrounding domains that prevent its expansion. Accordingly, they were not detected by aqueous ISEC technique in the least sulfonated polymers (306, 406, 606) and only little expanded polymer with high density (1.5 $nm^{-2}$) was observed (Fig. 8.4). The poor water swelling observed by means of laser technique on low sulfonated resins would be consistent with this observation (Fig. 8.2). At higher sulfonation degrees, the unsulfonated domain was highly reduced and cannot prevent the fully expansion of the least crosslinked polymer domain. As a result, the less dense gel-phase (0.1-0.4 $nm^{-2}$) was only detected by ISEC technique in the most sulfonated resins (806, D806A, D806B).

## 8.4 Conclusions

The PS-DVB polymer used in this work presented a heterogeneous crosslinking degree within the gel-phase. Thus, acid centers are placed in zones of the polymer with different density. At the initial sulfonation stage, acid centers are only placed in the least dense domain of the polymer mass. At higher functionalization degrees, acid centers are also located in the least accessible zones of the resin.

Catalytic tests revealed the dependencies of the selectivity to EOE on the different polymer domain. The last sulfonated domain of the polymer is poorly accessible for OcOH molecules. As a result, the centers located in this domain are inefficient to produce EOE and DNOE. In contrast, the entire polymer domain is accessible for EtOH and DEC molecules. Accordingly, the latest acid centers added are only efficient to produce DEE.

It can be concluded that the EOE formation occurs mainly in the initially sulfonated, least dense zone. In contrast, DEE is formed in the whole polymer matrix. Therefore, for production of long chain ethers such as EOE or DNOE; which are preferred as diesel fuels using of partially sulfonated in macroreticular exchanger catalysts would be advantageous.

Chapter 9

# Summary and outlook

## 9.1 Summary

Ethyl octyl ether is a bioethanol-derived component that has excellent properties as diesel fuel. This work proved that ethyl octyl ether can be produced successfully in liquid-phase at the temperature range of 130-190ºC by using acidic ion-exchange resins, as suitable and economic catalysts. The use of two promising reactants that can be a renewable compound source, ethanol and diethyl carbonate, have been explored. Both reactants are able to ethylate 1-octanol and form the desired product. However, an identical industrial drawback is observed on both reactants, the loss of ethyl groups to form diethyl ether, which is not suitable as diesel compound.

In order to minimize the diethyl ether formation, and in this way, to maximize the ethyl octyl ether production; several commercial acidic resins were tested, or else, prepared and subsequently tested. The best catalysts are those allowing 1-octanol to access to most sulfonic groups of the catalyst. Such desired properties can be achieved by decreasing the amount of crosslinking agent of resins, as a result, the resin has a high capacity to swell and at the same time a low gel-phase density. Another tailoring technique that lets 1-octanol to access to the vast majority of sulfonic groups is by locating them only in the least crosslinked domains of the gel-phase. Both tailoring techniques involve higher selectivity to ethyl octyl ether, which can be extrapolated to other bulky molecules. However, the former involves a reduction of the catalytic activity per volume unit of the catalyst bed, and the latter, per mass unit.

Interestingly for the resin designers and exploiters, it is proved that the Inverse Steric Exclusion Chromatography characterization technique allows predicting the catalyst performance in polar environments with high accuracy. In such a manner that polymeric catalysts having high specific volume of the swollen gel-phase and predominant domains with low polymer density are desired to enhance selectivity and yield to ethyl octyl ether formation.

The comparison between both ethylating agents, ethanol and diethyl carbonate, revealed that similar selectivity and yield can be potentially obtained over acidic resins. Nevertheless, diethyl carbonate is less competitive at shorter reaction times in a batch reactor, or at lower catalyst mass in continuous units, as a result of the slow decomposition of the required intermediate, ethyl octyl carbonate. On the other hand, the production of $CO_2$ via diethyl carbonate and the availability of ethanol nowadays suggest that use of the alcohol to form ethyl octyl ether is preferred.

Reaction rates to form ethyl octyl ether from ethanol and 1-octanol showed similar, or slightly higher, dependency on the temperature than that to form the main side product, diethyl ether. Thus, an enhancement of the reactor temperature clearly increases the feasibility of an ethyl octyl ether production unit. Accordingly, the use of chlorinated resins, which proved to be thermally stable up to 190ºC in the ethyl octyl ether production, is desired. Among the commercial ones, Amberlyst 70 is the most suitable catalyst in terms of selectivity to ethyl octyl

ether due to its low polymer density in aqueous swollen state. Such polymeric expansion should be taken into account to not block the liquid flow when fixed-bed reactors are employed. That is to say, Amberlyst 70 must be loaded to the reactor in a swollen state.

The relatively large values found of the thermodynamic equilibrium constant of ethyl octyl ether formation assure high conversion levels in an industrial etherification process. Interestingly, the equilibrium values of the formation of diethyl ether are around a half than those of ethyl octyl ether (150-190ºC). A comprehensive kinetic analysis enlightened that reaction rates to form ethyl octyl ether on Amberlyst 70 are strongly inhibited by the presence of water. Thus, reaction rates would be enhanced if most water is removed from bioethanol. Eventually, it was revealed that production of ethyl octyl ether is optimized by using a molar ratio of 1-octanol / ethanol of 1.4, a particle diameter of Amberlyst 70 of less than 0.63 mm and a reactor temperature of 190ºC. If it is desired to maximize the difference between the formation of ethyl octyl ether rate and the diethyl ether one, it is preferred to work on a higher excess of 1-octanol involving a 3.40 1-octanol / ethanol molar ratio.

## 9.2 Outlook

Catalyst screening data revealed that most catalytic performance can be qualitatively predicted by ISEC technique, as well as several quoted studies in an aqueous environment. Industrially, in most of the catalytic applications of ion-exchange resins, the catalysts operate in a partially or entirely swollen state. Some representative examples are the production of bisphenol-A, MTBE, ETBE or TAME. As it is well-known, the performance of comprehensive experimental catalytic tests is economically and timely consuming. Accordingly, in order to prepare or select an appropriated catalyst in these kinds of processes, ISEC measurements can provide economical and highly valuable information. Therefore, the development of a commercial ISEC technique can be really attracting from resin designers and exploiters. To the best of our knowledge, only two homemade ISEC experimental set-ups are worldwide available.

As concerns the resin design, the exploration of some novel ion-exchangers can lead to minimize the dramatic inhibitor effect of water on the reaction rates. In this line, the use of acylation agent before sulfonation of the polymer carrier is claimed to reduce the high hydrophilic character of the catalysts. Specifically for bioethanol derived ethers production, a higher catalyst affinity towards lipophilic reactants would most possibly hinder the alcohol adsorption on acid sites, but not in the same extent. The polarity of the compounds that influence the production of such compounds follows this trend: long chain alcohol < ethanol < water. The organic moiety of the long chain alcohol can contribute significantly to increase its concentration inside a lipophilic resin. Thus, selectivity to diethyl ether would be highly minimized. In addition, the loss of alcohol-resin affinity but also water-resin affinity could also lead to interesting results.

The present work explored the possibility of using bioethanol to ethylate 1-octanol, and in this way, to produce an excellent diesel fuel as ethyl octyl ether. Interesting conclusions have been drawn from a technical standpoint by using acidic ion-exchange resins as catalysts. In case, further research could be focused to overcome the difficulties of the scale up the process from lab to industrial case, by process simulations or the use of an experimental pilot reactor. Nonetheless, the low availability of 1-octanol nowadays implicates a too high price for ethyl octyl ether as a petroleum derived product. Thus, conclusions extracted in this thesis can also be qualitatively extrapolated to the synthesis of similar linear ethanol derived ethers. In this line, a comprehensive exploration of the availability of long chain alcohols, or else long chain olefins, available in the petroleum industry or, in the foreseeable future, in the promising biorefinery industry, can overcome the economical drawback.

## References


[1] BP, “Energy outlook 2030.” 2011.
[2] BP, “Statistical review of world energy 2011.” 2012.
[3] European Union, “DIRECTIVE 2009/28/EC.” 2009.
[4] US Energy Information Administration, “Annual energy review 2011.” 2012.
[5] European Biomass Industry Association, “Bioethanol production and use. Overview of the European market.” 2007.
[6] Edgard Gnansounou and Arnaud Daviat, “Ethanol fuel from biomass: a review,” *J Sci Ind Res*, vol. 64, pp. 809–821, 2005.
[7] K. L. Rock and M. Korpelshoek, “Increasing refinery biofuels production,” *PTQ Catal*, pp. 45–51, 2008.
[8] “European Fuel Oxygenates Association (EFOA),” 2013. [Online]. Available: http://www.efoa.org.
[9] A. C. Hansen, Q. Zhang, and P. W.L. Lyne, “Ethanol–diesel fuel blends—a review,” *Biores Tech*, vol. 96, pp. 277–285, 2005.
[10] E. Benazzi, “Gasoline and diesel imbalances in the Atlantic basin part 1: market outlook.” 2011.
[11] C. Millán, J. E. Gonzalez, F. Soriano, P. Aakko, C. Hamelinck, G. Vossen, and H. Kattenwinkel, “Blending ethanol in diesel.” 2007.
[12] D. Casanave, J. Duplan, and E. Freund, “Diesel fuels from biomass,” *Pure Appl Chem*, vol. 79, pp. 2071–2081, 2007.
[13] J. A. Melero, J. Vicente, M. Paniagua, G. Morales, and P. Muñoz, “Etherification of biodiesel-derived glycerol with ethanol for fuel formulation over sulfonic modified catalysts,” *Biores Tech*, vol. 103, pp. 142–151, 2012.
[14] D. Bradin, L. G. Grune, and M. Trivette, “Alternative fuel and fuel additive compositions,” U.S. Patent WO 2007/061903 A1, 2007.
[15] J. Eberhard, “Diesel fuel based on ethanol,” U.S. Patent 20100242347, 2010.
[16] G. A. Olah, “Cleaner burning and cetane enhancing diesel fuel supplements,” U.S. Patent US 5520710, 1996.
[17] M. Marchionna, R. Patrini, F. Giavazzi, M. Sposini, and P. Garibaldi, “High cetane ethers for the reformulation of diesel fuels,” presented at the 16th World Petroleum Congress, Calgary, Canada, 2000.
[18] G. C. Pecci, M. G. Clerici, F. Giavazzi, F. Ancillotti, M. Marchionna, and R. Patrini, “Oxygenated diesel fuels-structure and properties correlation,” presented at the Proc IX Int Symp Alcohols Fuels, Firenze, Italy, 1991, vol. 1, pp. 321–335.
[19] R. Patrini and M. Marchionna, “Process for the production of ethers from alcohols,” U.S. Patent US 6218583 B1, 2001.
[20] K. Seidel, C. Priebe, and D. Hollenberg, “Emulsions,” U.S. Patent US 5830483, 1998.
[21] A. Ansmann and B. Fabry, “Cosmetic preparations,” U.S. Patent US 6878379B2, 2005.
[22] C. Casas, R. Bringué, E. Ramírez, M. Iborra, and J. Tejero, “Liquid-phase dehydration of 1-octanol, 1-hexanol and 1-pentanol to linear symmetrical ethers over ion exchange resins,” *Appl Catal A Gen*, vol. 1, pp. 321–335, 2011.
[23] S. H. Brown, “Process for the production of symmetrical ethers from secondary alcohols,” U.S. Patent US 5444168, 1995.
[24] M. Poliakoff, W. K. Gray, T. M. Swan, S. K. Ross, S. Wieland, and S. Roeder, “Acid-catalyzed reactions,” U.S. Patent EP1185492, 2005.
[25] W. K. Gray, F. R. Smail, M. G. Hitzler, S. K. Ross, and M. Poliakoff, “The continuous acid-catalyzed dehydration of alcohols in supercritical fluids: a new approach to the cleaner synthesis of acetals, ketals, and ethers with high selectivity,” *J Am Chem Soc*, vol. 121, pp. 10711–10718, 1999.
[26] R. Bringué, M. Iborra, J. Tejero, J. F. Izquierdo, F. Cunill, C. Fité, and V. J. Cruz, “Thermally stable ion-exchange resins as catalysts for the liquid-phase dehydration of 1-pentanol to di-n-pentyl ether (DNPE),” *J Catal*, vol. 244, pp. 33–42, 2006.
[27] E. Medina, R. Bringué, J. Tejero, M. Iborra, and C. Fité, “Conversion of 1-hexanol to di-n-hexyl ether on acidic catalysts,” *Appl Catal A Gen*, vol. 374, pp. 41–47, 2010.
[28] S. D. Alexandratos, “Ion-exchange resins: a retrospective from Industrial and Engineering Chemistry Research,” *Ind Eng Chem Res*, vol. 48, pp. 388–398, 2009.

[29] B. Corain, M. Zecca, P. Canton, and P. Centomo, “Synthesis and catalytic activity of metal nanoclusters inside functional resins: an endeavour lasting 15 years,” *Phil Trans R Soc A*, vol. 368, 2010.
[30] P. F. Siril, H. E. Cross, and D. R. Brown, “New polystyrene sulfonic acid resin catalysts with enhanced acidic and catalytic properties,” *J Mol Catal A Chem*, vol. 279, pp. 63–68, 2008.
[31] S. Koujout and D. R. Brown, “Calorimetric base adsorption and neutralisation studies of supported sulfonic acids,” *Thermochim acta*, vol. 434, 2005.
[32] A. Biffis, B. Corain, M. Zecca, C. Corvaja, and K. Jerabek, “On the macromolecular structure and molecular accessibility of swollen microporous resins: a combined ESR-ISEC approach,” *J Am Chem Soc*, vol. 117, pp. 1603–1606, 1995.
[33] K. Jerabek, *Cross-evaluation of strategie, size-exclusion chromatography. (Inverse steric exclusion chromatography as a tool for morphology characterization)*. Washington: ACS Symposium Series 635, 1996.
[34] K. Jerabek, “Determination of pore volume distribution chromatography data from size exclusion,” *Anal Chem*, vol. 57, pp. 1595–1597, 1985.
[35] K. Jerabek, “Characterization of swollen polymer gels using size exclusion chromatography,” *Anal Chem*, no. 57, pp. 1598–1602, 1985.
[36] P. Centomo, K. Jerabek, D. Canova, A. Sassi, P. Canton, B. Corain, and M. Zecca, “Highly hydrophilic copolymers of N,N-dimethylacrylamide, acrylamido-2-methylpropanesulfonic acid, and Ethylenedimethacrylate: nanoscale morphology in the swollen state and use as exotemplates for synthesis of nanostructured ferric oxide,” *Chem Pub Soc Eu*, vol. 18, pp. 6632–6643, 2012.
[37] B. Corain, M. Zecca, and K. Jerabek, “Catalysis and polymer networks—the role of morphology and molecular accessibility,” *J Mol Catal A Chem*, pp. 3–20, 2001.
[38] J. Tejero, F. Cunill, M. Iborra, J. F. Izquierdo, and C. Fité, “Dehydration of 1-pentanol to di-n-pentyl ether over ion-exchange resin catalysts,” *J Mol Catal A: Chem*, vol. 182–183, pp. 541–554, 2002.
[39] M. R. Buchmeiser, *Polymeric materials in organic synthesis and catalysis*. Wiley-VCH, 2003.
[40] “Purolite website.” [Online]. Available: www.purolite.com.
[41] “Dow Chemical website.” [Online]. Available: www.dow.com.
[42] L. Hankova, L. Holub, and K. Jerabek, “Relation between functionalization degree and activity of strongly acidic polymer supported catalysts,” *React Funct Polym*, vol. 66, pp. 592–598, 2006.
[43] R. H. Perry and D. W. Green, *Perry’s chemical engineers’ handbook*, Seventh edition. McGraw-Hill, 1999.
[44] J. F. Izquierdo, F. Cunill, M. Iborra, J. Tejero, and C. Fité, *Cinética de las reacciones químicas*. Edicions de la Universitat de Barcelona, 2004.
[45] P. K. Kiviranta-Paakkonen, L. K. Struckmann, J. A. Linnekoski, and A. O. I. Krause, “Dehydration of the alcohol in the etherification of isoamylenes with methanol and ethanol,” vol. 37, pp. 18–24, 1998.
[46] S. C. M. Reis, E. R. Lachter, R. S. V. Nascimento, J. A. Rodrigues, and M. Garcia, “Transesterification of brazilian vegetable oils with methanol over ion-exchange resins,” *J Am Oil Chem Soc*, pp. 661–665, 2005.
[47] W. Liu and C. Tan, “Liquid-phase esterification of propionic acid with n-butanol,” *Ind Eng Chem Res*, vol. 40, pp. 3281–3286, 2001.
[48] D. Kapila, “Methods for preparing cycloalkylidene bisphenols,” U.S. Patent US 2005/0137428 A1, 2005.
[49] M. Girolamo, M. Lami, M. Marchionna, D. Sanflippo, M. Andreoni, A. Galletti, and G. Sbrana, “Methanol carbonylation to methyl formate catalyzed by strongly basic resins,” *Catal Lett*, vol. 1–2, pp. 127–131, 1996.
[50] A. Bellamy, “Reaction of supported fluoride ion with gaseous sulphur mustard,” *React Polym*, vol. 23, pp. 101–106, 1994.
[51] A. S. Ndou, N. Plint, and N. J. Coville, “Dimerisation of ethanol to butanol over solid-base catalysts,” *Appl Catal A Gen*, vol. 251, pp. 337–345, 2003.
[52] T. Tsuchida, S. Sakuma, T. Takeguchi, and W. Ueda, “Direct synthesis of n-butanol from ethanol over nonstoichiometric hydroxyapatite,” *Ind Eng Chem Res*, vol. 45, pp. 8634–8642, 2006.

[53] Y. Dekishima, E. I. Lan, C. R. Shen, K. M. Cho, and J. C. Liao, “Extending carbon chain length of 1-butanol pathway for 1-hexanol synthesis from glucose by engineered Escherichia coli,” *J Am Chem Soc*, vol. 133, pp. 11399–11401, 2011.
[54] E. Medina, R. Bringué, J. Tejero, M. Iborra, C. Fité, J. F. Izquierdo, and F. Cunill, “Dehydrocondensation of 1-hexanol to di-n-hexyl ether (DNHE) on Amberlyst 70,” presented at the European Congress of Chemical Engineering (ECCE-6), Copenhagen, 2007.
[55] T. Dogu and D. Varisli, “Alcohols as alternatives to petroleum for environmentally clean fuels and petrochemicals,” *Turk J Chem*, vol. 31, pp. 551–567, 2007.
[56] L. Petrus, E. J. Stamhuis, and G. E. H. Joosten, “Thermal deactivation of strong-acid ion-exchange resins in water,” *Ind Eng Chem Res*, vol. 20, pp. 366–371, 1981.
[57] D. M. Alonso, J. Q. Bond, J. C. Serrano-Ruiz, and J. A. Dumesic, “Production of liquid hydrocarbon transportation fuels by oligomerization of biomass-derived C9 alkenes,” *Green Chem*, vol. 12, pp. 992–999, 2010.
[58] P. Tundo, L. Rossi, and A. Loris, “Dimethyl carbonate as an ambident electrophile,” *J Org Chem*, vol. 70, pp. 2219–2224, 2005.
[59] P. N. Gooden, R. A. Bourne, A. J. Parrott, H. S. Bevinakatti, D. J. Irvine, and M. Poliakoff, “Continuous acid-catalyzed methylations in supercritical carbon dioxide: comparison of methanol, dimethyl ether and dimethyl carbonate as methylating agents,” *Org Process Res Dev*, vol. 14, pp. 411–416, 2010.
[60] P. Tundo, F. Trotta, G. Moraglio, and F. Ligorati, “Continuous-flow processes under gas-liquid phase-transfer catalysis (GL-PTC) conditions: the reaction of dialkyl carbonates with phenols, alcohols, and mercaptans,” *Ind Eng Chem Res*, vol. 27, pp. 1565–1571, 1988.
[61] B.C. Dunn, C. Guenneau, S.A. Hilton, J. Pahnke, and E.M. Eyring, “Production of diethyl carbonate from ethanol and carbon monoxide over a heterogeneous catalyst,” vol. 16, pp. 177–181, 2002.
[62] N. Roh, B.C. Dunn, E.M. Eyring, R.J. Pugmire, and H. Meuzelaar, “Production of diethyl carbonate from ethanol and carbon monoxide over a heterogeneous catalytic flow reactor,” *Fuel Process Technol*, vol. 83, pp. 27–38, 2003.
[63] T. Sakakura and K. Kohno, “The synthesis of organic carbonates from carbon dioxide,” *Chem Commun*, pp. 1312–1330, 2009.
[64] N. Keller, G. Rebmann, and V. Keller, “Catalysts, mechanisms and industrial processes for the dimethylcarbonate synthesis,” *J Mol Catal A Chem*, vol. 317, pp. 1–18, 2010.
[65] G. Centi and S. Perathoner, “Opportunities and prospects in the chemical recycling of carbon dioxide to fuels,” *Catal Today*, vol. 148, pp. 191–205, 2009.
[66] H. Kurakata, Y. Izumi, and K. Aika, “Ethanol synthesis from carbon dioxide on Ti02-supported [RhloSe] catalyst,” *Chem Commun*, pp. 389–390, 1996.
[67] Y. Izumi, “Selective ethanol synthesis from carbon dioxide: roles of rhodium catalytic sites,” *Platinum Met Rev*, vol. 41, pp. 166–170, 1997.
[68] T. Sakakura, J. Choi, and H. Yasuda, “Transformation of carbon dioxide,” *Chem Rev*, vol. 107, pp. 2365–2387, 2007.
[69] Rohm and Haas Company, “Lab. Proc. for Testing AmberlystTM Polym. Catal,” 2004.
[70] J. Tejero, C. Fité, M. Iborra, J. F. Izquierdo, F. Cunill, and R. Bringué, “Liquid-phase dehydrocondensation of 1-pentanol to di-n-pentyl ether (DNPE) over medium and large pore acidic zeolites,” *Microporous Mesoporous Mater*, vol. 117, pp. 650–660, 2009.
[71] R. Nel and A. Klerk, “Dehydration of C5-C12 linear 1-alcohols over η-Alumina to fuel ethers,” *Ind Eng Chem Res*, vol. 48, pp. 5230–5238, 2009.
[72] P. Tundo, F. Arico, A. Rosamilia, and E. Memoli, “Synthesis of dialkyl ethers by decarboxylation of dialkyl carbonates,” *Green Chem*, vol. 10, pp. 1182–1189, 2008.
[73] S. Pros, “Synthesis of ethyl octyl ether over acidic ion-exchange resins,” University of Barcelona, 2009.
[74] S. Ihm, M. Chung, and K. Park, “Activity difference between the internal and external sulfonic groups of macroreticular ion-exchange resin catalysts in isobutylene hydration,” *Ind Eng Chem Res*, vol. 27, pp. 41–45, 1988.
[75] D. Zhu, F. Mei, L. Chen, W. Mo, T. Li, and G. Li, “An efficient catalyst Co(salophen) for synthesis of diethyl carbonate by oxidative carbonylation of ethanol,” *Fuel*, vol. 90, pp. 2098–2102, 2011.
[76] “Orion Instruments website, dielectric constants data.” [Online]. Available: http://orioninstruments.com/html/tools/dielectric.aspx.

[77] S. R. Samms, S. Wasmus, and R. F. Savinell, “Thermal stability of Nafion® in simulated fuel cell environments,” *J Electrochem Soc*, vol. 143, pp. 1498–1504, 1996.
[78] J. Zhang, L. Zhang, H. Liu, A. Sun, and R. Liu, *Electrochemical technologies for energy storage and conversion*. Weinheim (Germany): Wiley-VCH, 2012.
[79] D. M. Alonso, J. Q. Bond, D. Wang, and J. A. Dumesic, “Activation of Amberlyst-70 for alkene oligomerization in hydrophobic media,” *Top Catal*, vol. 54, pp. 447–457, 2011.
[80] G. V. Samsonov and V. A. Pasechnik, “Ion exchange and the swelling of ion-exchange resins,” *Russ Chem Rev*, vol. 38, pp. 547–565, 1969.
[81] B. C. Gates, J. S. Wisnouskas, and H. W. Heath, “The dehydration of t-butyl alcohol catalyzed by sulfonic acid resin,” *J Catal*, vol. 24, pp. 320–327, 1972.
[82] B. C. Gates and W. Rodriguez, “General and specific acid catalysis in sulfonic acid resin,” *J Catal*, vol. 31, pp. 27–31, 1973.
[83] R. Thornton and B. C. Gates, “Catalysis by matrix-bound sulfonic acid groups: olefin and paraffin formation from butyl alcohols,” *J Catal*, vol. 34, pp. 275–287, 1974.
[84] R. Bringué, J. Tejero, M. Iborra, J. F. Izquierdo, C. Fité, and F. Cunill, “Water effect on the kinetics of 1-pentanol dehydration to di-n-pentyl ether (DNPE) on Amberlyst 70,” *Top Catal*, vol. 45, pp. 181–186, 2007.
[85] A. A. Kiss, F. Omota, A. C. Dimian, and G. Rothenberg, “The heterogeneous advantage: biodiesel by catalytic reactive distillation,” *Top Catal*, vol. 40, pp. 141–150, 2006.
[86] J. M. Aragon, J. M. R. Begas, and L. G. Jodra, “Catalytic behavior of macroporous resins in catalytic processes with water production. Activation and inhibition effects in the kinetics of the self-condensation of cyclohexanone,” *Ind Eng Chem Res*, vol. 32, pp. 2555–2562, 1993.
[87] M. Iborra, C. Fité, J. Tejero, F. Cunill, and J. F. Izquierdo, “Drying of acidic macroporous styrene-divinylbenzene resins,” *React Polym*, vol. 21, pp. 65–76, 1993.
[88] N. Bothe, F. Döscher, J. Klein, and H. Widdecke, “Thermal stability of sulphonated styrene-divinylbenzene resins,” *Polym*, vol. 20, pp. 850–854, 1979.
[89] R. Bringué, E. Ramírez, C. Fité, M. Iborra, and J. Tejero, “Kinetics of 1-pentanol etherification without water removal,” *Ind Eng Chem Res*, vol. 50, 2011.
[90] B. L. Yang, S. B. Yang, and R. Q. Yao, “Synthesis of ethyl tert-butyl ether from tert-butyl alcohol and ethanol on strong acid cation-exchange resins,” *React Funct Polym*, vol. 44, pp. 167–175, 2000.
[91] U. Limbeck, C. Altwicker, U. Kunz, and U. Hoffmann, “Rate expression for THF synthesis on acidic ion exchange resin,” *Chem Eng Sci*, vol. 56, pp. 2171–2178, 2001.
[92] B. C. Gates and J. N. Johanson, “Langmuir-Hinshelwood kinetics of the dehydration of methanol catalyzed by cation exchange resin,” *AIChE J*, vol. 17, pp. 981–983, 1971.
[93] J.G. Nunan, K. Klier, and R.G. Herman, “Methanol and 2-methyl-1-propanol (isobutanol) coupling to ethers and dehydration over Nafion H: selectivity, kinetics, and mechanism,” *J Catal*, vol. 139, pp. 406–420, 1993.
[94] J. Gangadwala, S. Mankar, and S. Mahajani, “Esterification of acetic acid with butanol in the presence of ion-exchange resins as catalysts,” *Ind Eng Chem Res*, vol. 42, pp. 2146–2155, 2003.
[95] A. Delion, B. Torck, and M. Hellin, “Equilibrium constant for the liquid-phase hydration of isobutylene over ion-exchange resin,” *Ind Eng Chem Res*, vol. 25, pp. 889–893, 1986.
[96] R. Bringué, J. Tejero, M. Iborra, J. F. Izquierdo, C. Fité, and F. Cunill, “Experimental study of the chemical equilibria in the liquid-phase dehydration of 1-pentanol to di-n-pentyl ether,” *Ind Eng Chem Res*, vol. 46, pp. 6865–6872, 2007.
[97] R. Bringué, J. Tejero, M. Iborra, C. Fité, J. F. Izquierdo, and F. Cunill, “Study of the chemical equilibrium of the liquid-phase dehydration of 1-hexanol to dihexyl ether,” *J Chem Eng Data*, vol. 53, pp. 2854–2860, 2008.
[98] C. Casas, C. Fité, M. Iborra, J. Tejero, and F. Cunill, “Study of the chemical equilibrium of the liquid-phase dehydration of 1-octanol to 1-(octyloxy)octane,” *J Chem Eng Data*, vol. 58, pp. 741–748, 2013.
[99] R. Wittig, J. Lohmann, and J. Gmehling, “Vapor-Liquid Equilibria by UNIFAC Group Contribution. 6. Revision and Extension,” *Ind Eng Chem Res*, vol. 42, pp. 183–188.
[100] G. Pilcher, A. S. Pell, and D. Coleman, “Measurements of heats of combustion by flame calorimetry,” *J Trans Faraday Soc*, vol. 60, pp. 499–505, 1963.
[101] J. B. Pedley, R. D. Naylor, and S. P. Kirby, *Thermochemical data of organic compounds*. New York: Chapman and Hall, 1986.

[102] P. Kitchaiya and R. Datta, “Ethers from ethanol. 2. reaction equilibria of simultaneous tert-amyl ethyl ether synthesis and isoamylene isomerization,” *Ind Eng Chem Res*, vol. 34, pp. 1092–1101, 1995.
[103] “National Instititute of Standards and Technology database (NIST), US Department of Commerce.” [Online]. Available: http://nist.gov/.
[104] Y. M. Naziev, M. M. Bashirov, and Y. A. Badalov, “Experimental study of isobaric specific heat of higher alcohols at high pressures,” *J Eng Phys*, vol. 51, pp. 1459–1464, 1986.
[105] J. C. Miltenburg, H. Gabrielova, and K. Ruzicka, “Heat capacities and derived thermodynamic functions of 1-hexanol, 1-heptanol, 1-octanol, and 1-decanol between 5 K and 390 K,” *J Chem Eng Data*, vol. 48, pp. 1323–1331, 2003.
[106] M. W. Chase, *NIST-JANAF Thermochemical Tables*, 4th ed. J Phys Chem Ref Data, Monogr 9, 1998.
[107] R. W. Gallant, *Physical properties of hydrocarbons*, vol. Chapter 28. Lousiana: Gulf Publishing Company, 1970.
[108] R. C. Reid, J. M. Prausnitz, and B. E. Poling, *The properties of gases and liquids*, 4th ed., vol. Chapter 5. New York: McGraw-Hill, 1987.
[109] S. P. Verevkin, “Improved Benson increments for the estimation of standard enthalpies of formation and enthalpies of vaporization of alkyl ethers, acetals, ketals, and ortho esters,” *J Chem Eng Data*, vol. 47, pp. 1071–1097, 2002.
[110] J. M. Smith and H. C. Ness, *Introduction to chemical engineering thermodynamics*, vol. Chapter 15. New York: McGraw-Hill, 1987.
[111] C. Mosselman and H. Dekker, “Enthalpies of Formation of n-Alkan-1-ols,” *J Chem Soc, Faraday Trans 1*, vol. 71, pp. 417–424, 1975.
[112] K. Pihlaja and J. Heikkil, “Heats of combustion. Diethyl ether and 1,1-diethoxyethane,” *Acta Chem Scand*, vol. 22, pp. 2731–2732, 1968.
[113] J. W. Murrin and S. Goldenhagen, “Determination of the C-O bond energy from the heats of combustion of four aliphatic ethers,” U.S. Naval Powder Factory Research and Development Department, 1965.
[114] R. González, “Performance of Amberlyst 35 in the synthesis of ETBE from ethanol and C4 cuts,” University of Barcelona, 2011.
[115] K. Jerabek, J. Odnoha, and K. Setinek, “Kinetics of the synthesis of bisphenol A,” *Appl Catal*, vol. 36, 1988.
[116] F. Cunill, J. Tejero, C. Fité, M. Iborra, and J. F. Izquierdo, “Conversion, selectivity, and kinetics of the dehydration of 1-pentanol to di-n-pentyl ether catalyzed by a microporous ion-exchange resin.,” *Ind Eng Chem Res*, vol. 44, pp. 318–324, 2005.
[117] J. D. Kemp, “Process for the esterification of isobutene,” U.S. Patent US Patent US3678099, 1972.
[118] L. P. McMaster and E. R. Gilliland, “Preparation and characterization of a modified ion-exchange resin,” *Ind Eng Chem Prod Res Dev*, vol. 11, pp. 97–105, 1972.
[119] H. Widdecke, J. Klein, and N. Bothe, “The influence of neighbouring group effects on the stability and reactivity of ion exchange polymers,” *Makromol Chem Suppl*, vol. 6, pp. 211– 226, 1984.
[120] E. G. Lundquist, “Catalyzed esterification process,” U.S. Patent US Patent 5426199.
[121] S. Blagov, S. Parada, O. Bailer, P. Moritz, D. Lam, R. Weinand, and H. Hasse, “Influence of ion-exchange resin catalysts on side reactions of the esterification of n-butanol with acetic acid,” *Chem Eng Sci*, no. 61, pp. 753–765, 2006.
[122] M. Kotora, C. Buchaly, P. Kreis, and A. Gorak, “Reactive distillation -experimental data for propyl propionate synthesis,” *Chem Pap*, vol. 62, pp. 65–69, 2008.
[123] J. Lange, W. D. Graff, and R. J. Haan, “Conversion of furfuryl alcohol into ethyl levulinate using solid acid catalysts,” *ChemSusChem*, vol. 2, pp. 437–441, 2009.
[124] C. Pirola, C. L. Bianchi, D. C. Boffito, G. Carvoli, and V. Ragaini, “Vegetable oil deacidification by Amberlyst: study of the catalyst lifetime and a suitable reactor configuration,” *Ind Eng Chem Res*, vol. 49, pp. 4601–4606, 2010.
[125] M. Cadenas, R. Bringué, C. Fité, E. Ramírez, and F. Cunill, “Liquid-phase oligomerization of 1-hexene catalyzed by macroporous ion-exchange resins,” *Top Catal*, vol. 54, no. 998–1008, p. 2011.
[126] M. Granollers, J. F. Izquierdo, and F. Cunill, “Effect of macroreticular acidic ion-exchange resins on 2-methyl-1-butene and 2-methyl-2-butene mixture oligomerization,” *Appl Catal A Gen*, vol. 345–346, pp. 163–171, 2012.

## Nomenclature

| | |
|---|---|
| $a_i$ | catalytic activity on the reaction i with respect to fresh catalyst |
| $a_j$ | activity of component j |
| $a_{\infty,i}$ | terminal activity of reaction i |
| a, b, c, d | temperature dependence coefficients |
| $a_j$, $b_j$, $c_j$, $d_j$ | polynomial form coefficients of heat capacities expressions of compound j |
| CS | conventionally sulfonated |
| $C_{p,(l)}$ | molar heat capacities in the liquid-phase of the compounds j (J/(mol·K)) |
| DCE | 1,2-dichloroethane |
| DEC | diethyl carbonate |
| DEE | diethyl ether |
| $d_p$ | catalyst particle diameter (mm) |
| $d_{pore}$ | catalyst pore diameter (nm) |
| DOC | di-n-octyl carbonate |
| DNOE | di-n-octyl ether |
| DVB | divinylbenzene |
| EA | ethylating agent, referring to ethanol or diethyl carbonate |
| $E_a$ | apparent activation energy (kJ/mol) |
| EMT | external mass transfer |
| EOC | ethyl octyl carbonate |
| EOE | ethyl octyl ether |
| ER | Eley-Rideal |
| ETBE | ethyl tert-butyl ether |
| EtOH | ethanol |
| $F_j$ | molar flow rate of species j (mol/h) |
| $[H^+]$ | acid capacity (meq $H^+$/g) |
| i | reaction i |
| $I_H$ | van't Hoff integration constant |
| $I_K$ | Kirchoff equation integration constant |
| IMT | internal mass transfer |
| ISEC | Inverse Steric Exclusion Chromatography |
| j | compound j |
| k | compound k |
| $k_{d,i}$ | rate constant of reaction i decay ($h^{-1}$) |
| $k_i$ | kinetic constant of reaction i (mol/(h·g)) |
| $K_a^i$ or $K_{eq,i}$ | reaction equilibrium constant of reaction i using compound activities |
| $K_x^i$ | reaction equilibrium constant of reaction i using compound molar fractions |
| $K_\gamma^i$ | reaction equilibrium constant of reaction i using compound activity coefficients |
| $K_j$ | adsorption equilibrium constant of compound j |

| | |
|---|---|
| $K_\Gamma$ | Poynting correction factor |
| LHHW | Langmuir-Hinshelwood-Hougen-Watson |
| n | number of active sites that take part in the surface reaction |
| NIST | National Institute of Standards and Technology of US |
| OcOH | 1-octanol |
| OS | oversulfonated |
| P | pressure (bar) |
| PS-DVB | polystyrene-divinylbenzene |
| q | volume flow rate (mL/min) |
| $r_i$ | reaction rate of reaction i (mol/(h·$g_{cat}$)) or (mol/(h·$kg_{cat}$)) |
| $r_i^0$ | initial reaction rate of reaction i (mol/(h·$kg_{cat}$)) |
| $R_{OcOH/EA}$ | molar ratio of 1-octanol with respect to ethanol or diethyl carbonate |
| $S_{BET}$ | surface area in dry state obtained by BET method ($m^2$/g) |
| $S_j^k$ | selectivity of reactant j toward product k (%, mol/mol) |
| $S^0_{(l)}$ | liquid-phase molar entropy (J/(K·mol)) |
| SiC | silicon carbide |
| SS | surface sulfonated or low sulfonated |
| SSR | sum of squared errors |
| SSRR | sum of squared relative errors |
| T | temperature (ºC) |
| $t_0$ | initial time of the activity decay (h) |
| US | United States |
| V | mean particle volume in liquid ($cm^3$) |
| $V_0$ | mean particle volume of dried resin in air ($cm^3$) |
| $V_j$ | molar volumes of compound j (L/(mol)) |
| $V_{pore}$ | pore volume in dry stat ($cm^3$/g) |
| $v_s$ | superficial velocity (cm/s) |
| $V_{sp}$ | specific volume of the swollen phase ($cm^3$/g) |
| $W_{cat}$ | catalyst mass (g) |
| x | molar fraction (mol/mol) |
| $X_j$ | conversion of reactant j (%, mol/mol) |
| $Y_j^k$ | yield of reactant j toward product k (%, mol/mol) or (%, g/g) |
| $\Delta_r G^0_{(l)}$ | standard free energy change of reaction in liquid-phase (kJ/mol) |
| $\Delta_r H^0_{(l)}$ | standard molar enthalpy change of reaction in liquid-phase (kJ/mol) |
| $\Delta_f H^0_{(l)}$ | liquid-phase standard molar enthalpy change of formation (kJ/mol) |
| $\Delta_r S^0_{(l)}$ | standard molar entropy change of reaction in liquid-phase (J/(mol·K)) |
| ΣS | sum of individual surface area ($m^2$/g) |
| $\Sigma V_{pore}$ | sum of individual pore volumes ($cm^3$/g) |
| $\rho_j$ | liquid density of compound j (g/$cm^3$) |
| $\rho_s$ | skeletal density of resins (g/$cm^3$) |

| | |
|---|---|
| $M_j$ | molecular weight of compound j (mol/g) |
| σ | active center |
| $v_j$ | stoichometric coefficient of compound j |
| $\gamma_i$ | activity coefficient of compound j |

## List of Tables

## List of Figures

# Resum del treball (català)

## Resum curt

Des del 1900, la població mundial s'ha més que quadruplicat, els ingressos econòmics de la qual ha augmentat en un factor de 25 i el consum d'energia per un factor de 23. En els proper anys no s'espera un creixement de la demanda energètica dels països ja desenvolupats, però sí de les economies emergents, amb Xina liderant majoritàriament aquesta demanda. A conseqüència de polítiques de suport a les energies renovables, els alts preus del petroli i les innovacions tecnològiques, es preveu que aquestes seguiran tenint una ràpida expansió. Entre elles, el bioetanol es preveu que tindrà un creixement exponencial en els propers anys.

El bioetanol té grans propietats en motors d'ignició, i actualment és mesclat amb les gasolines o usat directament. No obstant, utilitzar bioetanol per produir èters com l'ETBE, TAME i TAEE millora substancialment la qualitat de la gasolina, a més de ser energèticament més eficient. De la mateixa manera, la utilització de bioetanol per produir compostos diesel seria una forma d'incrementar la producció de diesel (deficitària a Europa), i tan o més important, de millorar-ne la qualitat i així reduir les emissions nocives de material particulat, òxids de nitrogen, sofre i compostos volàtils. Un èter derivat del bioetanol que té excel·lents propietats com a combustible diesel és l'etil octil èter.

L'objectiu d'aquest treball és l'estudi de la producció d'etil octil èter en fase líquida mitjançant catalitzadors heterogenis. Això implica la selecció dels reactius i catalitzadors més adequats des d'un punt de vista de rendiment i selectivitat. A més, l'estudi termodinàmic i cinètic de la reacció en permeten tan el disseny com la optimització del procés.

Els assajos catalítics s'han realitzat en un reactor de tanc agitat operant en discontinu i en un reactor tubular operant en continu. El reactor discontinu s'ha utilitzat per la selecció dels millors catalitzadors i per l'estudi termodinàmic de la reacció; i el reactor tubular per estudiar l'evolució de l'activitat catalítica al llarg del temps i per realitzar-ne l'estudi cinètic. Ambdós reactors han treballat a 25 bars de pressió i en un rang de temperatures de 130 a 190ºC. L'anàlisi de les mostres s'ha realitzat en un cromatògraf equipat amb un TCD, injectades directament des del reactor. Els reactius utilitzats han sigut etanol, dietil carbonat i 1-octanol. La majoria de catalitzadors utilitzats han sigut resines poliestirèniques de bescanvi iònic. Les resines seleccionades tenien diferent capacitat àcida, grau d'encreuament, estructura reticular i estabilitat tèrmica.

Els resultats experimentals han mostrat que el compost etil octil èter es pot formar mitjançant l'etilació de 1-octanol a partir de dos reactius provinents d'origen renovable, l'etanol i el dietil carbonat. No obstant, la mateixa problemàtica econòmica és observada en ambdós compostos, la pèrdua de grups etils en la formació de dietil èter; el qual, tot i provenir d'una font totalment renovable, no presenta tan bones propietats com a component diesel com l'etil octil èter.

Per tal de minimitzar la formació de dietil èter, i d'aquesta forma, maximitzar la producció d'etil octil èter, diverses resines àcides de bescanvi iònic comercials han sigut assajades, o bé,

preparades i assajades. S'ha observat que els millors catalitzadors eren els que permeten al 1-octanol accedir a la majoria de grups sulfònics del catalitzador. Aquest tipus de resines són les que posseeixen un menor quantitat d'agent reticulant, concretament de divinilbenzè. Una altra tècnica per permetre al 1-octanol accedir a la gran majoria de centres actius és col·locant els grups sulfònics només en el domini menys reticulat de la fase gel. Ambdós tècniques impliquen una major selectivitat cap a etil octil èter, extrapolable a altres molècules voluminoses. Tot i això, cal tenir present que la primera tècnica implica una reducció en la eficiència per unitat de volum del llit catalític, i la segona, per unitat màssica. Un fet molt rellevant observat en aquest treball és que la caracterització de les resines mitjançant de cromatogràfica inversa d'exclusió de grandaria permet predir l'activitat catalítica en un medi polar amb gran exactitud. D'aquesta forma, les resines àcides que presenten un elevat volum específic de fase gel inflada i en les que predomina els dominis de baixa densitat polimèrica són les més desitjades per incrementar la selectivitat i el rendiment cap a etil octil èter.

La comparació del dos agents etilants, etanol i dietil carbonat, ha revelat que es poden obtenir similars selectivitats i rendiments en temps de reacció elevats mitjançant resines àcides de bescanvi iònic. Tanmateix, l'ús de dietil carbonat és menys competitiu en temps de reacció curts, a conseqüència de la lenta descomposició de l'intermedi de la reacció, l'etil octil carbonat. A més, la formació de $CO_2$ via dietil carbonat i la més alta disponibilitat d'etanol suggereix que l'ús de l'alcohol és preferit des d'un punts de vista tan industrial com ambiental.

L'estudi termodinàmic ha revelat que els valors relativament alts de la constant termodinàmica d'equilibri químic en la formació de l'etil octil èter asseguren alts nivells de conversió en un procés industrial. A més, s'ha observat que la constant d'equilibri de la reacció competitiva de formació de dietil èter té valors inferiors en el rang de temperatures explorat, fet que en limitaria la seva formació. Finalment, un exhaustiu estudi cinètic ha revelat que la velocitat de formació d'etil octil èter a partir d'etanol i 1-octanol és altament inhibit per l'adsorció de l'aigua en els centres actius d'Amberlyst 70. Per això, l'extracció de l'aigua provinent del bioetanol afavoriria la producció d'etil octil èter. Finalment, s'ha observat que les velocitats de reacció són optimitzades utilitzant una raó molar 1-octanol / etanol de 1.4, un diàmetre de partícula menor a 0.63 mm d'Amberlyst 70 i una temperatura de reactor de 190ºC. En el cas de voler maximitzar la diferència entre la formació d'etil octil èter i dietil èter, és preferible treballar amb un excés més elevat de 1-octanol fins a una raó molar de 1-octanol / etanol de 3.4.

## Resum llarg

## 1. Introducció

Des del 1900, la població mundial s'ha més que quadruplicat, els ingressos econòmics de la qual ha augmentat en un factor de 25 i el consum d'energia per un factor de 23. En els proper anys no s'espera un creixement de la demanda energètica dels països ja desenvolupats, però sí de les economies emergents, amb Xina liderant majoritàriament aquesta demanda. A conseqüència de polítiques de suport a les energies renovables, els alts preus del petroli i les innovacions tecnològiques, es preveu que aquestes seguiran tenint una ràpida expansió. Entre elles, el bioetanol es preveu que tindrà un creixement exponencial en els propers anys [1-5].

El bioetanol té grans propietats en motors d'ignició, i actualment és mesclat amb les gasolines o usat directament. No obstant, és preferible la utilització del bioetanol per tal de produir etil èters, com ara l'etil ter-butil èter o l'etil ter-amil èter; degut a que l'adició d'aquests components millora substancialment la qualitat de la gasolina, a més de ser energèticament més eficient [6,7]. Anàlogament, la utilització de bioetanol per produir compostos diesel seria una forma d'incrementar la producció de diesel (deficitària a Europa), i tan ho més important, de millorar-ne la qualitat i així reduir les emissions nocives de material particulat, òxids de nitrogen, sofre i compostos volàtils [8,9]. Un èter derivat del bioetanol que té excel·lents propietats com a combustible diesel és l'etil octil èter (EOE) [10].

El EOE és un èter asimètric de 10 àtoms de carboni, $C_{10}H_{22}O$ (Fig. 1), té un contingut d'oxigen del 10 % en pes, una temperatura d'ebullició de 187ºC, una densitat $d_4^{20}$ de 0.771, un índex de cetanatge de 97 i satisfactòria lubricitat. A més de les seves excel·lents propietats com a component diesel, també pot ser utilitzat en una gran varietat d'usos industrials com a component de colorants, pintures, cautxús, resines i lubricants [10-13].

Fig. 1: Estructura del EOE.

Els èters lineals poden ser sintetitzats a partir de la deshidratació d'alcohol lineals primaris mitjançant catalitzadors àcids. La deshidratació d'alcohols s'ha demostrat com un tipus de reacció molt útil per obtenir èters lineals com ara el dimetil èter, di-n-butil èter, di-n-pentil èter o el di-n-octil èter [14,15]. Típicament, la deshidratació d'alcohols s'ha catalitzat industrialment a partir d'àcid sulfúric. No obstant, els catalitzadors sòlids tenen avantatges com ara una més fàcil separació. En aquesta línia, s'ha provat que les resines de bescanvi iònic poden catalitzar reaccions de deshidratació d'alcohols cap a èters simètrics lineals amb gran selectivitat (97-99%) [15].

Les resines de bescanvi iònic són molt útils degut a que després de la seva utilització es poden separar fàcilment per filtració, com també es poden utilitzar en columnes. A la Fig. 2 es pot observar un exemple de perles de resines de bescanvi iònic. Les resines de bescanvi iònic poden ser utilitzades com a catalitzadors, tan com a substitut de l'àcid sulfúric com per immobilitzar catalitzadors metàl·lics [16]. La majoria de resines de bescanvi iònic comercials estan formades per un copolímer de poliestirè-divinilbenzè (PS-DVB). Les resines PS-DVB àcides són atractives ja que, comparades amb altres catalitzadors àcids, exhibeixen unes concentracions més altes de grups àcids (~5 meq $H^+$/g) [15]. Pel contrari, la força àcida d'aquestes és més baixa que la dels típics catalitzadors inorgànics com les zeolites [17]. L'activitat catalítica de les resines àcides està totalment condicionada per l'accessibilitat dels seus centres actius [15]. Així, sembla obvi que, prèviament a l' utilització de qualsevol resina és necessari el seu estudi morfològic.

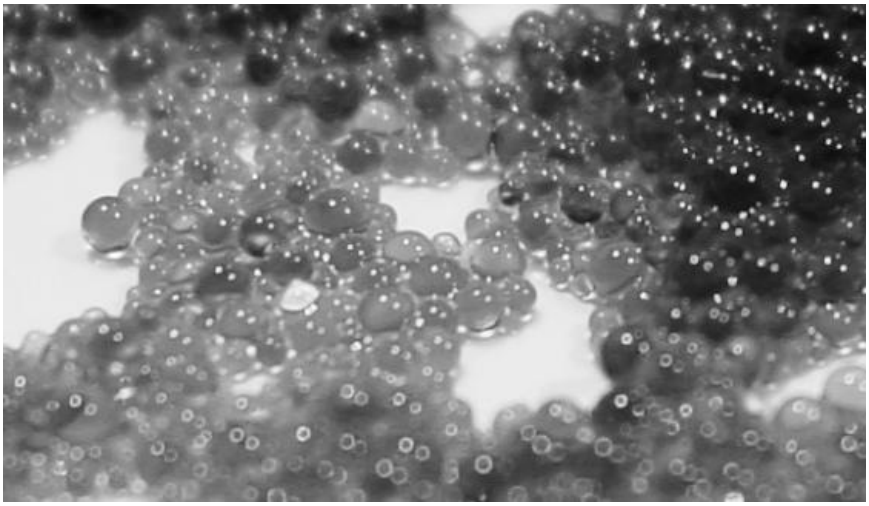

Fig. 2: Perles de resines de bescanvi iònic.

Les resines PS-DVB estan dividies morfològicament en dos grups : les tipus gel i les macroreticulars. Les resines tipus gel estan copolimeritzades sense l'ús de porífer i la seva porositat només apareix en estat inflat. En canvi, en la polimerització de les resines macroreticular es fa ús d'un dissolvent (porífer) que crea porus permanents. Els dos tipus de resines veuen molt augmentada la seva superfície porosa en medi polar. Així, la morfologia de les resines no pot ser caracteritzada per tècniques convencionals com ara l'adsorció de nitrogen o la intrusió de mercuri ja que aquestes tècniques precisen de mostres completament seques. Fins a la data, la única tècnica que permet caracteritzar les resines en medi inflat és la Cromatografia Inversa d'Exclusió de mida (ISEC). Aquesta tècnica ha permès trobar correlacions entre la morfologia del polímer i la seva activitat catalítica [18-20].

A part de l'acidesa i l'accessibilitat de les resines, es tan o més important, conèixer com evoluciona la seva activitat amb el temps. Les resines àcides, al ser un material polimèric, tenen com a important desavantatge la pèrdua de centres actius a altes temperatures, típicament per sobre de 120-150ºC. Tot i així, algunes resines tenen estabilitat tèrmica fins a 190ºC degut a que han estat prèviament clorades [17].

Finalment, per tal de dissenyar un reactor químic de formació de EOE mitjançant resines àcides de bescanvi iònic, és imprescindible modelar la reacció mitjançant expressions cinètiques. Quan s'usa un catalitzador sòlid és necessari que, almenys un dels reactius s'adsorbeixi a la superfície del catalitzador. Per tant, la reacció química està formada per un procés complex, on diferents etapes elementals tenen lloc (Fig. 3).

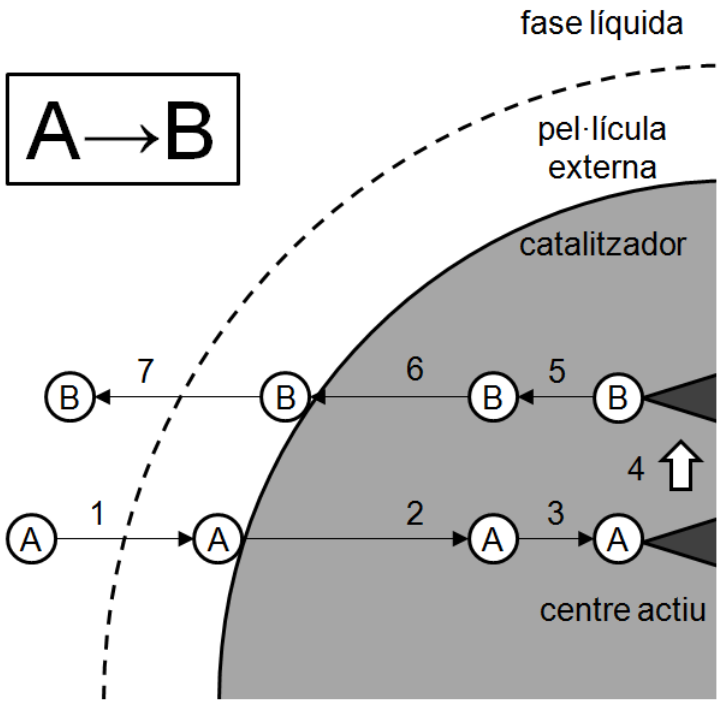


Fig. 3: Etapes del procés catalític en la reacció A → B.

1. Difusió del reactiu de la fase líquida fins a la superfície del catalitzador.
2. Difusió del reactiu a través del catalitzador
3. Adsorció del reactiu al centre actiu
4. Reacció química entre espècies adsorbides o entre espècies adsorbides amb espècies en fase líquida.
5. Desorció del producte de reacció.
6. Difusió del producte a través del catalitzador.
7. Difusió del producte des de la superfície del catalitzador fins la fase líquida.

En catàlisis heterogènia, els models clàssics provenen de la isoterma de Langmuir, basats en 2 hipòtesis: a) la superfície conté un nombre fix de centres actius b) tots els centres actius són idèntics c) la reactivitat dels centres actius no depèn de la quantitat o la natura dels compostos presents a la superfície durant la reacció. En els formalismes de Langmuir-Hinselwood-Hougen-Watson (LHHW) la reacció és entre espècies adsorbides, mentre que en el formalisme Eley-Rideal alguna de les espècies no està adsorbida [21]. En ambdós casos, el procediment

general es basa en proposar una etapa limitant de velocitat i desenvolupar una expressió que s'adapti als resultats experimentals.

L'objectiu d'aquest treball és estudiar el procés catalític per obtenir el compost EOE. Això involucra la selecció de la millor forma d'obtenir aquest producte i el millor catalitzador possible. A més, un cop seleccionat el procés òptim, es realitzarà un estudi termodinàmic i cinètic del procés que pugui ser útil en per la industria.

Concretament, es aquest treball s'avalua la producció de EOE a partir de la deshidratació d'etanol (EtOH) amb 1-octanol (OcOH) a partir de resines àcides PS-DVB de bescanvi iònic, totes elles comercials. L'activitat catalítica de moltes resines es compara i s'estableixen relacions entre l'estructura de les resines amb la seva activitat catalítica. A continuació, s'estudia la formació de EOE a partir d'una mescla de OcOH amb dietil carbonat (DEC). De nou, la influència de l'estructura dels catalitzadors es relaciona amb la seva activitat catalítica. A continuació, l'eficiència dels dos agents etilants proposats, EtOH i DEC, es compara utilitzant els millors catalitzadors trobats.

Un cop seleccionat la millor via d'obtenció del producte, s'avalua l'estabilitat dels millors catalitzadors a alta temperatura i amb la presència d'aigua en el medi a temps de reacció llargs. En aquest punt, es selecciona el millor catalitzador, en relació a activitat i estabilitat, s'obtenen dades de l'equilibri químic de la reacció i d'un model cinètic capaç de predir les velocitats de reacció. Finalment, s'explora la possibilitat d'incrementar la selectivitat cap a EOE a partir de la preparació i utilització de catalitzadors parcialment sulfonats.

## 2. Experimental

En aquest treball es va fer ús de 17 resines àcides comercials de diferent estructura, contingut de DVB, grau de sulfonació i estabilitat tèrmica. També, es van utilitzar 2 resines bàsiques, una zeolita i dos alúmines, totes elles comercials. A part, es van preparar i assajar 6 resines àcides parcialment sulfonades.

L'estudi de la formació de EOE es va realitzar mitjançant dos dispositius experimentals, un reactor de tanc agitat operant en discontinu i un tubular de llit fix operant en continu. El reactor de tanc agitat té un volum nominal de 100-mL. La temperatura va estar controlada per un forn elèctric. La pressió de treball va ser de 25 bar, mitjançant nitrogen. Una sortida del reactor estava connectada directament a una vàlvula de mostreig que injectava el líquid a un cromatògraf GLC. Un esquema del reactor es pot observar en la Fig. 4.

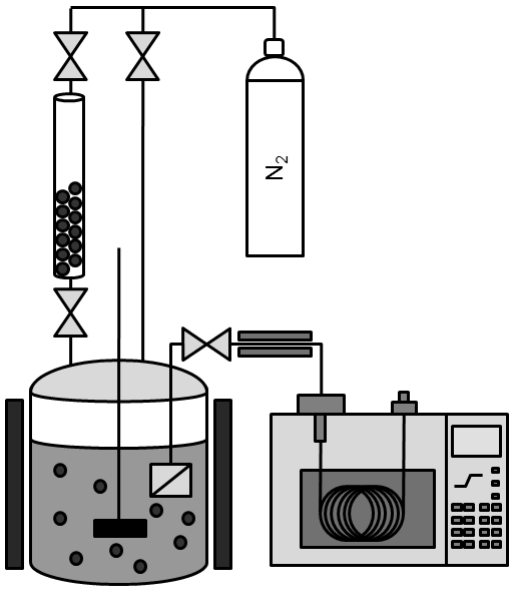


Fig. 4: Esquema de la instal·lació del reactor de tanc agitat.

Previ al seu ús, les resines van ser assecades a 110ºC en un forn a pressió atmosfèrica i posteriorment a 110ºC a 0.01 bar. El reactor va ser carregat amb 70 ml de la mescla de reactius, pressuritzat a 25 bar, agitat a 500 rpm i escalfat fins la temperatura desitjada (130-190ºC). Quan la mescla arribava a la temperatura, s'injectava el catalitzador ubicat en un cilindre extern, a partir de canvi de pressions. En alguns experiments el catalitzador va ser introduït directament amb la mescla de reactius. Els experiments van tenir una durada entre 6 i 150 hores. La composició del sistema va ser analitzada durant l'experiment.

El segon reactor usat, de llit fix, té un volum nominal de 20-mL. La mescla líquida era bombejada mitjançant dos bombes. La pressió aplicada va ser de 25 bar a partir d'una vàlvula reguladora de líquid, ubicada a la sortida del reactor. El llit catalític va consistir en una mescla homogènia de catalitzador i inert (quars o SiC partícules). La temperatura va ser controlada a partir d'un forn elèctric. Un esquema del reactor es pot observar en la Fig. 5.

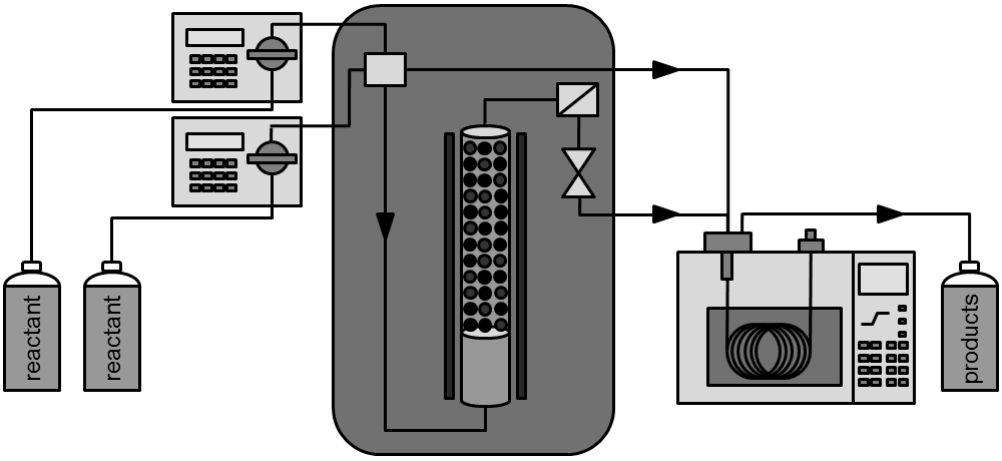


Fig. 5: Esquema de la instal·lació del reactor de llit fix.

Previ al seu ús, les resines van ser assecades a 110ºC en un forn a pressió atmosfèrica i posteriorment a 110ºC a 0.01 bar. Les resines seques eren diluïdes amb l'inert i introduïdes al reactor. La mescla de reactius va ser mesclada i pre-escalfada a la càmera calenta. El caudal volumètric va estar comprès entre 0.25 i 6.7 ml/min. Un cop el reactor estava totalment inundat de líquid, era pressuritzat i escalfat a la temperatura desitjada (150-190ºC). Els experiments van tenir una durada de 2 a 70 hores. La composició del sistema va ser analitzada a la sortida del reactor durant l'experiment.

## 3. Resultats i discussió

EOE va ser format amb èxit a partir de la deshidratació entre OcOH i EtOH mitjançant resines àcides de bescanvi iònic. Tanmateix, la selectivitat cap a l'asimètric EOE (15-46%) va ser molt més baixa que les obtingudes en èters simètrics a partir d'un alcohol (58-99 %) [15], com a resultat de que la síntesis de EOE competeix amb la formació dels corresponents èters simètrics, el dietil èter (DEE) (43-83 %) i de di-n-octil èter (DNOE) (43-83%).

La morfologia de les resines es va mostrar com un factor decisiu per tal d'optimitzar la producció de EOE. La selectivitat cap a EOE va ser incrementada en resines de tipus gel i macroreticulars amb baix contingut de DVB, degut a que tenen més espai entre cadenes en medi polar, sent Amberlyst 121 i Dowex 50Wx2 les resines més adequades en termes de maximització del rendiment. Degut a l'alta selectivitat cap a EOE i la seva alta estabilitat tèrmica, Amberlyst 70 també és un catalitzador atractiu per sintetitzar EOE.

EOE també va ser format amb èxit a partir de DEC i OcOH. Primerament té lloc la transesterificació de DEC amb OcOH a etil octil carbonat. Seguidament, el carbonat es descompon a EOE. L'assaig de catalitzadors, resines àcides i bàsiques de bescanvi iònic, una zeolita, i dos alúmines, va mostrar que les conversions, selectivitats i rendiments més alts van ser aconseguits mitjançant resines àcides de bescanvi iònic.

Anàlogament a la formació de EOE a partir de deshidratació d'alcohols, la síntesi de EOE a partir de DEC també va estar lligada a l'estructura de les resines, ja que com es pot observar a la Fig. 6A, resines amb semblant capacitat àcida van mostrar diferents rendiments. L'accessibilitat de les molècules va ser afavorida en resines amb gran capacitat d'inflament ($V_{sp}$) com s'observa a la Fig. 6B. Així, els catalitzadors amb una fase polimèrica molt expandida són els més adequats per tal de produir EOE. Aquests requisits es poden trobar en resines de baix contingut de DVB.

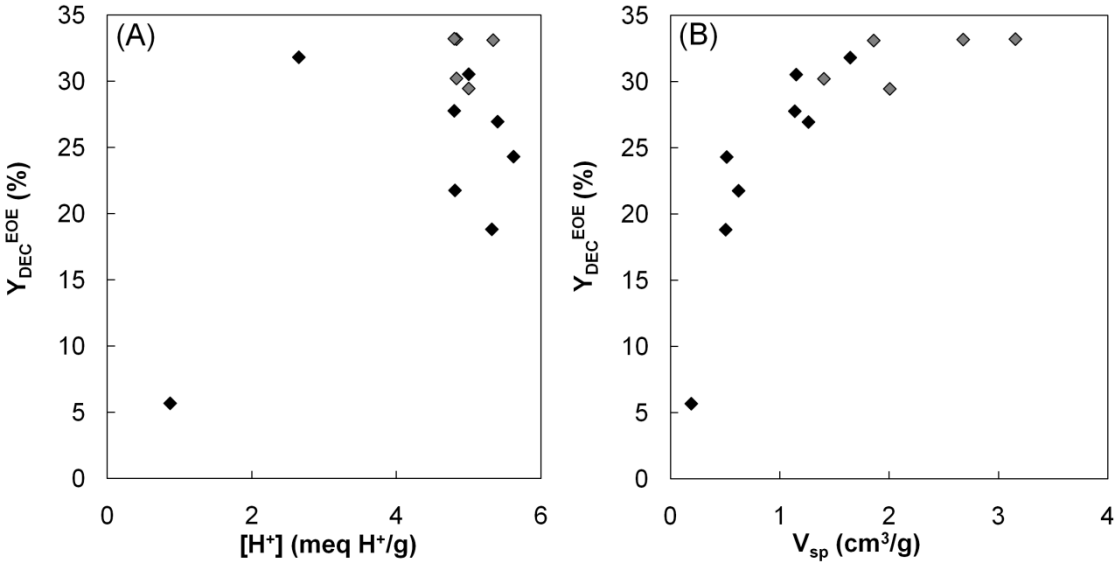


Fig. 6: Influència de la capacitat àcida de les resines (A) i el Vsp en el rendiment cap a EOE respecte a DEC a 8h. T=150ºC, $R_{OcOH/DEC}$ =2, $W_{cat}$=2 g, 500 rpm. ♦Macroreticular; ♦Tipus gel.

La formació de EOE a partir de mescles OcOH / EtOH, o bé, OcOH / DEC mitjançant l'ús de resines àcides amb baix contingut de DVB va ser comparat. Es va observar que el major inconvenient en ambdós reaccions és la pèrdua de grups etils per produir DEE. Com a conseqüència, la selectivitat cap a EOE respecte a l'agent etilant, DEC o EtOH, va ser relativament baixa (40-50 % a 8 hores de reacció).

A temps llargs (48 hores), les conversions, selectivitats i els rendiments a EOE obtinguts van ser similar en ambdós sistemes, com es pot observar a la Figura 7 (A, B i C, respectivament). No obstant, les velocitat de reacció de formació de EOE van ser lleugerament més altes en el sistema OcOH / EtOH. Per tant, EtOH és considerat com l'agent etilant més adequat per formar EOE mitjançant resines àcides a temps de reacció curts i DEC només es pot mostrar competitiu a temps de reacció llargs, o en unitat en continu, en reactors sobredimensionats. A més a més,

l'alta disponibilitat de EtOH en el mercat i la producció d'aigua com a subproducte suggereix que l'ús de EtOH és més recomanat que de DEC per tal de formar EOE.

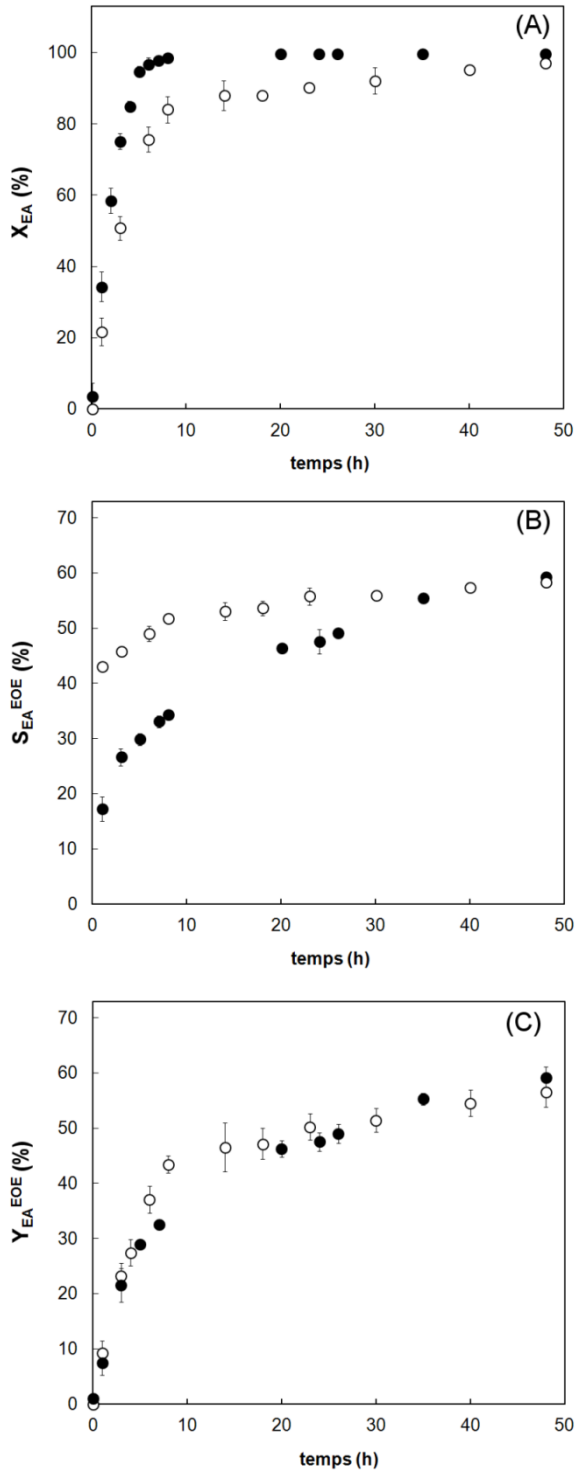


Fig. 7: Conversió (A), selectivitat (B) i rendiment (C) a EOE respecte l'agent etilant. (○ EtOH; ● DEC). Dowex 50Wx2, T=150ºC, $R_{OcOH/EtOH}$= $R_{OcOH/DEC}$=2, $W_{cat}$=2g.

Amb la finalitat d'obtenir velocitats de reacció de formació de EOE a partir de EtOH i OcOH més elevades, i així fer més competitiu el procés, es va explorar l'augment de temperatura de treball a 190ºC. Dowex 50Wx2, la millor resina a 150ºC, va perdre una quantitat rellevant de centres actius a 190ºC. La pèrdua de grups sulfònics va ser incrementada per la presència de l'aigua formada per la deshidratació de OcOH i EtOH.

Al contrari, la dessulfonació no va ser important a 190ºC en les resines Amberlyst 70 i Purolite CT 482, mostrant-se així tèrmicament estables a aquesta temperatura. Les velocitats de reacció van decréixer amb el temps d'operació fins a aconseguir un nivell d'activitat constant, però inferior que l'inicial. Aquest comportament va ser atribuït a que l'adsorció de l'aigua en la resina que competeix amb EtOH i OcOH pels centres actius, mostrant clarament una inhibició de les velocitats reacció. Tot i que, tan aviat com l'aigua és eliminada de les resines, les activitats van ser recuperades. A la Fig. 8 es pot observar com les resines reutilitzades van mostrar similar comportament cinètic que les resines fresques.

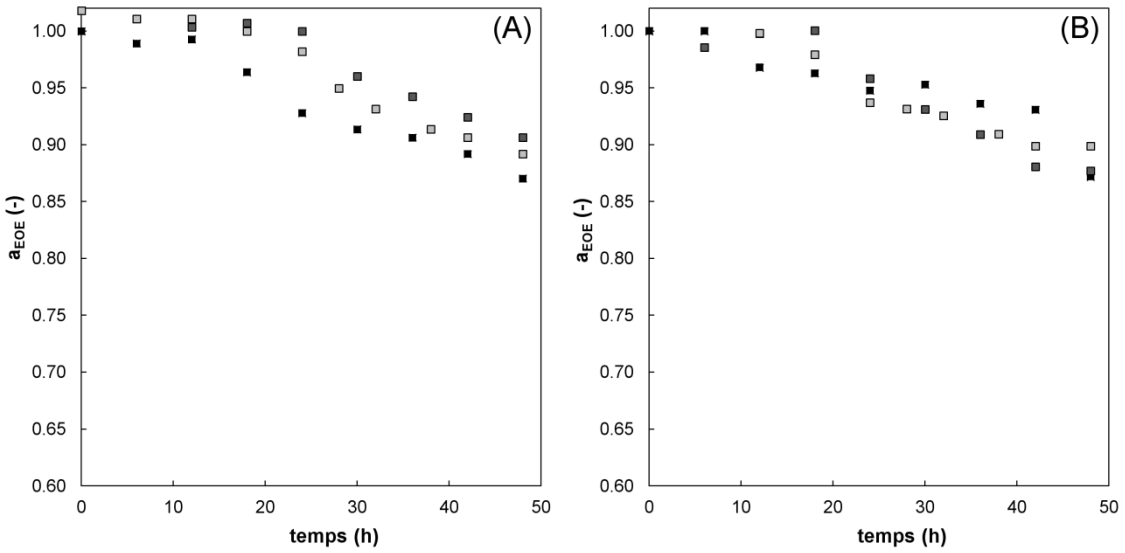


Fig. 8: Evolució de l'activitat catalítica de la formació de EOE amb el temps a partir de EtOH i OCOH sobre Purolite CT482 (A) i sobre Amberlyst 70 (B) a 190ºC. $R_{OcOH/EtOH}$=10, q=0.25 ml/min, P=25 bar (■ 1$^{er}$ cicle; ♦ 2$^{nd}$ cicle; ▲ 3$^{er}$ cicle).

En paral·lel, els resultats experimentals van indicar que les resines no estaven completament inflades a l'inici de l'experiment. Com a resultat, la difusió de OcOH i de molècules voluminoses va estar dificultat en les primeres hores d'operació. No obstant, a mesura que avança el temps d'operació, l'aigua alliberada va actuar com a solvent i va inflar la resina. Així, la caiguda d'activitat catalítica va ser menys pronunciada cap a èters amb més limitacions estèriques (EOE i DNOE) que cap a l'èter amb menys limitacions (DEE).

En l'estudi d'equilibri químic es va observar que els valors obtinguts de constants d'equilibri van ser més alts en el cas de la formació de EOE a partir de EtOH i OcOH que de la formació de DEE a partir de dos molècules de EtOH. A partir de la dependència amb la temperatura de les constants d'equilibri (veure Fig. 9), es va provar que les dos reaccions de deshidratació d'alcohols eren exotèrmiques.

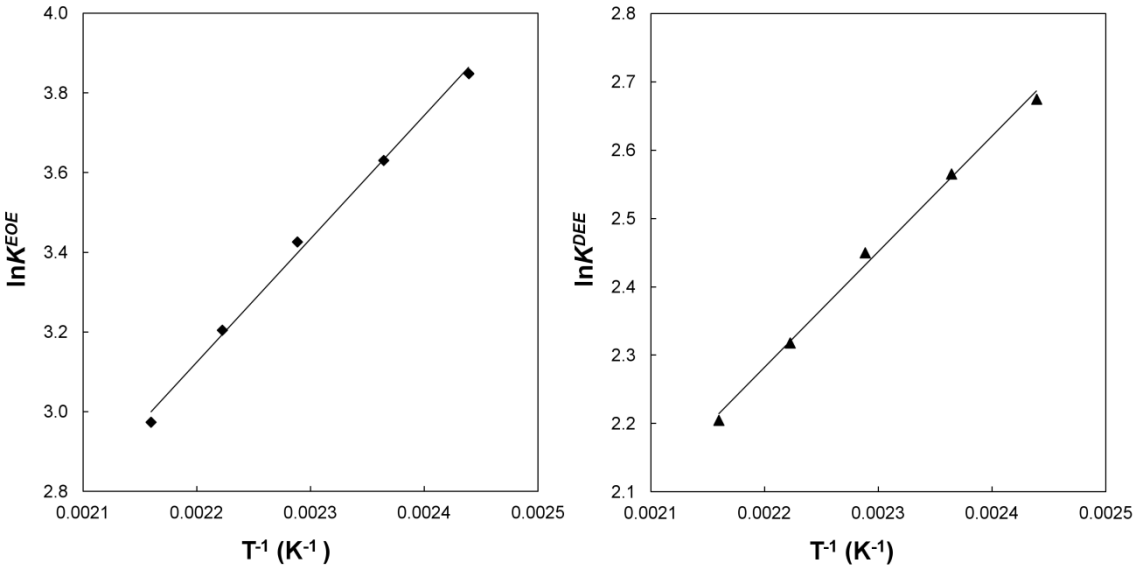


Fig. 9: Variació de ln K amb 1/T considerant constant la $\Delta_r H_{(l)}^0$ en el rang de temperatures explorat. (A) reacció de síntesis de EOE; (B) reacció de síntesis de DEE.

Les variacions d'entalpia de les reaccions obtinguts a 25ºC trobades va ser de -(18.9 ± 1.3) kJ/mol per la formació de EOE, i de -(12.1 ± 0.9) kJ/mol per la formació de DEE. Pel que fa a la variació d'entropia de la reacció, les dos van mostrar valors negatius, -(13.6 ± 4.2) J/(K·mol) per la formació de EOE, i de -(7.6 ± 2.1) J/(K·mol) per la formació de DEE. Quant a la entalpia de formació estàndard i la entropia molar de EOE els valors obtinguts van ser de -(436 ± 7) kJ/mol i de -(434 ± 11) J/(K·mol), respectivament.

Pel que fa a l'estudi de les velocitats de reacció, un model cinètic en termes d'activitat dels components per tal de descriure la formació de EOE i DEE (eq. 1 i 2, respectivament) és proposat.

$$r_{DEE}\left[\frac{mol}{h\cdot g}\right]=\frac{2.10\cdot10^{11}\exp(-100/RT)\left(a_{EtOH}^2-a_{DEE}a_{water}/K_{eq,DEE}\right)}{a_{EtOH}+0.5a_{OcOH}+11.7a_{water}};\quad K_{eq,DEE}=\exp\left(\frac{1691}{T}-1.4\right)\qquad \text{eq. 1}$$

$$r_{EOE}\left[\frac{mol}{h\cdot g}\right]=\frac{7.04\cdot10^{11}\exp(-105/RT)\left(a_{EtOH}a_{OcOH}-a_{EOE}a_{water}/K_{eq,EOE}\right)}{a_{EtOH}+0.5a_{OcOH}+11.7a_{water}};\quad K_{eq,EOE}=\exp\left(\frac{3374.8}{T}-4.3\right)\qquad \text{eq. 2}$$

on R és expressat en kJ/(mol·K) i T en K. En la Fig. 10 es pot observar que les eq. 1 i 2 són capaces de predir els resultats experimentals tan per la formació de DEE (A) com per la formació de EOE (B). Les desviacions són semblants independentment del reactor usat, tanc agitat o llit fix, fet que incrementa la fiabilitat dels models.

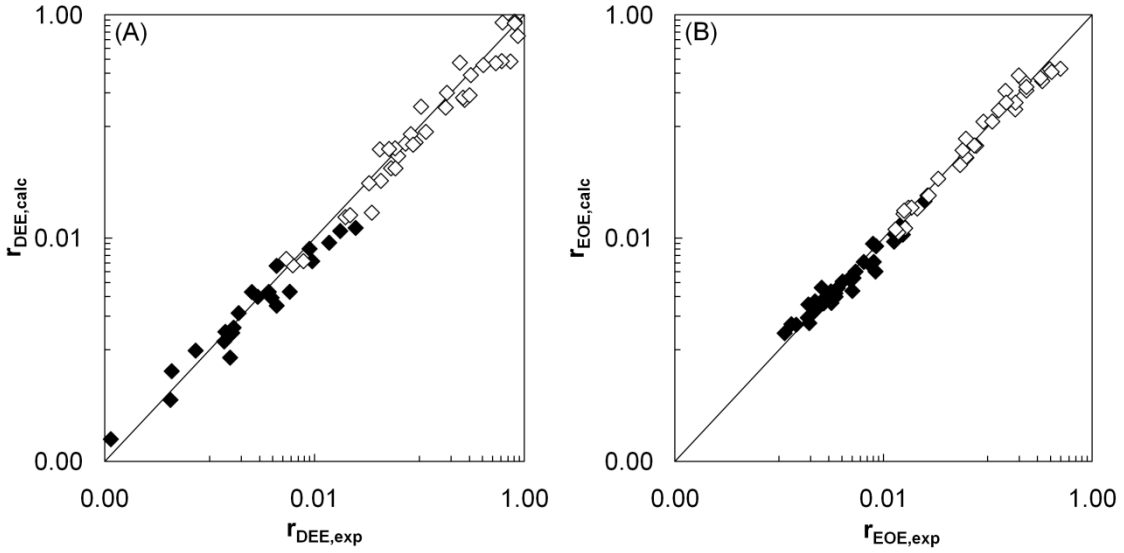


Fig. 10: Velocitats de reacció calculades mitjançant l'eq. 1 (A) i l'eq. 2 (B) versus les experimental. Símbols oberts representen els resultats obtinguts en el reactor de llit fix i símbols tancats usant el reactor de tanc agitat.

A partir del model proposat es pot inferir que la fracció de centres actius lliures és negligible i que només un centre actiu participa en l'etapa de la reacció en superfície, la qual és considerada com en l'etapa limitant de la velocitat de reacció. Les constant d'equilibri d'adsorció dels èters formats són negligibles comparades amb les dels alcohols i l'aigua. Així, pot ser considerat que tan el DEE com el EOE són alliberats directament a la fase líquida. Pel contrari, les velocitats de reacció es van mostrar molt sensibles a la presència d'aigua al medi, manifestant clarament un efecte inhibidor. Les energies d'activació aparent obtingudes van ser de 105 ± 4 kJ/mol per la formació de EOE i de 100 ± 5 kJ/mol per la formació de DEE.

Finalment, es va explorar el comportament de les resines parcialment sulfonades en la reacció de síntesis d'etil octil èter. A partir de la preparació i assaig de resines àcides amb diferent grau de sulfonació, es va observar que les resines presenten un nivell de reticulació heterogènia dintre de la fase gel. Per tant, els centres actius van estar localitzats en zones de diferent densitat, i conseqüentment, de diferent accessibilitat. En l'etapa inicial de sulfonació, els centres àcids es van localitzar a la zona menys densa del polímer. A mesura que avança la sulfonació, aquests es van localitzar a la zona menys accessible del polímer.

Els assajos catalítics de resines parcialment sulfonades va revelar que la selectivitat cap a EOE depèn de la zona del polímer a on té lloc la reacció. Com es pot observar en la Fig. 11, les últimes zones sulfonades són molt poc accessible per les molècules de OcOH, i per tant, l'increment relatiu de conversió de OcOH amb la capacitat àcida és molt baix a alts nivells de

sulfonació. Conseqüentment, els últims centres àcids afegits a la resina són molt poc eficients en produir EOE. En canvi, tot el polímer és accessible per EtOH i DEC molècules, i així, aquestes zones només són eficients per tal de produir el subproducte DEE. D'aquesta forma, per la producció de molècules voluminoses com el EOE i el DNOE, l'ús de resines poc sulfonades pot ser avantatjós.

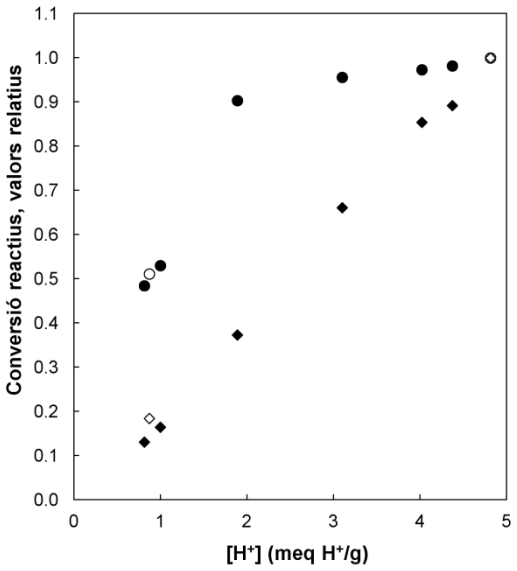


Fig. 11: Conversió relativa de OcOH (●) and EtOH (♦) com a funció de la capacitat àcida dels catalitzadors. (T=150ºC, P=25 bar, $R_{OcOH/EtOH}$=1, W=1g, t=6h). Els símbols tancats representen les resines preparades i els símbols tancats les resines comercials.

## 4. Conclusions

El compost EOE pot ser format mitjançant l'etilació de OcOH a partir de dos reactius d'origen renovable, EtOH i DEC. Les dos reaccions poden ser catalitzades mitjançant resines àcides de bescanvi iònic. Entre elles, les resines amb baix nivell de reticulació o les resines amb baix nivell de sulfonació afavoreixen la producció del compost desitjat EOE, en detriment del subproducte DEE.

Entre els dos agents etilants, EtOH i DEC, les mateixes selectivitats i rendiments poden ser obtingudes a temps de reacció llargs. Tanmateix, l'ús de DEC és menys competitiu en temps de reacció curts, com a resultat de la lenta descomposició de l'intermedi de reacció, l'etil octil carbonat. A més, la formació de $CO_2$ via dietil carbonat i la més alta disponibilitat d'etanol suggereix que l'ús de l'alcohol és preferit des d'un punts de vista tan industrial com ambiental.

L'estudi termodinàmic ha revelat que els valors relativament alts de la constant termodinàmica d'equilibri químic en la formació de l'etil octil èter asseguren alts nivells de conversió en un procés industrial. A més, s'ha observat que la constant d'equilibri de la reacció competitiva de

formació de dietil èter té valors inferiors en el rang de temperatures explorat, fet que en limitaria la seva formació.

En la formació de EOE a partir de la mescla EtOH / OcOH, la resina Amberlyst 70 s'ha mostrat com el catalitzador més adequat pel que fa a activitat i estabilitat tèrmica. L'estudi cinètic ha permès proposar una expressió mecanístic que és capaç de predir les velocitats de reacció tan en un reactor de tanc agitat com en un reactor de llit fix. Aquestes velocitats de reacció són altament inhibides per la presència d'aigua en el medi.

## Referències


[1] BP, "Energy outlook 2030." 2011.
[2] BP, "Statistical review of world energy 2011." 2012.
[3] European Union, "DIRECTIVE 2009/28/EC." 2009.
[4] US Energy Information Administration, "Annual energy review 2011." 2012.
[5] European Biomass Industry Association, "Bioethanol production and use. Overview of the European market." 2007.
[6] K. L. Rock and M. Korpelshoek, "Increasing refinery biofuels production," *PTQ Catal*, pp. 45–51, 2008.
[7] "European Fuel Oxygenates Association (EFOA)," 2013. [Online]. Available: http://www.efoa.org.
[8] A. C. Hansen, Q. Zhang, and P. W.L. Lyne, "Ethanol–diesel fuel blends—a review," *Biores Tech*, vol. 96, pp. 277–285, 2005.
[9] E. Benazzi, "Gasoline and diesel imbalances in the Atlantic basin part 1: market outlook." 2011.
[10] G. C. Pecci, M. G. Clerici, F. Giavazzi, F. Ancillotti, M. Marchionna, and R. Patrini, "Oxygenated diesel fuels-structure and properties correlation," presented at the Proc IX Int Symp Alcohols Fuels, Firenze, Italy, 1991, vol. 1, pp. 321–335.
[11] R. Patrini and M. Marchionna, "Process for the production of ethers from alcohols," U.S. Patent US 6218583 B1, 2001.
[12] K. Seidel, C. Priebe, and D. Hollenberg, "Emulsions," U.S. Patent US 5830483, 1998.
[13] A. Ansmann and B. Fabry, "Cosmetic preparations," U.S. Patent US 6878379B2, 2005.
[14] W. K. Gray, F. R. Smail, M. G. Hitzler, S. K. Ross, and M. Poliakoff, "The continuous acid-catalyzed dehydration of alcohols in supercritical fluids: a new approach to the cleaner synthesis of acetals, ketals, and ethers with high selectivity," *J Am Chem Soc*, vol. 121, pp. 10711–10718, 1999.
[15] C. Casas, R. Bringué, E. Ramírez, M. Iborra, and J. Tejero, "Liquid-phase dehydration of 1-octanol, 1-hexanol and 1-pentanol to linear symmetrical ethers over ion exchange resins," *Appl Catal A Gen*, vol. 1, pp. 321–335, 2011.
[16] B. Corain, M. Zecca, P. Canton, and P. Centomo, "Synthesis and catalytic activity of metal nanoclusters inside functional resins: an endeavour lasting 15 years," *Phil Trans R Soc A*, vol. 368, 2010.
[17] P. F. Siril, H. E. Cross, and D. R. Brown, "New polystyrene sulfonic acid resin catalysts with enhanced acidic and catalytic properties," *J Mol Catal A Chem*, vol. 279, pp. 63–68, 2008.
[18] K. Jerabek, *Cross-evaluation of strategie, size-exclusion chromatography. (Inverse steric exclusion chromatography as a tool for morphology characterization)*. Washington: ACS Symposium Series 635, 1996.
[19] K. Jerabek, "Determination of pore volume distribution chromatography data from size exclusion," *Anal Chem*, vol. 57, pp. 1595–1597, 1985.
[20] K. Jerabek, "Characterization of swollen polymer gels using size exclusion chromatography," *Anal Chem*, no. 57, pp. 1598–1602, 1985.
[21] R. H. Perry and D. W. Green, *Perry's chemical engineers' handbook*, Seventh edition. McGraw-Hill, 1999.

## Funding statement

This work was economically supported by the State Education, Universities, Research & Development Office of Spain (Project CTQ2010-16047). Trainee research staff grant was awarded by the University of Barcelona (APIF 2009-13).

## Acknowledgements

This Thesis does not only describe the daily work during four years, it also reflects an awesome period of my life. Luckily, I was not alone...

Thanks to my two supervisors **Javier** and **Eliana**, without whom the result of this work would have been much poorer. Through these years, you taught me a lot and you would easily realize that only by checking my first draft of the Cordova congress. I also want to express my gratitude to **Fidel** because four years ago you believed in me.

I would also like to thank **Montse**, **Carles**, **Roger**, **Marta**, **Madelin** and **Mari Ángeles** and because we have shared some nice moments (travels, meals...) and a lot of interesting discussions during my quotidian work. Special thanks go to **Carlos**, from the cradle to the grave (of my PhD period). As well, I feel really happy to have shared my lunch time (and much much more) with **Rafa**, **Xavi**, **Badia** and **Rodrigo**. Several students contributed directly or indirectly to this work and I would like to thank them for their input: **Pros**, **Pere**, **Adrian**, **Carlota**, **Sergio** and **Pedro**. Of course, “dícky moc” to **Jerabek**, and also to **Liba**, **Ladislav** and **Pavel** for helping me in my short but intense Praha stage, inside and outside the lab.

Further thanks to my co-teachers **María del Mar**, **Isabel** and others already quoted to coach me in my teaching duties. As my motivation for the research world began in The Netherlands, it’s a pleasure to thank to the people that enthused me indirectly about doing a PhD: **Celio**, **Joan**, **Roma**, **Laura**, **Can** and **Katja**.

Com que entendre la interacció entre molècules és molt més fàcil que entre persones, vull acabar expressant una total gratitud per la meva **família**, em sap greu pels altres però la meva és la millor! Com també el suport rebut pels meus **amics** en aquests quatre anys. Finalment, gràcies, **Anna,** per haver-me acompanyat en aquest camí. Fa 4 anys, en els agraïments, vaig demanar que la vida no ens allunyés dels nostres somnis. I no tan sols no ens n’ha allunyat, sinó que n’hem complert molts i ens n’han sorgit de nous. Així que tan sols desitjo que en els propers anys no perdem la innocència per seguir somiant, i ningú ha dit que hagi de ser fàcil...

“recte endavant és no anar gaire lluny” Le Petit Prince